DETERMINATION OF THERAPEUTIC EFFECTS OF MULTIFUNCTIONAL MICELLE-BASED NANOCARRIERS ON BREAST CANCER CELLS

A Thesis Submitted to
the Graduate School of Engineering and Science of İzmir Institute of Technology in Partial Fulfillment of the Requirement for the Degree of

MASTER OF SCIENCE

in Molecular Biology and Genetics

by
Gizem Tuğçe ULU

July 2019

İZMİR

We approve the thesis of **Gizem Tuğçe ULU**

Examining Committee Members:

Prof. Dr. Yusuf BARAN
Molecular Biology and Genetics, İzmir Institute of Technology

Assoc. Prof. Dr. Bünyamin AKGÜL
Molecular Biology and Genetics, İzmir Institute of Technology

Asst. Prof. Dr. Mona EL KHATIB
Molecular Biology and Genetics, Abdullah Gül University

19 July 2019

Prof. Dr. Yusuf BARAN
Supervisor, Molecular Biology and Genetics, İzmir Institute of Technology

Prof. Dr. Volkan SEYRANTEPE
Head of Department of Molecular Biology and Genetics, İzmir Institute of Technology

Prof. Dr. Aysun SOFUOĞLU
Dean of the Graduate School of Engineering and Science, İzmir Institute of Technology

ACKNOWLEDGMENTS

I offer my deepest gratitude to my supervisor Prof. Dr. Yusuf BARAN for his encouragements, critical discussions, and advice throughout my life. I am learning from him not to wear a title under my job, but to wear a heart on my job.

I am also thankful to my laboratory members and friends, Yağmur KİRAZ, Sevim Beyza GÜRLER, Erez UZUNER, Mustafa ÖZTÜRK, Polen YUNUS, and Melisa ÇETİNKAYA.

I would like to thank our colloborator group, Prof. Dr. Sevil DİNÇER İŞOĞLU and her Ph.D. candidate Nazende Nur AKŞİT.

I would like to thank my friends, Sena ATICI, Yağmur Ceren Ünal, Esra BİLGİÇ, Sefayi Merve ÖZDEMİR, Züleyha KANPARA CİVAŞ, Cihan Civan CİVAŞ, Merve TORUN, Taha Buğra GÜNGÜL, Büşra ACAR, Seren KEÇİLLİ, Nihan AKTAŞ, and İsmail TAHMAZ.

My special thanks to my parents and my brother, for encouragement throughout my life and their great support.

I would like to thank Prof. Dr. Çağlar KARAKAYA, Assoc. Prof. Gülistan MEŞE ÖZÇİVİCİ and her master student Yağmur Ceren ÜNAL, and Assoc. Prof. Özden YALÇIN ÖZUYSAL and her master student Elif Günyüz for opening their labs to my studies.

I would like to thank Specialist Özgür OKUR for analysis with BD FacsCanto Flow Cytometry in IZTECH-BIOMER.

I would like to thank Prof. Dr. Ayşe Elif ERSON BENSAN and Prof. Dr. Sevil DİNÇER İŞOĞLU for provided cell lines.

I am thankful to my jury members, Assoc. Prof. Bünyamin AKGÜL and Asst. Prof. Mona El KHATIP, for their helpful suggestions and comments that provide to be a helpful for prospective studies in this field.

I would like to thank Katherine Willcox for proof reading.

I would like to thank Asst. Prof. Çiğdem Tosun and Prof. Dr. Ali Çağır for their advice.

This study was supported by the research grant from The Scientific and Technological Research Council of Turkey entitled as “Development of Breast Cancer Targeted, More Stable, Double-Moiety pH-Sensitive, Drug-Conjugated, Multifunctional Micelle-Based Nanocarriers and Investigation of Their *in vitro* Efficiency” and numbered as 116R057.

ABSTRACT

DETERMINATION OF THERAPEUTIC EFFECTS OF MULTIFUNCTIONAL MICELLE-BASED NANOCARRIERS ON BREAST CANCER CELLS

Breast cancer is the most common and frequent cause of death among women composed to all types of cancer. Current treatment protocols do not provide complete cure or selective drug delivery while targeted therapy can provide an important avenue for successful treatment of breast cancer.

In this study, therapeutic effects of drug-conjugated nanocarrier system with enhanced stability and double moiety pH-sensitivity on breast cancer (SKBR-3- HER-2-positive), normal breast epithelial (MCF-10A, HER-2-negative) and chronic myeloid leukemia (K562, HER-2-negative) cells were determined. With this approach, SKBR-3 cells were targeted by single nanocarriers having selectivity with unused peptide ligand (HER-2), stability with cross-linking of core moiety, and cleavage by two sites of pH-effect and drug release properties. After physicochemical characterization of micelle-based nanocarriers, cytotoxic, apoptotic and cytostatic effects of doxorubicin conjugated micelles were determined.

Doxorubicin conjugated micelles with HER-2 peptide (DOX-HER-2-NCs) had more cytotoxic effects on HER-2 positive cells. Additionally, intracellular amounts of doxorubicin is higher in SKBR-3 cells with applied DOX-HER-2-NCs as determined by fluorescence imaging. The apoptosis rate was increased on SKBR-3 at 50% cell growth inhibition (IC50) as determined by Annexin-V/Propidium iodide double staining. However, there was not any significant change in loss of mitochondrial membrane potential. Additionally, DOX-HER-2-NCs resulted in cell cycle arrest at G2/M-phase in response to IC50 value. Besides, protein level of Bcl-2 did not change while protein level of Bax and Caspase-3 were increased as determined by Western Blotting. This project provides novel and more effective treatment of breast cancer by using multifunctional properties of nanocarriers.

ÖZET

ÇOK FONKSİYONLU MİSEL NANOTAŞIYICILARIN MEME KANSERİ HÜCRELERİ ÜZERİNDEKİ TERAPÖTİK ETKİLERİNİN BELİRLENMESİ

Tüm kanser türleri karşılaştırıldığında meme kanseri kadınlarda en sık rastlanan ve ölüme neden olan bir kanser türüdür. Mevcut tedavi yöntemleriyle tam bir tedavi olmadığından dolayı ilaçların seçici taşınması ve hedeflenmesi yöntemlerinin geliştirilmesiyle meme kanserinin tedavisi için önemli bir adım taşımaktadır.

Bu çalışmada, geliştirilmiş stabilite ve çift-yarı pH duyarlılığına sahip ilaç konjuge edilmiş taşıyıcı misellerin terapötik etkileri, meme kanseri hücreleri (SKBR3-HER-2-pozitif), normal meme epitel hücreleri (MCF-10A, HER-2-negatif) ve kronik miyeloid lösemi hücrelerinde (K562, HER-2-negatif) incelenmiştir. Bu yaklaşım için daha önce kullanılmayan peptid ligand (HER-2) ile seçiciliği, çekirdek kısmın çapraz bağlanması ile stabilitesi, iki pH-etki bölgesi ile ayrılması ve ilaç salım özellikleri ile SKBR-3 hücreleri hedeflenmiştir. Misel bazlı nanotaşıyıcıların fizikokimyasal karakterizasyonundan sonra, Doxurobicin ile konjuge misellerin sitotoksik, apoptotic, sitostatik etkileri belirlenmiştir.

HER-2 peptidli olan doksorubisin konjuge misellerin (DOX-HER-2-NTs) HER-2 pozitif hücrelerinde daha sitotoksik olduğu belirlendi. Aynı zamanda, DOX-HER-2-NTs uygulanan SKBR-3 hücrelerinde Doxurobicin seviyesinin daha yüksek olduğu florasans görüntülemesi ile gözlemlendi. Annexin-V/Propidium iyodür çift boyamasına göre, SKBR-3 hücrelerinde IC50 (%50 inhibitor konsantrasyonu) değerinde apoptotsis oranı artmıştır. Ancak, mitokondrial potansiyelinde önemli bir değişim olmadığı gözlemlenmiştir. Ek olarak, IC50 değerindeki DOX-HER-2-NTs hücre döngüsüde G2/M-fazında tutuklamaya neden olduğu hücre döngüsü analizi ile belirlenmiştir. Western bloting çalışmalarında ise Bcl-2 protein oranı değişmezken Bax ve Kaspaz-3 proteini artmaktadır. Bu çalışma çok işlevli nanotaşıyıcılar kullanılarak meme kanseri hastaları için yeni ve daha etkili bir tedavi yönteminin geliştirilmesi planlanmaktadır.

To My Brother Berkay Berkant ULU,

To My Parents,

and To All Children's Smiles

TABLE OF CONTENT

LIST OF FIGURES

Figure **Page**

Figure **Page**

Figure **Page**

LIST OF TABLES

Table **Page**

CHAPTER 1

INTRODUCTION

Cancer is a major health problem worldwide and is called a global burden of disease. According to statistical analysis, approximately 18.1 million people have been diagnosed with cancer and 9.6 million people have died in 2018. Around 18% of total cancer deaths are caused by lung cancer, followed by breast cancer at 11.6% (1).

Cancer is known as uncontrolled cell growth and division. Cancer cells have the potential to invade and spread to other parts of the body (2, 3). Many reasons have been identified to induce cancer initiation and progression such as tobacco use, excessive consumption of alcohol, lack of physical activity, diet, obesity, infections, environmental pollution, and one's genetic background (4). Determining the causes of cancer is crucial in attempting to solve the problem. The certain signs and symptoms of cancer are supported by screening tests. Early detection is critical to determine the treatment of cancer (5). Cancer treatment is based on the type of cancer, stage at diagnosis, duration of continued treatment, overall health of patients, and lifestyle (6, 7). Chemotherapy, immunotherapy, surgery, radiotherapy, stem cell transplantation, hormone therapy, and targeted therapy are the standard types of cancer treatment (8, 9). The purpose of chemotherapy is to kill cancer cells by using chemicals that targets cell division and suppress cell proliferation, but this application causes many side effects in patients (10). Immunotherapy provides the regulation of the immune system by using checkpoint inhibitor or cell transplantation (11). Surgery aims to remove tumor and tumor microenvironment. This treatment is also preferred to reduce and prevent the spread of tumors or metastasis (12). Additionally, surgery is boosted with radiotherapy to kill cancer cells with high-dose radiation. This therapy is selected to reduce the tumor and decrease its effect before surgery (13). Chemotherapy and radiotherapy cause unwanted complications in the immune system and stem cell transplantation allows for a more efficient solution, which is preferred in leukemia or lymphoma patients (14). For breast cancer and prostate cancer, hormone therapy can be favored to regulate the aid of the

hormones in protection from cancer progression (15, 16). In addition, developing technology helps to find causes of cancer initiation and progression with a new signaling pathway that supplies innovative treatment application to overcome cancer as well as generate diagnosis and prognosis. High-throughput screening technology is an important factor in terms of the role of molecules in different signaling pathways such as PI3K/AKT, PD-L1, Notch, and Wnt signaling pathways (17-19). Targeted and personalized therapy can be listed under this type of treatment strategies. Efficiency and precision of the treatment for cancer are determined by genetic testing and health history of patients (20, 21). For targeted therapy, specific molecules, which are involved in cell growth, proliferation, invasion, and migration are used to block cancer progression and metastasis (22-24). Molecularly targeted drugs are developed by using a patient's genes, proteins or other small molecules. Targeted therapy also avoids frequent drug administration, use of high dose, and unwanted toxicities for conventional therapies. These barriers can be overcome by using different nanoparticles with their targeted molecules for cancer signaling pathways (25-27).

Conjugated nanoparticles with cell-specific targeting properties or cross-linking agents are used to target specific cells. These targeting features have a specific affinity for differential expression of antigens. For example; trastuzumab conjugated nanoparticles are developed to target HER-2 positive or overexpressed breast cancer cells but not normal cells (28). Also, nanoparticles are modified to target peptide, antibodies, and non-coding RNA (siRNA, miRNA, piRNA) to increase the effects of drugs and targets as well as circulation time. Despite the advantages of targeted therapy using nanoparticles, some limitations prevent achieving targets, such as the accumulation of nanoparticles in unwanted organs in patients (29-31).

Moreover, drug-conjugated nanoparticles fortified with multiple markers is necessary to increase drug efficiency by targeted drug delivery to overcome heterogeneous tumor environment and cancer.

1.1 Breast Cancer

Breast cancer is the most common type of cancer observed in women and forms in breast tissue. In 2018, about 2 million people were diagnosed with breast cancer, which corresponds to 11.6% of 36 types of cancer. Also, 626,679 people have died because of

breast cancer, which represents 6.6% in 36 types of cancer. In addition, the cumulative risk of breast cancer is 5.03% for ages from birth to 74 (1).

Many factors cause breast cancer such as age, high rate of drinking alcohol, imbalance of hormone in the body, family history, inherited mutation (BRCA1, BRCA2, and other genes), hereditary, and genetic factors (32). According to statistical analysis, 5% to 10% of breast cancer cases are determined for the inherited mutation (33). Additionally, the other major factor in breast cancer is nonhereditary factors with respect to studies about international and interethnic differences in incidence (34).

The age of the patient, tumor size, location or size of axillary lymph nodes, histologic type of the tumor, hormone-receptor and pathological results are prognostic factors that are important for prediction of progression and treatment of breast cancer as well as the outcome of disease (35). This information is used to determine the type of cancer. Due to its ability to spread from breast tissue to other parts of breast tissue, breast cancer is divided into two categories, known as non-invasive breast cancer (carcinoma in situ) and invasive breast cancer. Non-invasive breast cancer is found in the ducts of the breast, is called ductal carcinoma in situ (DCIS), and does not spread to other parts of the body. On the other hand, invasive breast cancer that develops in breast ducts is known as invasive ductal breast cancer and can spread to other tissues but not necessarily (36).

Mammographic screening and genetic testing are used for the diagnosis of breast cancer (37). After the diagnosis of breast cancer, treatment strategies for breast cancer is decided by using the subtypes, stage, and location of breast tumor (38). Furthermore, targeted therapy is developed for breast cancer such as trastuzumab, pertuzumab, and lapatinib (39). Trastuzumab and pertuzumab are monoclonal antibodies that are used both in early and late stages of breast cancer (40, 41). On the other hand, lapatinib is a type of kinase inhibitor that is used for metastatic breast cancer. Lapatinib inhibits EGFR effectively (42). It can also be taken with other chemo-drugs and hormone therapy that increase response rate and overall survival rate (43, 44). However, these drugs have side effects for breast cancer patients. Using trastuzumab or pertuzumab cause heart damage (congestive heart failure) for breast cancer patients (45). After using lapatinib, the skin of hand and feet become sore and red which is called hand-foot syndrome (46). For this problem, an innovative approach is developed by using nanobiotechnology to produce nanoparticle-drugs, which has less cytotoxic and genotoxic effects for healthy cells.

Nanobiotechnology, therefore, became a groundbreaking approach for targeted therapy in the battle against breast cancer.

1.2 Molecular Subtypes of Breast Cancer

Breast cancer is a heterogeneous cancer type that has different subtypes based on biological properties. The six different molecular subtypes of breast cancer are luminal A, luminal B, HER-2 enriched, basal-like, claudin-low, and normal breast cancer. Each molecular subtype has different properties in terms of hormone receptor and growth factor expression level, which are estrogen, progesterone, and HER-2 receptors. These subtypes are determined by cell morphology and immunohistochemical analysis (47). Differences of subtypes cause various symptoms, prognosis, diagnosis as well as a treatment due to the differences in the molecular subtypes that lead to different outcomes, which is important to provide precise identification of molecular subtypes for treatment to overcome breast cancer (48). So, the rate of survival and mortality can differ according as molecular subtypes. Luminal A subtype has a high prognosis rate together with a high survival rate (49). On the other hand, the basal-like subtype has a low prognosis rate, which brings low survival rate (50, 51).

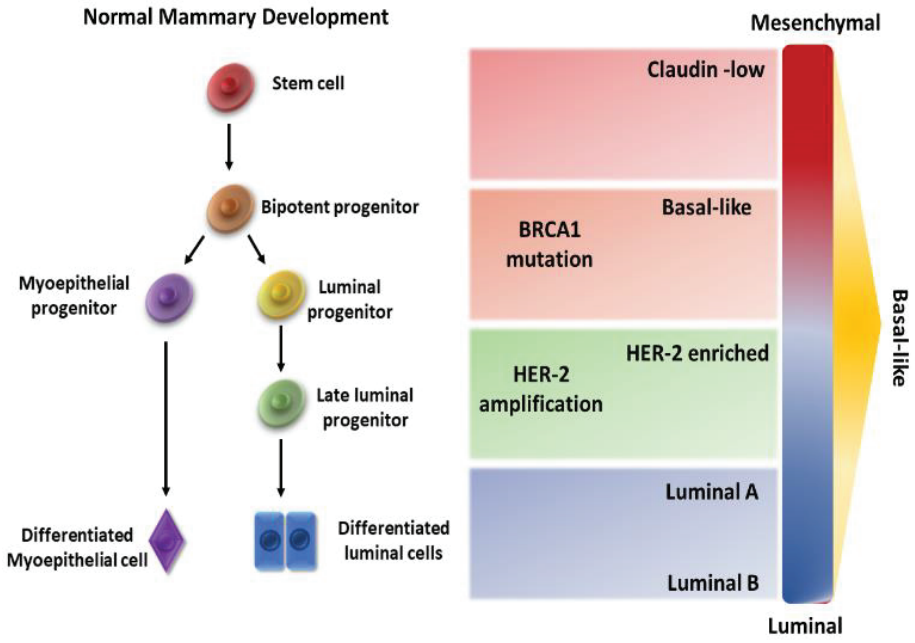

Figure 1.1 The putative model of normal mammary development and intrinsic molecular subtypes of breast cancer cells.

According to a hospital-based study by Zuo *et. al*., the survival rates of patients with I, II, III and IV stage were 97.1%, 92.6%, 75.6%, and 42.7%, respectively. However, the survival rates of patients with Luminal A, Luminal B, HER-2 overexpression and basal-like were 92.6%, 88.4%, 83.6%, and 82.9%, respectively. Therefore, the determination of the stage or subtypes of breast cancer is important to determine the survival rate and prognosis of cancer (52).

1.2.1 Luminal A

Luminal A breast cancer is known as hormone receptor-positive (estrogen and progesterone receptor-positive), HER-2 negative and low Ki67 (proliferating cell nuclear antigen) (53). In addition to that, luminal epithelial cytokeratins (CK)-8, CK-18 and gene-related to estrogen receptor which are LIV1 (zinc transporter ZIP6 or SLC39A6; solute carrier family 39 zinc transporter, member 6), hepatocyte nuclear factor 3 alpha (FOXA1), X-box binding protein 1 (XBP1), GATA binding protein 3 (GATA3), B cell lymphoma 2 (BCL2), erbB3 and erbB4 are also characterized as luminal A (54). 30-70 % of breast cancer is luminal A which has a better prognosis compared to other subtypes of breast cancer, which leads to high survival and low recurrence rate (55).

1.2.2 Luminal B

Luminal B breast cancer is defined as hormone receptor-positive (estrogen and progesterone receptor-positive) and either HER-2 positive or HER-2 negative. 30% of HER-2 positive breast cancer is characterized as luminal B subtypes (54). 10-20% of breast cancer is determined as luminal B, which also have a lower rate of survival and a higher rate of recurrence compared to luminal A (55). Genes related to cell proliferation including avian myeloblastosis viral oncogene homolog (v-MYB), gamma-glutamyl hydrolase (GGH), lysosome-associated transmembrane protein 4-beta (LAPTMB4), nuclease sensitive element-binding protein 1 (NSEP1) and cyclin E1 (CCNE1) are used for characterization of luminal B (56). Additionally, Ki67 is also used for determination of luminal B. Many studies are found to specify differences between luminal A and luminal B. Ki67 is one of the potential markers to be used for this purpose. However,

Ki67 marker is limited in terms of standardization (threshold values) of Ki67 expression level to be using clinical studies (57).

The survival rate of luminal B breast cancer patients is similar to HER-2 enriched and basal-like subtypes which are identified as a high-tumor risk (58). Moreover, luminal B subtypes are more insensitive to paclitaxel or doxorubicin during chemotherapy compared to HER-2 enriched and basal-like subtypes (59). Given this limitation, recent studies focus on alternative growth factor in the signaling pathway of breast cancer. Fibroblast growth factor receptor 1 (FGFR1), HER1, phosphoinositide 3 kinases (PI3K), catalytic alpha polypeptide, and sarcoma proto-oncogene (Src) are the five main growth factors (60). Therewithal, several antibodies and small molecule inhibitors are developed to suppress FGFR1 in recent studies because FGFR1 has a role in oncogenesis and resistance. Over-amplification of FGFR1 gene cause poor prognosis for luminal B subtypes. Recently, inhibitors of FGFR1 has been tested in clinical studies (61).

1.2.3 HER-2-Enriched

HER-2- enriched breast cancer patients have hormone receptor-negative (estrogen and progesterone receptor-negative) and positive HER-2 (overexpressed HER-2 receptor). HER-2 receptor is encoded by HER-2 gene that also acts as a proto-oncogene on chromosome 17q21 (62). HER-2 receptors actualize dimerization and phosphorylation of HER-2 extracellular domains. This phosphorylated tyrosine kinase residue effects different signaling pathways that are related to cell proliferation, survival, differentiation, angiogenesis, invasion, and metastasis (24, 63).

15-20% of breast cancer is HER-2 enriched. Overexpression of HER-2 induces aggressiveness as determined by different *in vitro* and *in vivo* studies. (55).

HER-2 enriched breast cancer has a poor prognosis with a tendency to metastasize other organs and develop resistance to hormone therapy, but they are sensitive to cytotoxic agents such as doxorubicin that blocks topoisomerase-2 activity. The topoisomerase-2 gene is located on chromosome 17, which provides an advantage to target HER-2 gene (64). Development of gene screening technology led to improve new therapeutic drug design.

1.2.4 Basal-Like

Triple-negative/basal-like breast cancer is defined as the hormone receptor-negative (estrogen and progesterone receptor) and HER-2 negative (65). They are not expressed, so basal myoepithelial markers which are a high level of CK5, CK 14, CK 17 and laminin are used for the determination of this subgroup. Besides, p-cadherin, fascin, caveolins 1 and 2, alpha-beta crystallin and epidermal growth factor receptor (EGFR) are overexpressed in basal-like breast cancer (66). Additionally, mutations in tumor protein 53 (TP53) gene are found in basal-like breast cancer patients that also affect genomic instability by dysregulating the retinoblastoma (Rb) pathway (67).

5-15% of breast cancer is triple-negative/basal-like (55). This subtype is aggressive and has a poor prognosis compared to luminal A and luminal B types (68). The basal-like subgroup is defined by high proliferation, heterogeneity, metastases, and incidence of relapse (69). The absence of ER, PR, and HER-2 protein expression cause lack of immunohistochemical classification. Instead of this technique, gene expression microarray analysis is used to define basal-like subgroup (70).

These groups have drug resistance that also induces aggressiveness by signaling pathways such as mTOR and TGFβ signaling pathways (71). BRCA1 (breast cancer susceptibility gene 1) is expressed in basal-like breast cancer with Ki67 basal cytokeratin, TP53, EGFR, and p-cadherin. So, this molecule and their related signaling pathway are used in targeted therapy for these subgroups. For example, poly-ADP ribose polymerase (PARP) enzyme has an important role in DNA double-strand breaks. So, the PARP enzyme inhibitor is used to target deficient BRCA1 pathway for this subgroup (72, 73).

1.2.5 Claudin-Low

Claudin-low breast cancer is a type of basal-like subgroup. This group has low expression of claudins 3, 4 and 7, occludin and e-cadherin that have roles in cell-cell adhesion and tight junctions. Additionally, some genes related to epithelial to mesenchymal transition and stem cell properties are highly expressed. Also, this subgroup has poor clinical outcomes to overcome cancer (74).

1.2.6 Normal Breast

Normal breast cancer tumors correspond to 5-10% of all breast tumors (54). This subgroup is characterized by using the classification of intrinsic subtypes with fibroadenomas and normal breast samples (75). This subgroup has a lack of expression of ER, PR, and HER-2 and thus is classified as basal-like breast cancer. However, the expression level of CK5 and EGFR is negative. By their gene expression level in this subgroup, the prognosis is similar to luminal and basal-like cancers (76).

In 2011 and lately in 2013 St. Gallen International Breast Cancer Conferences, the effects of molecular classification were discussed and accepted in the role of treatment approaches on breast cancer. Panel members decided to use new therapeutic approaches that will be based on the intrinsic subtypes of breast cancer. The subtypes of breast cancer are determined by microarray, which is supported by immunohistochemistry (77, 78).

1.2.7 Molecular Biology of Breast Cancer

In recent years, many studies provided new knowledge about the biology of breast cancer by developing high throughput technologies. The nature of diseases is examined in depth with a comparatively large number of samples. Breast cancer consists of six intrinsic subtypes which are luminal A, luminal B, HER-2-enriched, basal-like, claudin-low and normal breast. However, this classification is not standardized. Large scale and valuable information can provide the characterization of each subgroup. The biology of the tumor, microenvironment, and their features lead to an understanding of signaling pathways that provide a determination of progression of cancer, administration of tumor and treatment of cancer. In addition, the determination of genes and proteins in signaling pathways provide improvements for targeted therapy for breast cancer (79).

1.2.7.1 Signaling Pathways in Breast Cancer

According to the cancer genome atlas drawing on 9,125 samples from 33 cancer types, 10 main signaling pathways have been found to have roles in generating of the hallmarks of cancer, which are cell growth, progression, and death by regulation of cell cycle, Hippo, Myc, Notch, Nrf2, PI-3-Kinase/Akt, Ras, PTPs, TGFβ signaling, p53 and

β-catenin/Wnt. In addition, 99% of tumors have a role in at least one of the signaling pathway. However, targetable drugs can be used in 57% of tumors to alter these pathways to overcome cancer (80). So, signaling pathways have an important role in the identification of targeting cancer specifically for promising cancer treatment. Breast cancer is regulated by different pathways which are used to understand tumor heterogeneity and improve new therapeutic strategies.

Basal-like breast cancer is a more aggressive type of breast cancer. Three main signatures, namely retinoblastoma tumor suppressor (RB1), PTEN, and TP53, regulate metastasis not only in this subgroup of the breast but also other malignancy types (81, 82). Loss of RB1 and PTEN and TP53 mutation induces tumorigenesis by activation of Myc, β-catenin/Wnt, and PI-3-Kinase/Akt signaling pathways. RB1 has an anti-proliferative effect in cells by inhibition of E2F1 transcription factor that has a role in the regulation of cell cycle. Phosphorylation of cyclin-dependent kinase 4/cyclin D (CDK4/cyclin D) and CDK2/cyclin E complex inactivate RP phosphorylation that mediates cell cycle progression. For this purpose, Witkiewicz et al. focused on targeting of loss of RB by using CDK4/cyclin D inhibitor that induces activation of RB (83). Besides, dephosphorylating phosphatidylinositol 3,4,5-trisphosphate (PIP3) is dephosphorylated by PTEN, which is called an antagonist of phosphatidylinositol 3-kinase (PI3K) signaling. Inhibition of PI3K induces tumor dissemination and relapse by increasing mitochondrial activity (84).

The Hippo signaling pathway, which is mediated by Hippo transducer, Yes-associated protein (YAP), and tafazzin (TAZ) have a role in hallmarks of cancer as well. Inhibition of YAP/TAZ blocks epithelial-to-mesenchymal transition (EMT) and invasion in breast cancer (85). Besides, this pathway consists of a kinase cascade. Two core signatures, which are mammalian STE20-like protein kinase-1 (MST1) and the large tumor suppressor 1 (LATS1) and LATS2 have a role in the activation/deactivation of the Hippo pathway. MST1 and LATS1/2 regulate activation of YAP/TAZ. Suppression of LATS1/2 induces EMT and metastasis of breast cancer via inhibition of YAP/TAZ (86). YAP/TAZ acts as pro-tumorigenic and induces focal adhesion. These properties are important for metastasis progression. Focal adhesion composes dynamic structure for cells, which mediates cytoskeleton modeling. The dynamics of focal adhesion (assembly-disassembly of focal adhesion) mediate controlling cell migration/invasion, proliferation, and survival by inducing focal adhesion kinase. An increase in focal adhesion kinase

expression induces metastasis with poor diagnosis and prognosis (87). In addition, phosphorylation of focal adhesion kinase induces Src, Shc, PI3K, PLC-γ, and Ras pathways (88).

Myc is known as an oncogene that mediates transcription factors which mediate cellular processes including cell growth, proliferation, re-entry, adhesion, metabolism, death, and angiogenesis (89, 90). In addition, Myc signaling pathway affects multiple processes in breast cancer cells such as regulation of tumor progression and drug-resistance in cells.

Notch signaling induces cell proliferation and tumor recurrence (91). This pathway has a role in invasion and intravasation of breast cancer (92). In addition, Notch signaling is critical for treatment of chemo-resistant cancer stem-like cell. This signaling pathway is controlled by 5 different substrates and 4 receptors, which are Jagged-1, Jagged-2, Delta-like-1, 3, 4, and Notch1-4, respectively. The correlation between Notch and its ligand Jagged-1 causes poor prognosis. The high level of Jagged-1 induces stem cell self-renewal in luminal subtypes of breast cancer. Additionally, overexpression of Notch1, Notch3, and Notch4 receptors cause metastasis and an aggressive tumor of breast cancer. So, high co-expression of Jagged and Notch have a role in the survival rate of breast cancer patients (93). Notch signaling has a role in Akt and NF-κB signaling. Hossain *et. al*. demonstrates that Jagged-1 increase Akt phosphorylation with Notch1 dependent pathway that induces respiration in mitochondria that also have a role in transcription of survival genes. So, they focused on the combination of pharmacological Notch inhibitor with Akt or NF-κB inhibitors to develop therapeutic applications for breast cancer (94).

The lack of glucose in cancer cells stimulates expression of nuclear factor erythroid-derived 2-like 2 (Nrf2) to induce anti-oxidants as well as autophagy by regulation of cytoprotective genes expression and efflux transporters. Nrf2 is known as a master regulator in autophagy (95, 96). Keap1/ Nrf2 pathway has a role in cellular metabolism for adaptation of glucose deprivation. Autophagy causes a decrease of p63 which causes Keap1 to bind to Nrf2 transcription factor. So, Nrf2 protein degradation increases, which leads to an increase in antioxidant activity (95). On the other hand, the Nrf2 signaling pathway also mediates drug resistance mechanism by induction of P-glycoprotein (P-gp) and breast cancer resistance protein (BCRP). P-gp and BCRP are

efflux transporters that play a critical role in the accumulation of toxic and endogenous substrates in the cells. At this point, the selection of drugs based on the Nrf2 signaling pathway is important for the treatment of resistant breast cancer (97, 98).

The phosphatidylinositol 3-kinase (PI3K)/Protein Kinase B (PKB, Akt) pathway has a critical role in cancer progression, metastasis, and drug-resistance. Activation of Akt induces activation of Ras, PI3K, and loss of PTEN (99). Three different isoforms of Akt are found, which are Akt1 (PKBα), Akt2 (PKBβ) and Akt3 (PKBγ). Each isoform has specific features in cellular processes (100). Ubiquitin-modifying enzymes regulate the post-translational modification of Akt. Activation of BRCA1 is related to K48-linked ubiquitination by the Akt pathway. BRCA1 bind to phosphorylated Akt1 which induces K48-linked ubiquitination. This ubiquitination provides proteasomal degradation of Akt1. On the other hand, K43-linked ubiquitination processes induce activation of Akt1 by stimulating nuclear translocation of Akt1 (101-103). Also, the activation/deactivation of p21 and p27 is modulated by Akt-dependent phosphorylation. The function of p21 and p27 causes cell proliferation and poor prognosis. Overexpression of p21, cytoplasmic translocation of p21 or p27 are used as a biomarker of the aggressive tumor with poor prognosis in breast cancer (104).

TGF-β signaling inhibits cell proliferation, which is important for breast cancer progression. Inducing HER-2/EGFR signaling replaces TGF-β signaling pathways, which changes cellular progression from anti-proliferation to cancer initiation and progression. Inhibition of HER-2/EGFR induces TGF-β signaling, which causes epithelial-mesenchymal transition and cell migration because HER-2/EGFR signaling is related to Akt pathway with an accumulation of Smad3, which has a role in epithelial-mesenchymal transition and cell migration (105). According to Kunihiro *et. al*., inhibition of Smad dependent/ TGF-β signaling blocks breast cancer bone metastasis initiation and progression (106).

Protein tyrosine phosphatases (PTPs) have an important role in the phosphorylation of tyrosine kinase that regulates tumorigenesis. PTPs also called as TCPTP, is an intracellular non-transmembrane phosphatase (107). TCPTP has a role in the regulation of epidermal growth factor and Janus activated kinase/signal transducers and activators of transcription signaling (JAK/STAT) (108). The two main groups in TCPTP are 48 kDa variant (TC48) and the 45 kDa variant (TC45) (109). While the TC48

is located in the endoplasmic reticulum, TC45 is found in the nucleus. These two main groups have a role in tyrosine kinase phosphorylation-dependent signaling pathways, which regulate cell growth by regulation of cell cycle checkpoints and cell stress by dysregulation of the endoplasmic reticulum. So, deletion or overexpression of TC48 and TC45 contributes to treatment strategies in breast cancer (110, 111).

All of these signaling pathways have important roles in breast cancer initiation, progression, and invasion and are regulated by different molecules, which can be regulated/inhibited by their specific inhibitors.

Different signaling pathways regulate cellular processes during breast cancer progression. Cell proliferation, cell growth, cell death, apoptosis, drug resistance, cell adhesion and metastasis are main processes in regulation (Figure 2).

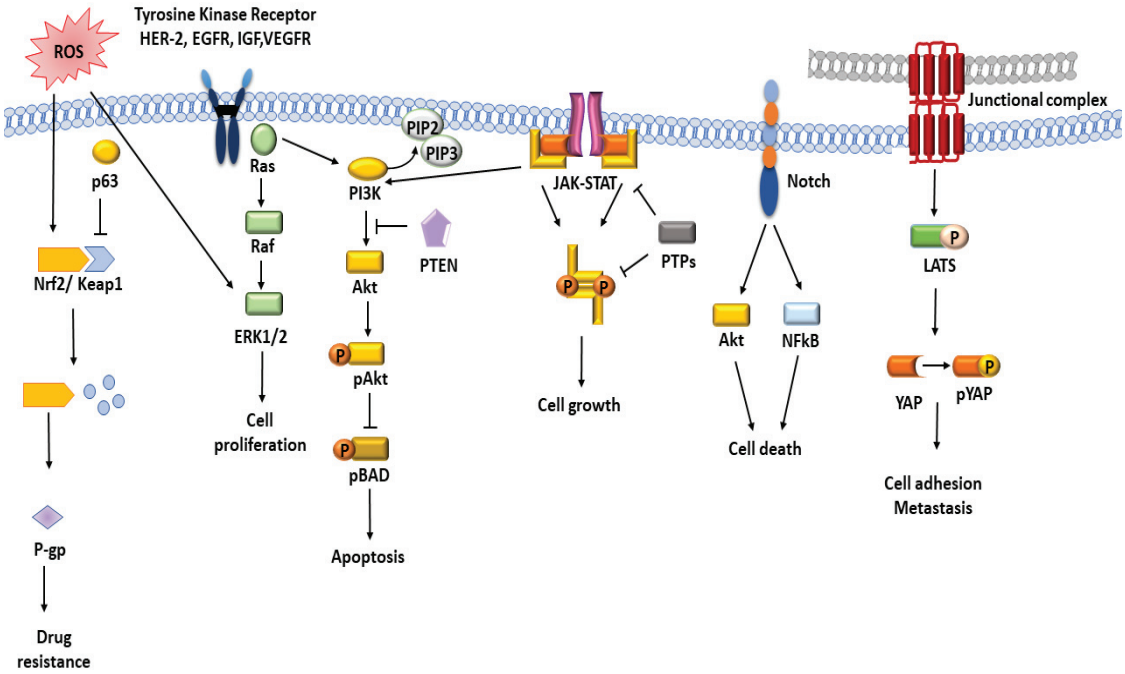

Figure 1.2. The main signaling pathways in breast cancer progression.

The determination of these signaling pathways is important because the regulation of molecules control cencer initiation and progression. So, different threatment approach will be developed by actication/deactivation of these molecules.

1.2.7.2 HER-2 Signaling Pathway

Human epidermal growth factor is a member of the epidermal growth factor family and has a role in the stimulation of cell growth, proliferation, survival, and differentiation via different signaling pathway in cancer (63). Four group members, HER-1, HER-2, HER-3, and HER-4, are found that are also known as ErbB1, ErbB2, ErbB3, and ErbB4, respectively (112). HER receptor consists of a cysteine-rich extracellular ligand-binding site. These receptors have a tyrosine kinase catalytic activity domain. The autophosphorylation of tyrosine kinase residue induces dimerization of this receptor. This process involves different signaling pathways which regulate cellular proliferation, transcription, motility and apoptosis inhibition. (113).

HER-1 members were the first tyrosine kinase discovered by Carpenter G. et al in 1978. They showed, for the first time, the regulation of biochemical reaction by the formation of epidermal growth factor receptor complex (114). HER-2 receptor is 185 kD transmembrane glycoprotein, which is located on human chromosome 17 (17q12). Overexpression of HER-2 which modulates carcinogenesis and tumorigenesis, is found in breast, gastric, lung, ovary, colon, and bladder cancer (115).

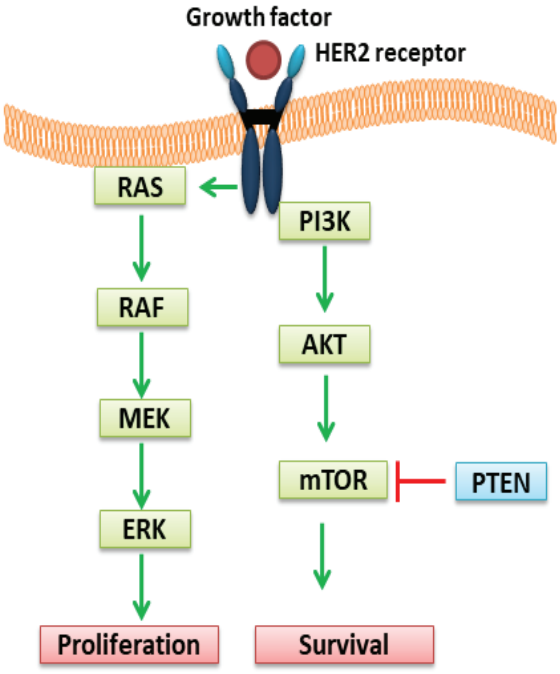

Figure 1.3. The role of HER-2 on two main signaling pathways.

HER-2 has important roles in different signaling pathways such as PI3K/AKT and RAF/MEK/ERK that regulate cell proliferation and survival in breast cancer (Figure 3).

The PI3K/Akt/mTOR pathway has a role in cell growth. This signaling pathway is regulated by phosphorylation of HER-2, which is determined as a key effector (116). Also, different studies showed that the expression levels of another tyrosine kinase such as insulin-like growth factor I receptor (IGF1R) affects the same pathway, the PI3K/Akt/mTOR pathway, and MAPK. Dysregulation of IGF1R is seen in malignant transformation. Overexpression of IGF1R is induced by HER-2 and HER-3, which is activated by PI3K signaling pathway. Figitumumab and metformin are used to inhibit IGF1R ligand binding. They can be used with HER-2 inhibiting agents as a combination treatment for HER2+ metastatic breast cancer (117).

1.2.7.3 Signaling Pathways in Therapeutic Advances

HER-2 overexpression of breast cancer is identified to target HER-2 with agents such as trastuzumab, pertuzumab, trastuzumab emtansine (T-DM1) and small molecules tyrosine kinase inhibitors of HER-2 (118).

Activation of PI3K by mutation of PIK3CA or loss of PTEN induce resistance in HER-2 targeted therapies, which causes poor prognosis after trastuzumab treatment. To overcome this, different inhibitors are used as combination drug treatment, such as mTOR inhibitors, which are used to overcome trastuzumab resistance in HER-2-riched breast cancer. Moreover, the regulation of Cyclin D1/CDK4 has a role in the resistance of HER-2 inhibition. The inhibition of CDK4/6 suppressed mTORC1. The efficiency of the combination of CDK4/6 and HER2 inhibitors are determined in transgenic and PDX breast cancer mouse models by Goel *et. al*. (119)

The presence or absence of HER-2 expression has an important role in the progression of breast cancer and drug resistance. Jordan *et. al*. showed the role of HER-2 positive and HER-2 negative circulating tumor cells and the evolution of metastatic breast cancer. They analyzed the circulation of breast cancer cells in 19 women. They found that 84% of ER-positive/ HER-2 negative primary tumors gained HER-2 positive properties. HER-2 positive circulating tumor cells have more proliferative properties. Also, HER-2 negative cells are responsible for the activation of Notch and DNA damage

signaling pathways that cause resistance to cytotoxic chemotherapy. However, Notch inhibition induces sensitivity of treatment in breast cancer. According to their results, paclitaxel treatment or Notch inhibitors supply sustainable treatment by suppression of tumorigenesis (120).

PTEN mutation is related to cancer progression and resistance in overexpressed HER-2 breast cancer. Ebbesen *et. al*. showed that suppression of PTEN triggered cancer progression. On the other hand, increased PTEN causes cancer regression. They demonstrated the relationship between PTEN and MEK signaling pathway to identify the role of MEK inhibitors with PTEN mutation on therapy-resistant breast cancer patients (121).

α-Lipoic acid, also called as thiotic acid, has a role in mitochondrial activation by enzymes such as pyruvate dehydrogenase and α-ketoglutarate dehydrogenase. These enzymes have a key role in cellular metabolism. Different studies showed beneficial effects of α-Lipoic acid in breast cancer treatment. α-Lipoic acid induces apoptosis and inhibits cell proliferation in breast cancer. In addition, Tripathy *et. al*. demonstrated that α-Lipoic acid inhibits cell migration and invasion by TGF-β signaling pathway and reduction of matrix metalloproteinase-9 (MMP-9) expression (122).

Estrogen positive tumor represents 70% of all breast cancers. For this group, aromatase inhibitors are used in the therapy but these cells gain resistance during chemotherapy. For this problem, combination drug treatment is used with an aromatase inhibitor and CDK4/6 inhibitors, or mTOR inhibitors (123). Entinostat, also known as histone deacetylase inhibitor, is used in metastatic estrogen receptor-positive breast cancer patients. Preclinical studies show that luminal subtypes are more sensitive to entinostat compared to basal-like breast cancer owing to Myc signaling (124).

In the last decade, the mortality rate of breast cancer decreased due to the significant improvements in molecular approaches for targeted therapy. ER or HER-2 are main targeting molecules for inhibition of cancer initiation and progression (125).

In addition, regulation of different signaling pathways is important to mediate cellular processing of breast cancer cells. Besides, the regulation of signaling pathways has a role in the treatment of breast cancer. So, the determination of signaling pathways or the investigation of molecules in signal transduction is crucial to find new therapeutic approaches for breast cancer.

1.2.8 Treatment of Breast Cancer

Immunohistochemistry (IHC) for identification of protein expression and fluorescence in-situ hybridization (FISH) for identification of gene amplification are two methods used for classification of HER-2 (+) in patients (126). After determination of breast cancer, the treatment strategies are determined to inhibit cancer progression. Generally, endocrine therapy, cytotoxic chemotherapy, and anti-HER-2 agents are used in the treatment of metastatic breast cancer. However, these methods are limited to overcome cancer. So, novel drugs are necessary to target breast cancer cells. Understanding the molecular biology including signaling pathways of breast cancer allows for the development of new drugs.

1.2.8.1 Targeted Therapy for Breast Cancer

Human epidermal growth factor also called HER-2(+) is overexpressed in 20-30% of breast cancer patients (127). Aggressive phenotype is seen in HER-2(+) patients and is related to poor long term outcomes (128). Development of HER-2 targeting drugs (trastuzumab) for cancer treatment provides a 50% decrease in recurrence and 37% increase in survival rate in patients (129, 130).

In addition, five different HER-2 targeted therapeutic drugs have been approved by the FDA (131). Trastuzumab, pertuzumab, lapatinib, ado-trastuzumab emtansine, and neratinib are used for metastatic and adjuvant of HER2-positive breast cancer. These drugs are also used with a combination of other drugs to increase drug efficiency and overcome resistance (132).

Trastuzumab, which is HER-2 monoclonal antibody, provide improved outcomes for HER-2 early breast cancer. The use of trastuzumab decreases the death rate as well as recurrence. The mechanism of trastuzumab is to bind HER-2 transmembrane domain and inhibit dimerization (133). Pertuzumab is another humanized monoclonal antibody. Their mechanism is similar to trastuzumab but pertuzumab binds to dimerization domain and inhibits heterodimerization with other HER receptors. Combination of trastuzumab and pertuzumab is more effective than trastuzumab alone in neoadjuvant studies and provides an increased survival rate (134). On the other hand, metastatic breast cancer can gain

resistance to trastuzumab. In this event, alternative inhibitors are needed to inhibit HER-2 signaling pathway. One such inhibitor is Lapatinib, a selective tyrosine kinase inhibitor of HER-2 and EGFR. Lapatinib is also used with other inhibitors such as trastuzumab. They have complementary mechanism and synergy for anti-tumor activity in models of HER2-enriched breast cancer. The combination of lapatinib and trastuzumab significantly increases the response rate from chemotherapy and overall survival rate (135).

Ado-trastuzumab emtansine (T-DM1) is antibody-drug conjugated drugs that consist of anti-tumor features of HER-2 antibody and microtubule-disrupting agent which is called maytansinoid (DM1). After the conjugation of T-DM1 and HER-2, receptor-mediated endocytosis occurs and DM1 is released by proteolytic degradation with the lysosome (136). T-DM1 was approved by the U.S. Food and Drug Administration (FDA) in 2013 to use for patients with HER2-positive metastatic breast cancer who take trastuzumab and a taxane (137). Another tyrosine kinase inhibitor is neratinib, which inhibits HER-1, HER-2, and HER-4 for HER2-enriched metastatic breast cancer. This inhibitor blocks the activity of HER receptors irreversibly (138). It is used as a combination therapy with trastuzumab for HER-2 enriched breast cancer patients. According to Phase I/II study, neratinib and trastuzumab increase tumor activity in metastatic HER-2 enriched breast cancer. Also, there was no cardiac toxicity seen after application (139).

Targeting therapy has a critical role to overcome cancer. For these reasons, rapid development of targeting agents is necessary instead of traditional cytotoxic agents. The best example of this event is the improvement of T-DM1. Phase I study of T-DM1 was achieved in 2007 (140). After 2 years, the phase II study on the clinical application was examined in 2009 (141). Finally, this drug was approved by FDA in 2013 (142). The length of time for approval is only 6 years, which shows the necessity of targeted therapy for HER-2 enriched breast cancer.

Recently, the developing next-generation sequencing technique in clinical application provides new information about HER-2 biology. Moreover, new therapeutic drugs targeting HER-2 have been developed including small molecule inhibitors, antibody-drug conjugates, and nanocarriers. Palbociclib and abemaciclib are small molecule inhibitors of cyclin-dependent kinases (CDKs) 4 and 6 that reduce cell growth and proliferation (143, 144). Trastuzumab, pertuzumab, rituximab, and cetuximab are

antibody-drug conjugates drugs to solve many problems in chemotherapy to increase the efficiency on breast cancer cells (145). In addition, different nanoparticles are designed to improve targeted therapy. For example; polymeric, gold, and lipid nanoparticles are developed with specific agents-loaded to induce cytotoxic efficiency in cancer cells (146-148). Also, their specificity features are advanced by modified surface with conjugated specific antibodies and peptides (149, 150).

1.2.8.2 Role of Nanocarriers in Targeted Therapy of Breast Cancer

The death rate of breast cancer occurs due to drug resistance and metastasis to other organs such as lymph nodes, bone, lung, and liver. In the drug resistance mechanism

Multidrug resistance genes such as P-glycoprotein (P-gp/ABCB1), ABCG2, and BCRP also have critical roles in cancer progression and response to treatment (151). According to the literature in recent years, various targeted therapies are an improved approach to chemotherapy, immunotherapy with small molecules, proteins, and peptides, controlled-release drug delivery. However, these new methods have had limited success.

Nanoparticles are characterized by five different properties which are type, target, size, surface, and shape. These properties have important role in their physicochemical characterization. Each property demonstrates different outcomes in cells (Figure 4).

Developing nanotechnology promotes an increase in the therapeutic efficiency of drugs that is possible by an understanding of the relationship between tumor and tumor microenvironment. Using nanoparticles or nanocarriers supply to control the release of drugs, high loading capacity, and stability of drugs and less toxicity for normal healthy cells (152). Nanoparticles have multifunctional properties by modification of surface and core side that provide controlled anticancer agents to increase drug efficiency and overcome MDR (153, 154).

Two main groups are found as organic and inorganic nanoparticles. Dendrimers, micelles, liposomes, and ferrite are the type of organic nanoparticles. Also, iron nanoparticle, quantum dot, superparamagnetic iron oxide, and paramagnetic lanthanide iron nanoparticles are inorganic nanoparticles. Their synthesized methods are different in terms of drug attachment including encapsulation, covalent binding, and adsorption. (155, 156).

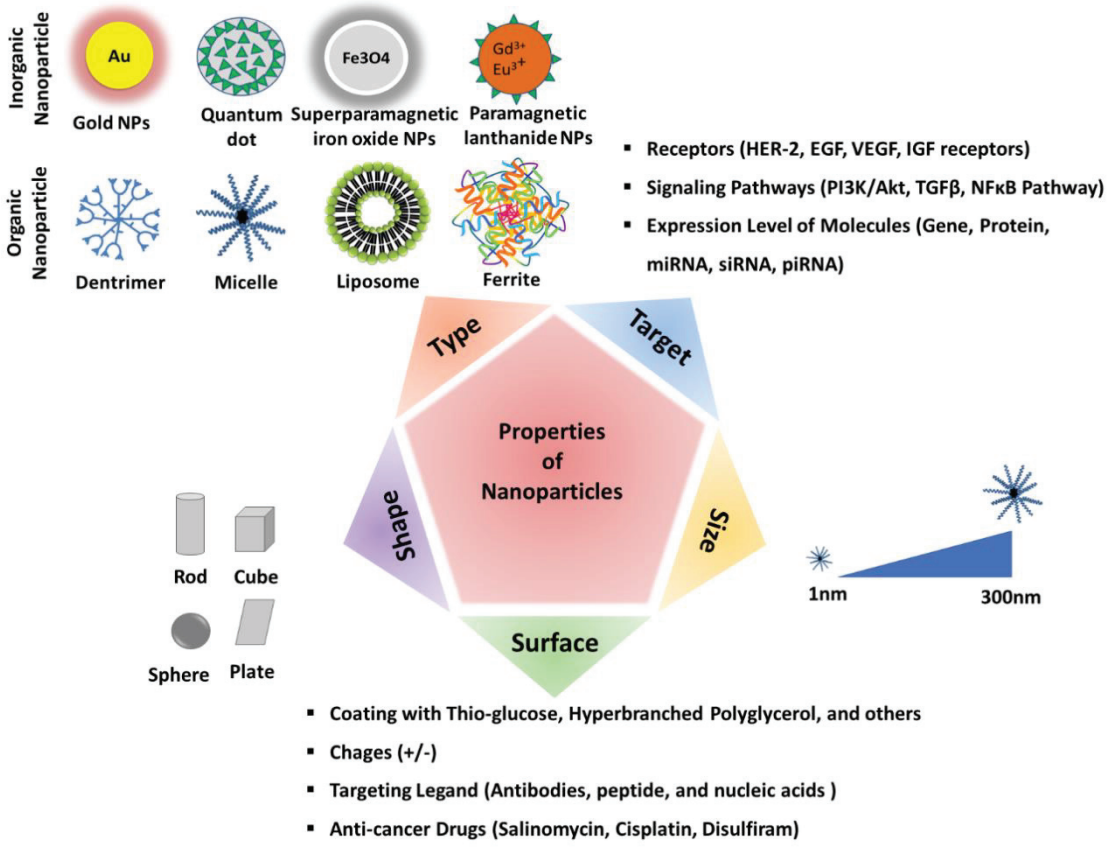

Figure 1.4 The different properties of nanoparticles.

Each type of nanoparticle has different properties, making them appropriate for different purposes. For example, liposomes are an early stage of drug delivery system for pharmaceutical nanocarriers. Liposomes have biocompatibility properties with inducing agent solubility that provides increasing drug efficiency. Additionally, they are bio-degradable and have low toxicity (157). On the other hand, quantum dots are other types of inorganic nanoparticles that have fluorescent imaging probes. These properties provide the tracking of quantum dots for imaging and sensory processes. Also, this type of nanoparticle has high toxicity that induces cell death by inducing the formation of reactive oxygen species (ROS). Quantum dots induce permeability by affecting cellular metabolism that ensures an advantage of using targeted therapy (158).

Moreover, micelle nanocarriers have a potential role in cancer diagnosis and treatment. They have biocompatibility and biodegradability, and their lipophilic properties enhance water solubility. According to *in vitro* studies, paclitaxel binds β-tubulin that block microtubulin formation. The water solubility of paclitaxel is 0.0015 mg/mL. The encapsulation of paclitaxel with micelles increase solubility from 0.0015

mg/mL to 2 mg/mL that increase drug efficiency by their hydrophobicity properties of micelles (159).

The receptors, which are HER-2, EGFR, vascular endothelial growth factor receptor (VEGFR), and IGF-IR are used to target inhibition of breast tumorigenesis for clinical treatment (Phases II and III) (160). Yamaguchi *et. al*. examined the effect of hyperbranched polyamidoamine coated silica nanoparticles with conjugated HER-2 antibody on radiosensitivity of SKBR-3 (HER-2 overexpressed breast cancer). According to results, SKBR-3 cell line is incubated with this synthesized nanoparticle. Next, they were exposed to X-ray radiation. Following that, these nanoparticles with radiation increased apoptosis on SKBR-3 (161). Li *et. al*. showed that the synthesized salinomycin-loaded polymer-lipid hybrid anti-HER2 nanoparticle increased cytotoxic effects on HER-2 positive breast cancer compared to non-targeted nanoparticles (162). EGFR peptides conjugated with PEGylated polylactic-co-glycolic acid (PLGA) nanoparticles that are loaded with curcumin are used to target EGFR expressed cells. According to results, PI3K signaling pathways are reduced and cytotoxic effects on cells increased. Moreover, its effectiveness increased with the increase in circulation time of curcumin (163).

All in all, nanoparticles have effectiveness that is an important role in the delivery of anti-cancer agents with conjugated factors. At this point, the determination of the molecular mechanism of cancer cells allows identification of the differences between cancer cells and normal healthy cells that highlight targeted therapy. Although many studies have been done so far, a different approach is necessary to improve the delivery system of nanoparticles and induce efficiency of drugs.

1.2.9 Aim of the Study

HER-2 enriched breast cancer type has overexpressed receptors on the surface of breast cancer cells (SKBR-3) resulting in poor prognosis and aggressivity. For targeted therapy of breast cancer, more stable core cross-linked micelles with a double-moiety pH-sensitivity were used to increase micelles stability and drug release at lysosomal pH that is provided by pH-sensitive hydrazone and acetal bonds. The micelles have many advantages such as biocompatible, biodegradable, easy modified, and easy functionalized to be used in targeted therapy. It also has dynamic structure. Thus, it cause some problem such as leaking out of drug, minimal circulation time, and optimal concentration for

micelles formation. So, the dymanic structure formation provide easy modified and easy functionalized but it is also called as disadvantage for micelles. In this project, core cross-linked micelles with a double-moiety pH-sensitivity provide stability of micelles that turns disadvantages into advantages.

Additionally, unused specific HER-2 peptide sequence (VSSTQDFP) is used to targeted HER-2. These properties also determined as the novelty of this project. pH-responsive nano-drug delivery system maintains drug efficiency that provides an accumulation of the drug in the tumor microenvironment. The using of peptide sequence has role in modification of size of NCs in satead of antibody. The increasing size of NCs is less than antibody. So, it can also provide targeted efficiency on cancer cells

The stability of drugs can be increased during blood circulation. Also, doxorubicin was used as anticancer agents for the treatment of breast cancer cells. According to the literature, various studies such as Nakanishi *et. al*. demonstrated that polymeric system with doxorubicin increases drug activity significantly compared to free doxorubicin (164). According to clinical studies and pharmacokinetic examination, micelles decrease the clearance of the doxorubicin by increasing half-life of drugs (165). In order to achieve this target in this project, maleimide-modified DOX are attached with micelles by using functionalized piridil disülfit (PDS) groups that increase drug loading and release efficiencies. Using of DOX also have imporrtnat role in tracking of micelles in cells thanks to flurosance properties of DOX molecule.

Sum up to, multifunctional doxorubicin-conjugated carrier system with enhanced stability and double moiety pH-sensitivity provide micelles stability and increase drug releasing capacity that also is strengthened by using unused peptide sequence for targeted therapy on HER-2 positive breast cancer (Figure 5). All of them are a new approach in the literature. Three different categorize which are free NCs, free HER-2-NCs, DOX-NCs and DOX-HER-2-NCs were synthesized to determine effects of micelles on SKBR-3 and MCF-10A cells for cytotoxic, apoptotic, and cytostatic effects. For first step, free NCs and free HER-2-NCs were determined to find cytotosic effects on SKBR-3 and MCF-10A. Next, cytotoxic, apoptotic and cytostatic effects of DOX-NCs and DOX-HER-2-NCs were determined on SKBR-3 and MCF-10A. Additionally, the effects of DOX-NCs and DOX-HER-2-NCs were determined on cell viability of co-culture of SKBR-3 and K562 cells.

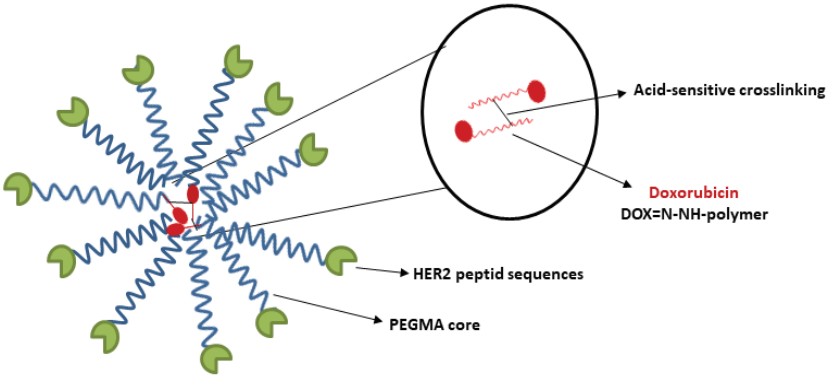

Doxorubicin: Anti-cancer agents, used as chemotherapeutic agents

Figure 1.5. Synthesized multifunctional micelle-based nanocarriers for using our purpose.

Afterward, *in vitro* efficiency of micelles was investigated on HER-2 positive SKBR3 cells and HER-2 negative MCF-10A breast cancer, as well as a co-culture system with SKBR-3 and K562 (HER-2 negative chronic myeloid leukemia). Firstly, the cytotoxic effects on cells lines were determined by using XTT cell proliferation assay and Trypan-blue staining assay. Furthermore, Co-culture of SKBR-3 and K562 highlighted drug selectivity in the same conditions that provide determination of drug efficiency. This approach provided a new perspective before *in vivo* studies. The DOX-HER-2-NCs was more effective on SKBR-3 cells drung co-culture application. So, the using of HER-2 peptide sequence increased drug efficiency on HER-2 positive cells. The uptake of DOX-NCs and DOX-HER-2-NCs on SKBR-3 and MCF-10A cells were determined by using fluorescence microscopy. Besides, the apoptotic effect of nanocarriers is determined by using Annexin-V/PI double staining. Besides, JC-1 mitochondrial potential assay was used to determine loss of mitochondrial membrane potential. Additionally, western blotting also was used to determine Bcl-2, Bax, and Caspase-3 protein levels. Cytostatic effects were determined by using flow cytometry.

The main propose of this project is to minimize the toxicity effect on healthy cells by showing high selectivity to breast cancer. This leads to an increase in the cytotoxic effects of doxorubicin on HER-2 positive breast cancer cells (Figure 6).

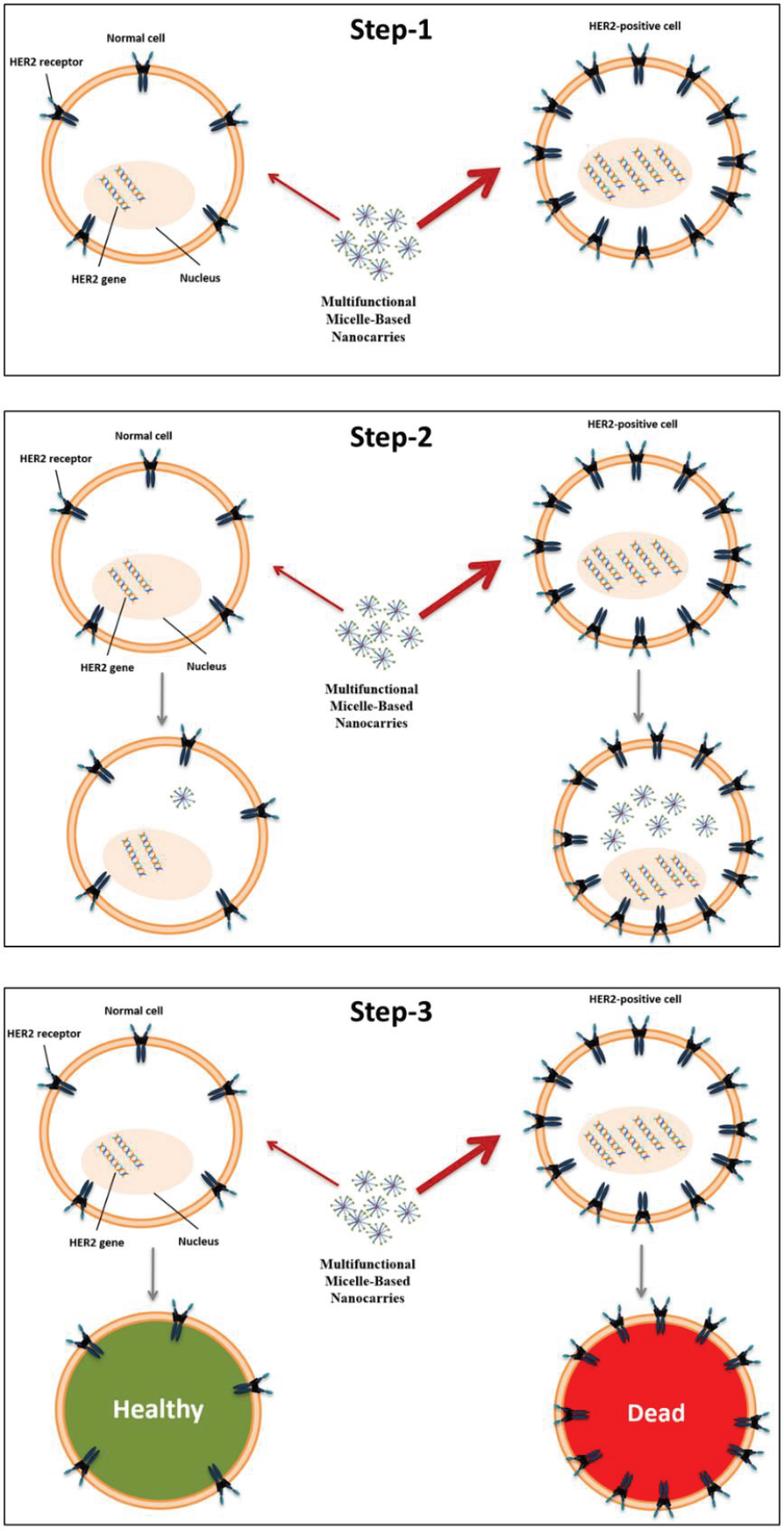

Figure 1.6. The main three steps in our expectation.

CHAPTER 2

MATERIALS & METHODS

2.1 Materials

In this study, different cell lines and chemicals were used to determine effects of multifunctional micelles-based nanocarriers on breast cancer.

2.1.1 Cell Lines

In this study, SKBR-3, MCF-10A, and K562 cell lines were used to determine the effect of NCs.

SKBR-3 is a human mammary gland/breast adenocarcinoma cell line that also is luminal-positive-HER-2. Its culture property is an adherent. This cell line was kindly provided by Prof. Dr. Sevil Dinçer İşoğlu, Abdullah Gül University, Kayseri, Turkey.

MCF-10A is a human mammary gland/breast non-tumorigenic breast cell lines that also is HER2-/-. Its culture property is an adherent. This cell line was kindly provided by Prof. Dr. Ayşe Elif Erson Bensan, Middle East Technical University, Ankara, Turkey.

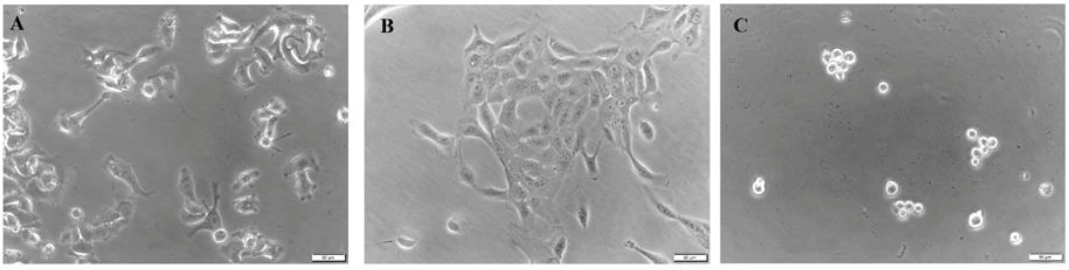

Figure 2.1. SKBR-3 (A), MCF-10A (B), and K562 (C) cell lines, Brightfields, Magnification: 20X.

K562 is chronic myelogenous leukemia (CML) cell line that is also characterized as non-HER2 expression. This cell line was used from our stock in laboratory.

2.1.2 Chemicals

All of the chemicals were used for cytotoxic, apoptotic, and genotoxic assays to determine the effects of multifunctional micelles-based nanocarriers on breast cancer

2.1.3 Cell Culture Chemicals

DMEM high glucose with L-glutamine and sodium pyruvate, Dulbecco's MEM Nutrient Mix F12 (1:1) with L-glutamine and HEPES, penicillin-streptomycin solution 100X, Dulbecco's phosphate buffer saline 10X (PBS), and trypsin-EDTA 1X in PBS were obtained by Euroclone. Fetal bovine serum (FBS) and horse serum were obtained by Gibco.

Epidermal growth factor, hydrocortisone, insulin and cholera toxin (usage permissions received) were obtained Sigma-Aldrich.

2.1.4 Nanocarriers

Different sizes and contents of nanocarriers were synthesized by Prof. Dr. Sevil Dinçer İşoğlu and her Ph.D. candidate, Nazende Nur Akşit. The physicochemical characterization of these nanocarriers was determined by Prof. Dr. Sevil Dinçer İşoğlu and Nazende Nur Akşit.

The size of NCs was determined by using Dynamic Light Scattering (DLS) by Nazende Nur Akşit.

All experiments were conducted with NCs-1 because their size is suitable for cell application. However, the effects of NCs-2 size on SKBR-3 and MCF-10A cells were determined.

Table 2.1 Different types of nanocarriers which were applied on cells to determine the effect of size of nanocarriers on breast cancer cells.

Nanocarrier	Size
Free NCs-1	80nm
Free HER-2-NCs-1	160nm
Free-NCs-2	115nm
HER-2-NCs-2	200nm
DOX-NCs-1	81nm
DOX-HER-2-NCs-1	134nm

2.1.5 Cell Proliferation and Viability Assay

XTT Cell Proliferation Assay Kit (Roche) and Trypan Blue powder dye were obtained from Sigma-Aldrich. Thermo ELECTRON CORPORATION Multiskan Spectrum was used for colorimetric analysis. Neubauer slide from MARIENSUPERIOR GERMANY was used to count viable cells.

2.1.6 Fluorescence Imaging

Paraformaldehyde (PFA) powder was obtained from Sigma-Aldrich. 4',6-Diamidino-2-Phenylindole, Dihydrochloride (DAPI) powder dye was obtained from Invitrogen™. Olympus-IX83 Fluorescence microscopy was used for microscopy studies.

During this step, the image was taken at the same exposure time to compare each image. Next, the ImageJ and FIJI programs were used for image processing.

2.1.7 Apoptosis Assay

Annexin V/PI dual staining apoptosis assay kit was provided by Biolegend. Flow cytometry was used for apoptosis and necrosis analysis.

JC-1 mitochondrial membrane potential assay kit was obtained from Cayman Chemical. Thermo ELECTRON CORPORATION Multiskan Spectrum was used for analysis.

2.1.8 Western Blotting

The expression level of apoptosis-related proteins was determined by Western Blotting.

2.1.9 Protein Isolation

Tris Buffer, which is called as cell lysis buffer was prepared by using 10mM Tris-HCl, 1mM EDTA, and 0.1% Triton-X.

2.1.10 Determination of Protein Concentration by BCA Assay

SMART™ BCA Protein Assay Kit (INtRON BIOTECHNOLOGY) was used to determine protein concentration.

2.1.11 Polyacrylamide Gel Electrophoresis (SDS-PAGE)

2-Mercaptoethanol, 4X Laemmli Sample Buffer, Mini PROTEAN® 3 System-Glass Spacer & Short Plates, 10X TGS (Tris/Glycine/SDS Buffer), 10X TBS (Tris-buffered saline), TGX Stain-Free™ FastCast™ Acrylamide Kit (10%), Prestained Protein SHARPMASS™ VI Protein MW marker, Trans-Blot® Turbo™ RTA Transfer Kit-PVDF(Mini-size Transfer Stacks and Mini-size PVDF membrane), Clarity™ Western ECL Substrate, TWEEN® 20, Trans-Blot® Turbo™ Transfer System, Mini PROTEAN® Tetra Cell System was obtained from BIO-RAD.

2.1.12 Transfer of Proteins from Gel to Membrane

1X Transfer Buffer was prepared by using TrisX, Glycine, and methanol. Trans-Blot® Turbo™ RTA Transfer Kit-PVDF and Trans-Blot® Turbo™ Transfer System were taken from BIO-RAD**.**

2.1.13 Detection of Desired Proteins by Specific Antibodies

ab32124-Anti-Bcl-2 antibody (E17), ab32503- Anti-Bax antibody (E63), ab184787- Anti-Caspase-3 antibody, ab9485- Anti-GAPDH antibody (Loading control), ab205718 Goat Anti-Rabbit IgG (HRP) was obtained from Abcam.

Clarity^{TM} Western ECL Substrate was taken from BIO-RAD.

FUSION SL VILBER LOURMAT imaging system is used for determination of protein bands.

2.1.14 Cell Cycle Assay

Triton X-100 was obtained from AppliChem. RNase-A, pancreas was obtained from Biomatik. Propidium iodide was obtained from Biolegend. Flow cytometry was used for the determination of the different cell cycle phases.

2.2 Methods

The cytotoxic, apoptotic, and genotoxic assays were used to determine the effects of multifunctional micelles-based nanocarriers on breast cancer

2.2.1 Maintenance of Cell Lines

In this study, SKBR-3, MCF-10A, and K562 cells cell lines were used. SKBR-3 cell lines and MCF-10A cell lines were used to compare the targeting efficiency of synthesized NCs separately. In addition to that, SKBR-3 and K562 cell lines were co-cultured that is important to determine the targeting efficiency of synthesized NCs in the same condition. Besides, co-culture application was brightened preliminary of *ex-vivo* evaluation and expectation of *in vivo* results.

Each cell lines were grown in different cell culture medium. These medium contents were shown at Table 2.2 and Table 2.3.

2.2.1.1 Preparation of Cell Culture Medium

SKBR-3, MCF-10A, and K562 cells were grown in different cell culture mediums. These mediums are indicated in the following table.

Table 2.2. The contents of DMEM high glucose with L-glutamine and sodium pyruvate.

Medium Contents	Rate of Content
Fetal Bovine Serum	10%
Penicillin/Streptomycin	1%

SKBR-3 and K562 cells were grown in DMEM high glucose with L-glutamine, sodium pyruvate, fetal bovine serum, and Penicillin/Streptomycin (Table 2).

Table 2.3. The contents of Dulbecco's MEM Nutrient Mix F12 (1:1) with L-glutamine and HEPES.

Medium Contents	Final Concentration or Rate of Content
Horse Serum	5%
Penicillin/Streptomycin	2Mm
Epidermal Growth Factor (EGF)	20 ng/ml
Hydrocortisone	0.5 µg/ml
Insulin	10 µg/ml
Choleratoxin	100 ng/ml

MCF-10A cells were grown in Dulbecco's MEM Nutrient Mix F12 (1:1) with L-glutamine, HEPES, horse serum, Penicillin/Streptomycin, EGF, hydrocortisone, insulin, and cholera toxin (Table 3).

DMEM high glucose with L-glutamine, sodium pyruvate, fetal bovine serum, and Penicillin/Streptomycin was prepared in 50ml falcon tube. Besides, Dulbecco's MEM Nutrient Mix F12 (1:1) with L-glutamine, HEPES, horse serum, Penicillin/Streptomycin, EGF, hydrocortisone, insulin, and cholera toxin was prepared in 500ml bottle.

2.2.1.2 Sterilization of the Materials

Before cell passage, all tips, glassware, distilled pure water (dH_2O) and ultra-pure water (ultra-dH_2O) were sterilized by autoclave at the special condition (Table 4).

Table 2.4. The type of sterilization types and their condition.

Type of sterilization	Temperature	Time
Tips and glassware	121 ^oC	20 minutes
dH_2O and ultra-dH_2O	121 ^oC	15 minutes

2.2.1.3 Thawing of Frozen Cell Lines

Cells were removed from -86^oC and were quickly defrosted in 37 ^oC water bath. As soon as ice crystals melted, the cells were taken into sterile falcon tube and fresh cell culture medium was added. Next, the falcon tubes were centrifuged at 600 rpm for 5 minutes. After centrifugation, the supernatant was removed, and the pellet was dissolved in 5 ml fresh medium. Lastly, the cells were put in 25 cm^2 flask. Generally, the cells were ready to use in the experiment after 3 passages.

2.2.1.4 Freezing of Cell Lines

Firstly, Mix1 and Mix2 solution were prepared for this step. The contents of these solution are shown at the following table (Table 5-6).

Table 2.5. The contents and the percentage of contents in cell freezing Mix1 medium.

Mix1 Contents	The percentage of contents
Fresh pure cell culture medium	60%
FBS	40%

Table 2.6. The contents and the percentage of contents in cell freezing Mix2 medium.

Mix2 Contents	The percentage of contents
Fresh pure cell culture medium	80%
DMSO	20%

The cells were frozen to use further studies. For this thesis, two different characterized cell lines, adherent and suspended cells, were used. For adherent cell lines (SKBR-3 and MCF-10A), the cell culture medium was removed and washed with 1X PBS. Then, 2ml trypsin-EDTA was added in 75 cm^2 flask and incubated in CO_2 incubator at 37 ^oC. After that, cells were collected with the 4ml medium in a falcon tube and were centrifuged at 600 rpm for 5 minutes. After centrifugation, the supernatant was removed, and the pellet was dissolved with 500µl of Mix1 solution as $2x10^6$ cells/cryogenic vial. Then, 500µl of Mix2 solution was added drop by drop in the cryogenic vial. After this application, these vials were put in the special box that contains isopropanol to protect the cells from having damaged. After one day, these vials were transferred in cryogenic box.

2.2.2 Determination of Cytotoxic Effect of NCs On Cells

The cytotoxic effect of NCs on SKBR-3 and MCF-10A were determined by XTT assay and trypan-blue staining. These two applications were based on cell proliferation and cell viability, respectively. In addition to that, their effects were determined in co-culture of SKBR-3 and K562 cell lines with trypan-blue staining.

2.2.2.1 XTT Cell Proliferation Assay

XTT assay from Roche (Cat. No. 11465015001, Roche) is a colorimetric assay that is used for quantification of cell growth, cell viability, and cytotoxicity.

Each types of cells were seeded differently because of their cell growth and doubling time. 5000 cells/well for SKBR-3 and 2000 cells/well for MCF-10A in 100µl

of medium were seeded in 96-well plate. After 24 hours, the different concentration of NCs were added in 4 replicated wells for each concentration value of NCs. After 48 hours and 72 hours, XTT labeling reagent: electron-coupling reagent were prepared as 50:1 dilution rate. Then, 50µl prepared XTT solution was added into each well. Next, 96-well plate was incubated in an incubator at 37 ^{o}C, %5 CO_2 for 6 hours. Finally, the formation of orange formazan dye was detected at 450nm with spectrometry from Thermo ELECTRON CORPORATION Multiskan Spectrum.

For determination of cytotoxic effects of NCs on cells, the wide range of NCs concentrations (1ng/ml, 5 ng/ml, 10 ng/ml, 50 ng/ml, 100 ng/ml, 500 ng/ml, 1 µg/ml, 10 µg/ml, 20 µg/ml, 50 µg/ml, 100 µg/ml) were applied on to the cells. According to the first result, the second and third replication were continued by 0.1 µg/ml, 1 µg/ml, 10 µg/ml, 100 µg/ml different size of NCs that consisted of free micelles and free micelles conjugated with HER-2 peptide. After this application, cytotoxicity of only Doxorubicin (DOX) was determined at 0.1 µM, 0.5 µM, 1 µM, 2 µM and 5 µM for SKBR-1 and 0.05 µM, 0.1 µM, 0.25 µM, and 1 µM for MCF-10A that was based on literature search. The efficiency of micelles which were DOX-loaded micelles and DOX-loaded micelles conjugated with HER-2-peptide were applied at 0.05 µM, 0.1 µM, 0.25 µM, and 1 µM doses.

2.2.2.2 Trypan Blue Staining-Cell Viability Assay

Trypan-blue dye (Sigma-Aldrich) is known as the dye exclusion method. This method was used to distinguish live and dead cells to quantify cell viability.

2.2.2.3 Trypan Blue Staining for SKBR-3 and MCF-10A cells

30.000 cells/well for SKBR-3 and 10.000 cells/well for MCF-10A in 500µl/well medium were seeded in 24-well plate. After 24 hours, the different concentration of micelles were added in 3 replicated wells for each concentration value of micelles. After 48 hours and 72 hours, the medium on cells was discharged and washed with 500µl/well 1X PBS. Next, 500µl/well trypsin-EDTA was added and incubated for 10-15 minutes. 500µl/well medium was added and suspended with pipetting. The 30µl medium was

added in 30µl trypan blue dye. Lastly, a 10µl mixture of trypan blue dye and cells were inoculated in Neubauer slide from MARIEN$_{\text{SUPERIOR GERMANY}}$ and collected number of live cells under the microscope (Carl Zeiss-12V DC 30W).

2.2.2.4 Trypan Blue Staining for co-cultured SKBR-3 and K562 cells

30.000 cells/well for SKBR-3 and 30.000 cells/well for K562 in 500µl/well medium were seeded in 24-well plate separately. After 24 hours, the medium on SKBR-3 was discharged and K562 cells are added in each well. The different concentration of NCs was added in 3 replicated wells for each concentration value of NCs. After 48 hours and 72 hours, the medium on cells was discharged and washed with 500µl/well 1X PBS. Next, 500µl/well trypsin-EDTA was added and incubated for 10-15 minutes. 500µl/well medium was added and suspended with pipetting. The 30µl medium was added in 30µl trypan blue dye. Lastly, a 10µl mixture of trypan blue dye and cells were inoculated in Neubauer slide from MARIEN$_{\text{SUPERIOR GERMANY}}$ and collected number of live cells under the microscope (Carl Zeiss-12V DC 30W).

2.2.3 Observation of Intracellular NCs Update

The taken DOX-loaded NCs and DOX-loaded NCs conjugated with peptide were determined by fluorescence microscopy (Olympus-IX83). Next, the fluorescence intensity density and co-localization analysis were determined by using Image-J and Fiji image processing programs, respectively.

2.2.3.1 Fluorescence Imaging (DAPI & DOX)

Firstly, the sterilized coverslip was placed on each well of the 6-well plate. 250.000 cells/well for SKBR-3 and 150.000 cells/well for MCF-10A in 500µl/well medium were seeded in a 6-well plate separately. After 24 hours, IC50 dose of DOX-loaded NCs and DOX-loaded NCs conjugated with peptide were added in well. After 48 hours, the medium on cells was aspirated and washed with 2ml/well 1X PBS twice. Next, 2ml/well 3.7% paraformaldehyde (PFA) was added and incubated for 20 minutes. After incubation, PFA on cells was discharged and washed with 2ml/well 1X PBS twice. Then,

1:500 DAPI (stock 5mg/ml) was added in each well and incubated at 30 minutes. A coverslip was placed on a slide. Lastly, slides were stored at 4 ^{o}C refrigerator overnight.

The 10 different images were taken at Alexa-555 for 210.5 ms. Then, image analysis based on fluorescence intensity density was done by using Image-J program. Also, 3 different images were taken at DOX and DAPI fluorescence. The co-localization values were determined by the Fiji program.

2.2.4 Determination of Apoptotic Effects of Micelles on Cells

In this study, the apoptotic effect of micelles on SKBR-3 and MCF-10A were determined by using Annexin V/PI dual staining apoptosis assay and JC-1 mitochondrial membrane potential assay. The viable, apoptotic and necrotic cells were shown by using Annexin V/PI dual staining apoptosis assay and the apoptotic cells also were shown by using JC-1 mitochondrial membrane potential assay that is based on the measurement of loss of mitochondrial membrane potential.

2.2.4.1 Annexin V/PI Double Staining Apoptosis Assay

Annexin V/PI Dual Staining Apoptosis Assay from BioLegend (Lot: B196507) is a fluorometric assay that was used to identify apoptotic and necrotic cells.

$5x10^5$ cells/well/2ml medium of SKBR-3 were seeded in 6-well plate. After 24 hours, IC50 and IC70 doses of DOX-NCs and DOX-HER-2-NCs were applied onto cells and incubated in CO_2 incubator at 37 ^{o}C, %5 CO_2 for 24 and 48 hours. After incubation, the medium was collected in falcon tubes. 1ml Trypsin-EDTA was added to each well. After incubation with Trypsin-EDTA, 4ml of medium was added in each well and collected in a falcon tube. Next, the cells were centrifuged at 800 rpm for 5 minutes. After centrifugation, the supernatant was removed, and the pellet was dissolved with 1X PBS. Then, the cells were centrifuged at 1000 rpm for 5 minutes. This step was replicated two times. The pellet was then dissolved with 200µl/well Annexin Binding Buffer (ABB). 2µl FITCH or/and 2µl PI were added according to Figure 7. The tubes were incubated at room- temperature for 15 minutes. Finally, apoptotic or necrotic cells were detected with flow cytometry.

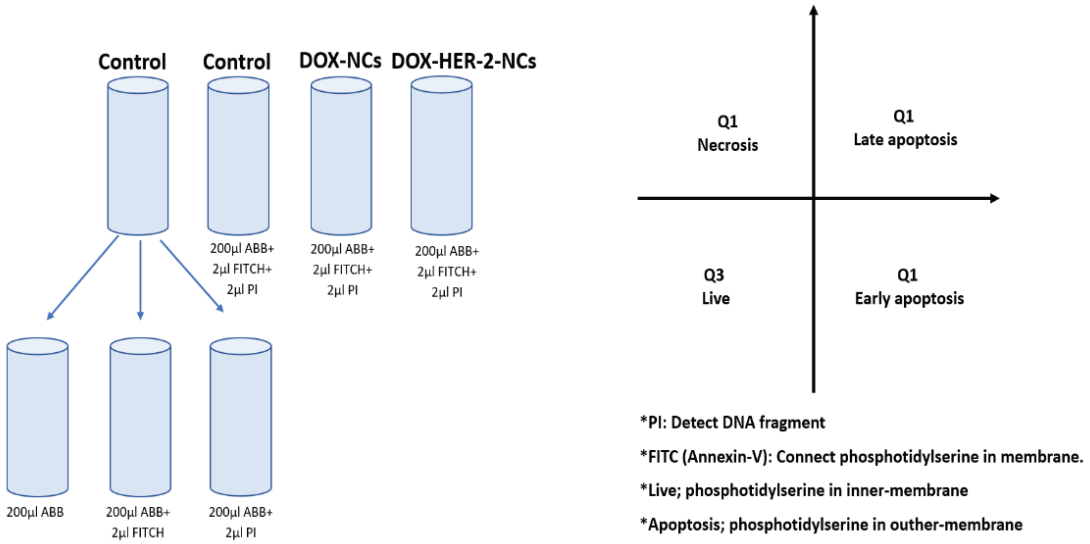

Figure 2.2. Annexin V/PI dual staining apoptosis assay application step and determination of quadrants.

2.2.4.2 JC-1 Mitochondrial Membrane Potential Assay

JC-1 Mitochondrial Membrane Potential Assay was obtained from Cayman (Cat. No. 10009172) and was used to determine the loss of mitochondrial membrane potential. JC-1 dye is known as a lipophilic, cationic, and fluorescent dye.

Before this step, the JC-1 Assay Buffer was prepared by dissolving 1 tablet in 100ml distilled water. Next, 1X JC-1 staining solution was prepared with culture medium.

5.000 cells/well of SKBR-3 in 100µl medium were seeded in 96-well plate. After 24 hours, the different concentration of micelles (DOX-NCs and DOX-HER-2-NCs) were added in 3 replicated wells for each concentration value of micelles. After 48 hours, 10µl/well of 1X JC-1 staining solution was added and incubated in an incubator at 37 ºC, %5 CO_2 for 20 minutes. After incubation, cells were centrifuged at 1000 rpm for 5 minutes. After centrifugation, the supernatant was removed, and the pellet was dissolved with 200µl of JC-1 assay buffer were added in each well. This step was replicated two times. Finally, JC-1 dye was detected at 535-595nm and 485-535nm with spectrometry from Thermo ELECTRON CORPORATION Multiskan Spectrum.

2.2.4.3 Western Blotting

This assay was used to identify expression level of specific proteins. In this study, the protein levels of Bcl-2, Bax, Caspase-3, and GAPDH were determined by western blotting.

2.2.4.3.1 Cell Lysis

$5x10^5$ cells/well/2ml medium of SKBR-3 were seeded in 6-well plate. After 24 hours, IC50 doses of micelles (DOX-NCs and DOX-HER-2-NCs) were added in cells and incubated in CO_2 incubator at 37 ^oC, %5 CO2 for 48 hours. After incubation, the medium was collected in falcon tubes. 1ml Trypsin-EDTA was added in each well. After incubation with Trypsin-EDTA, 4ml medium was added in each well and collect in a falcon tube. Next, the cells were centrifuged at 800 rpm for 5 minutes. After centrifugation, the supernatant was removed and the pellet was dissolved with 5ml of 1X PBS. Again, the cells were centrifuged at 800 rpm for 5 minutes. After centrifugation, 150µl of cell lysis buffer was added for each tube. They were centrifuged at 14.000 rpm for 20 minutes. After centrifugation, the supernatant (protein samples) was collected a new tube.

2.2.4.3.2 BCA Assay

BCA assay consists of two main steps which are the preparation of standards and working solution. 2.0 mg/ml BSA solution was found in SMART^{TM} BCA Protein Assay Kit. Different concentrations of protein standards were prepared to a determined protein concentration of a working solution (Table 7).

Working Solution (WS) was prepared by mixing 50:1, Solution A: Solution B. Then, 25 µl of each standards and unknown samples were put into a microplate well. Next, 200 µl of the Working Solution (WS) was added into each well and mixed by plate shaker for 30 seconds. Plate was incubated at 37°C for 30 minutes. Next, plate was cooled to room temperature. Finally, the absorbance of solution was measured at 562nm on spectrometry.

Table 2.7. Preparation of Diluted Albumin (BSA) Standards.

Tube	The volume of Diluent (µl)	Volume and Source of BSA	Final Concentration
1	0	300 µl of Stock	2,000 µg/ml
2	125	375 µl of Stock	1,500 µg/ml
3	325	325 µl of Stock	1,000 µg/ml
4	325	325 µl of tube 3 dilution	500 µg/ml
5	325	325 µl of tube 4 dilution	250 µg/ml
6	325	325 µl of tube 5 dilution	125 µg/ml
7	400	100 µl of tube 6 dilution	25 µg/ml
8	400	0	0 µg/ml

The protein concentrations of all unknowns were adjusted to the standard concentration before mixing with 2-Mercaptoethanol and 4X Laemmli Sample Buffer so that the final concentration of protein is the same for all samples. The mixture was incubated at 95 ºC for 10 minutes.

Acrylamide gel was prepared by using TGX Stain-FreeTM FastCastTM Acrylamide Kit (10%). This kit consists of resolver solution A, stacker solution A, resolver solution B, stacker solution B, %10 APS (ammonium persulfate), and TEMED. Firstly, 3ml resolver solution A and 3ml resolver solution B, 30 µl of %10 APS, and 3 µl of TEMED was mixed and loaded between glasses. After polymerization, 1ml stacker solution A and 1ml stacker solution B, 10 µl of %10 APS, and 2 µl of TEMED was mixed and loaded between glasses. 30 µl of samples were loaded into the wells. 4 µl of Standards (Prestained Protein SHARPMASS^{TM} VI Protein MW marker) were used in our studies as markers. The samples were run at 90 Volt and 19 Amper until the dye run off bottom of the gel (~ 1.5 hours).

2.2.4.3.3 Transfer of Proteins from Gel to Membrane

Proteins were transferred from 10% acrylamide gel to PVDF membrane. The membrane was wetted with methanol for 10 minutes, rinsed with dH2O and finally washed with 20% of methanol in 1X Transfer Buffer. Two pieces of transfer stacks were

washed with 20% of methanol in 1X Transfer Buffer. Next, the "sandwich" was assembled as 7 pieces of transfer stacks-gel-PVDF membrane-7 pieces of transfer stacks by using the Trans-Blot® TurboTM Transfer System for 25V, 2.5 Amper, and 17 minutes. When the transfer was finished, the membrane was immersed in 5% BSA solution at room temperature for 1 hour.

After incubation, BSA solution was removed and the prepared primary antibody solution was added at 4ºC for overnight. At the end of the primary antibody binding, 5 mL of 1% Tween in 1X TBS Buffer was added onto the membrane and incubated for 10 min at room temperature for three times. The buffer was replaced with BSA solution containing secondary antibody and incubated for 1 h at room temperature. At the end of the secondary antibody binding, 5 mL of 1% Tween in 1X TBS Buffer was added onto the membrane and incubated for 10 min at room temperature for three times. After removing all the buffers, the membrane was incubated with Clarity^{TM} Western ECL Substrate for 5 minutes. A membrane was exposed automated program by using FUSION SL VILBER LOURMAT imaging system.

Table 2.8. The using antibodies in determination of apoptotic protein.

Name of Antibody	Prepared solution type	Dilution rate
Bcl-2 (Primary Antibody)	%5 BSA in TBS-Tween	1:1000
Bax (Primary Antibody)	%5 BSA in TBS-Tween	1:1000
Caspase-3 (Primary Antibody)	%5 BSA in TBS-Tween	1:2000
GAPDH (Loading control)	%5 BSA in TBS-Tween	1:2500
IgG (Secondary Antibody)	%5 BSA in TBS-Tween	1:3000

2.2.5 Determination of Cytostatic Effect of Micelles on Cells

In this study, the cytostatic effect of micelles on SKBR-3 and MCF-10A were determined by using cell cycle assay. This method was used to show cell cycle arrest or cell growth/survival in stages of the cell cycle, which are G1, S, and G2. The using cell cycle analysis provided to determine cell cycle arrest after drug application to understand effect mechanism of drug on cell cycle of SKBR-3.

2.2.6 Cell Cycle Analysis with using Propidium Iodide Staining

Cell cycle analysis depends on the quantitation of DNA content in cells. For this purpose, propidium iodide (PI) which is DNA-binding dye was used to measure a fluorescent intensity in G0/G1, S, and G2/M phases.

$5x10^5$ cells/well/2ml medium of SKBR-3 were seeded in 6-well plate. After 24 hours, IC20, IC50, and IC80 doses of micelles (DOX-NCs and DOX-HER-2-NCs) were added in cells and incubated in CO_2 incubator at 37 ^oC, 5% CO2 for 48 hours. After incubation, the medium was collected in falcon tubes. 1ml Trypsin-EDTA was added in each well. After incubation with Trypsin-EDTA, 4ml medium was added in each well and collect in a falcon tube. Next, the cells were centrifuged at 800 RPM for five minutes. After centrifugation, the supernatant was removed and the pellet was dissolved with 1ml of cold 1X PBS and placed in the icebox for 15 minutes. Next, 4 ml of (-20^{o}C) 100% Ethanol was added and waited in the refrigerator at -20^{o}C overnight. Next, the cells were centrifuged at 800 rpm for 5 minutes. After centrifugation, the supernatant was removed and the pellet was dissolved with 1ml of cold 1X PBS. Again, the cells were centrifuged at 800 RPM, 5 minutes. After centrifugation, the supernatant was removed and the pellet was dissolved with 1 ml of 1X PBS-(0.1%) Triton X 100. Next, 100 µl RNase-A was added and incubated at 37^{o}C for 30 minutes. After incubation, 100 µl PI was added and incubated at room temperature for 10 minutes. Finally, the different phases of the cell cycle was detected with flow cytometry in IZTECH-BIOMER.

2.2.7 Image Processing and Statistical Analysis

In this study, Image J and Fiji programs were used to determine fluorescence intensity density and co-localization analysis, respectively. Additionally, the GraphPad Prism 7 program was also used for the draw all graphs and statistical analysis.

R-total value represents co-localization value. If it is closed to “1”, two different images from different fluorescence wavelengths are co-localized and determined by Pearson's correlation coefficient.

Statistical analysis was done using t-test, $p<0.05$:*; $p<0.01$:**; $p<0.001$:*** were considered significant. The error bars represent the standard deviations.

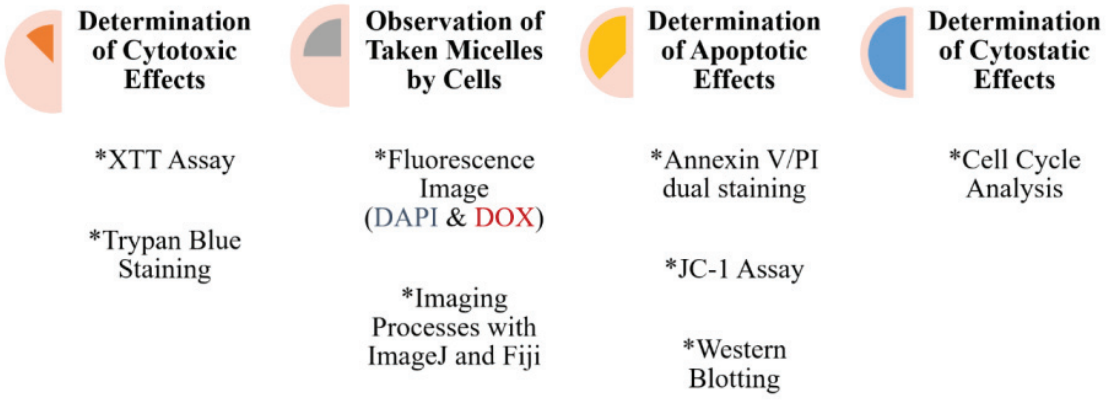

Figure 2.3. Experimental flow chart for this project.

CHAPTER 3

RESULTS & DISCUSSIONS

3.1 Free NCs and free HER-2-NCs did not affect cell proliferation of SKBR-3 and MCF-10A cells

The cytotoxic effects of free-NCs and HER-2-NCs on SKBR-3 and MCF-10A was explored by step-wise increasing concentrations (0.1- to 100 μg/ml) of both NCs at 48 and 72h.

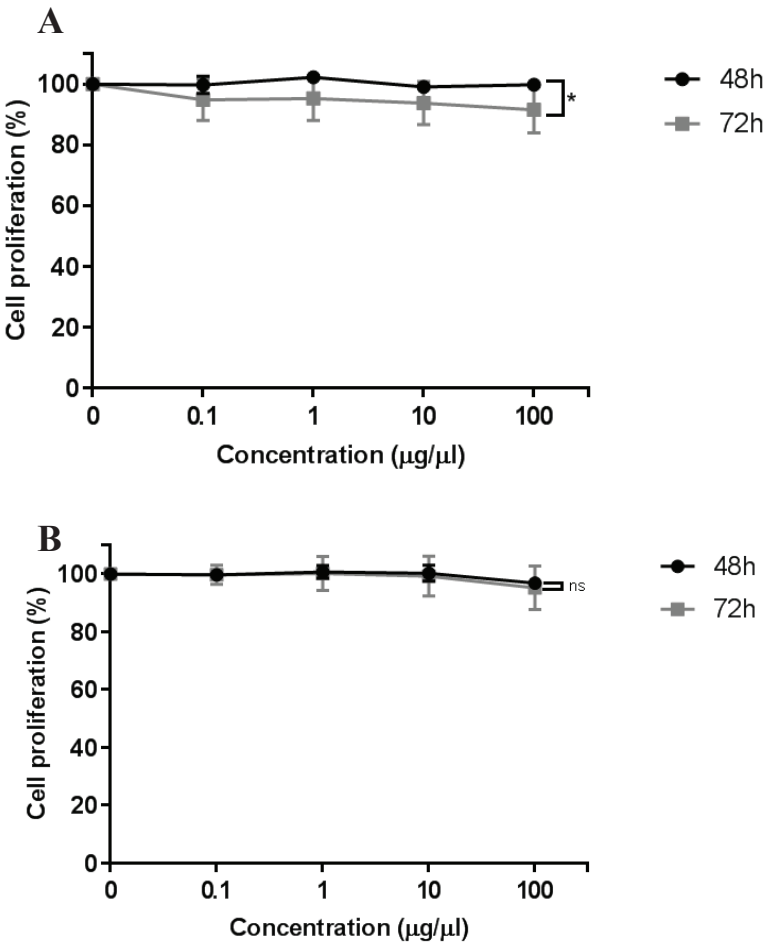

Figure 3.1. Cytotoxic effects of free NCs on cell proliferation of SKBR-3 (A) and MCF-10A (B) cells at 48- and 72h.

Cytotoxic effects of free NCs on SKBR-3 cells were determined by XTT cell proliferation assay. Experiments were conducted in triplicate in at least three independent experiments, and statistical analysis was done using paired t-test, and $p<0.05$:*; $p<0.01$:**; $p<0.001$:*** were considered significant. The error bars represent the standard deviations. The error bars are not seen when they are smaller than the thickness of the lines on the graphs (Figure 3.1).

As shown in Figure 3.1A, SKBR-3 cells continued to survive upon exposure to free NCs which were referred to that free NCs did not exhibit cytotoxic properties at both 48- and 72h. Besides, there was no significant change as compared to both control-trails. However, comparison of 48- and 72h application had significant change, but cell proliferation is approximately 80-90% that was shown non-toxicity.

In Figure 3.1B, exposure of free NCs on MCF-10A cells did not exhibit cytotoxic properties at both 48- and 72h. Besides, there was no significant change as compared to both control-trails and 48- and 72h. According to the comparison of Figure 3.1A and Figure 3.1B, free NCs cause similar effects on both SKBR-3 and MCF-10A cells.

Next, Figure 3.2A demonstrated the effect of free HER-2-NCs on SKBR-3 cells which did not exhibit cytotoxic properties at both 48- and 72h that is similar to free NCs. Besides, there was no significant change as compared to both control-trails and 48- and 72h.

Additionally, Figure 3.2B showed that MCF-10A cells were also grown upon exposure to free HER-2-NCs. The results showed that there were no significant cytotoxic effects on MCF-10A at 48- and 72h that were also similar to free NCs.

Overall, the free NCs and conjugation of HER-2 peptide sequence on NCs did not induce cytotoxicity on cells. Additionally, this property supports the advantage of nanocarriers which is biocompatible. This point also provided to controlling cytotoxicity effects of DOX on cancer cells that also formed by releasing of DOX on cells.

After this determination, the effect of size of nanocarriers was identified by using cell proliferation assay. Also, the physicochemical characterization of nanocarriers has an important role in cellular processes.

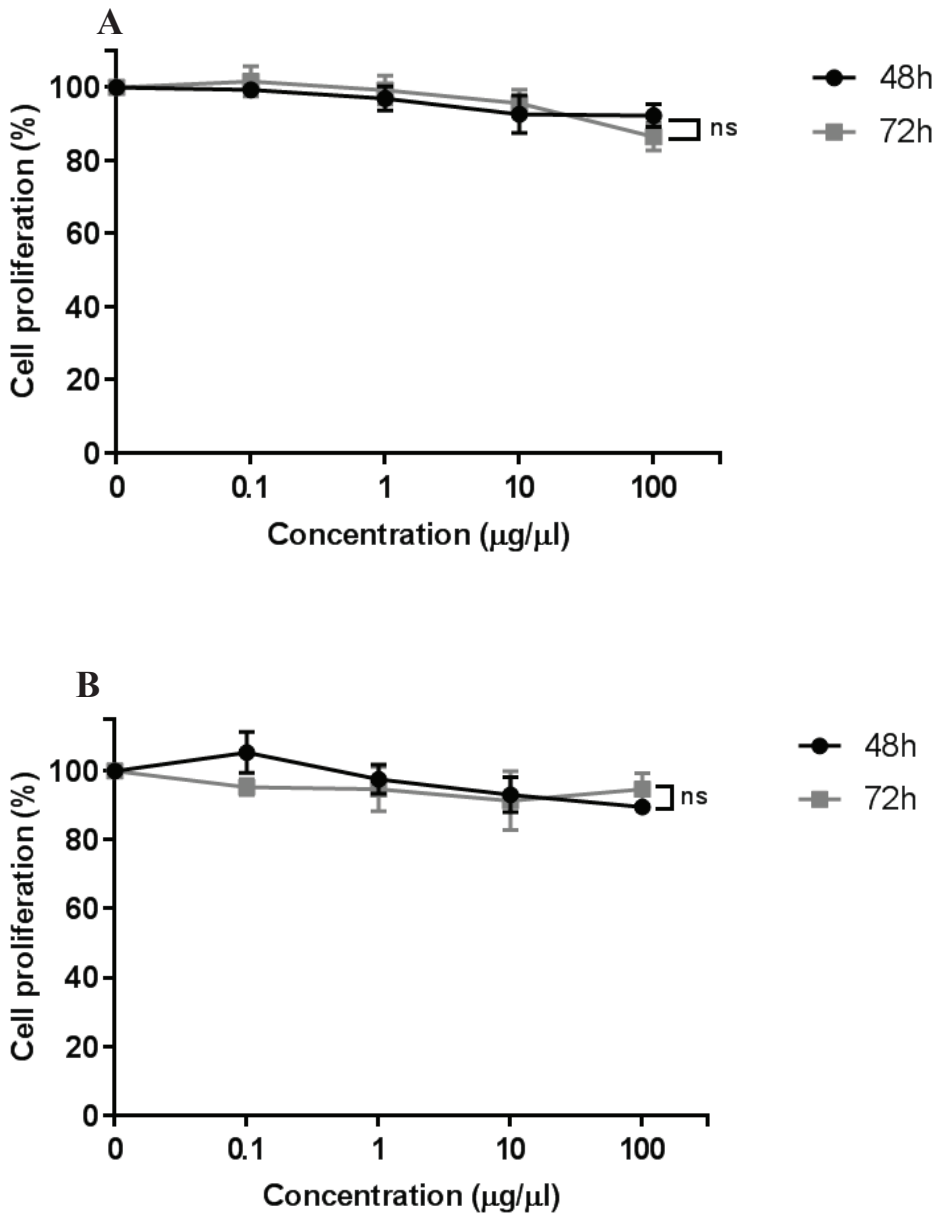

Figure 3.2. Cytotoxic effect of free HER-2-NCs on cell proliferation of SKBR-3 (A) and MCF-10A (B) cells at 48- and 72h.

Cytotoxic effects of free HER-2-NCs were determined by XTT cell proliferation assay for SKBR-3. Experiments were done in triplicate in at least three independent experiments, and statistical analysis was done using paired t-test, $p<0.05$:*; $p<0.01$:**; $p<0.001$:*** were considered significant. The error bars represent the standard deviations. The error bars are not seen when they are smaller than the thickness of the lines on the graphs (Figure 3.2)

3.2 Increasing size of free NCs and free HER-2-NCs did not affect cell proliferation of SKBR-3 and MCF-10A cells significantly

The cytotoxic effects of higher size of free-NCs-2 and HER-2-NCs-2 on SKBR-3 and MCF-10A cells was explored by step-wise increasing concentrations (0.1- to 100 μg/ml) of both NCs at 48- and 72h.

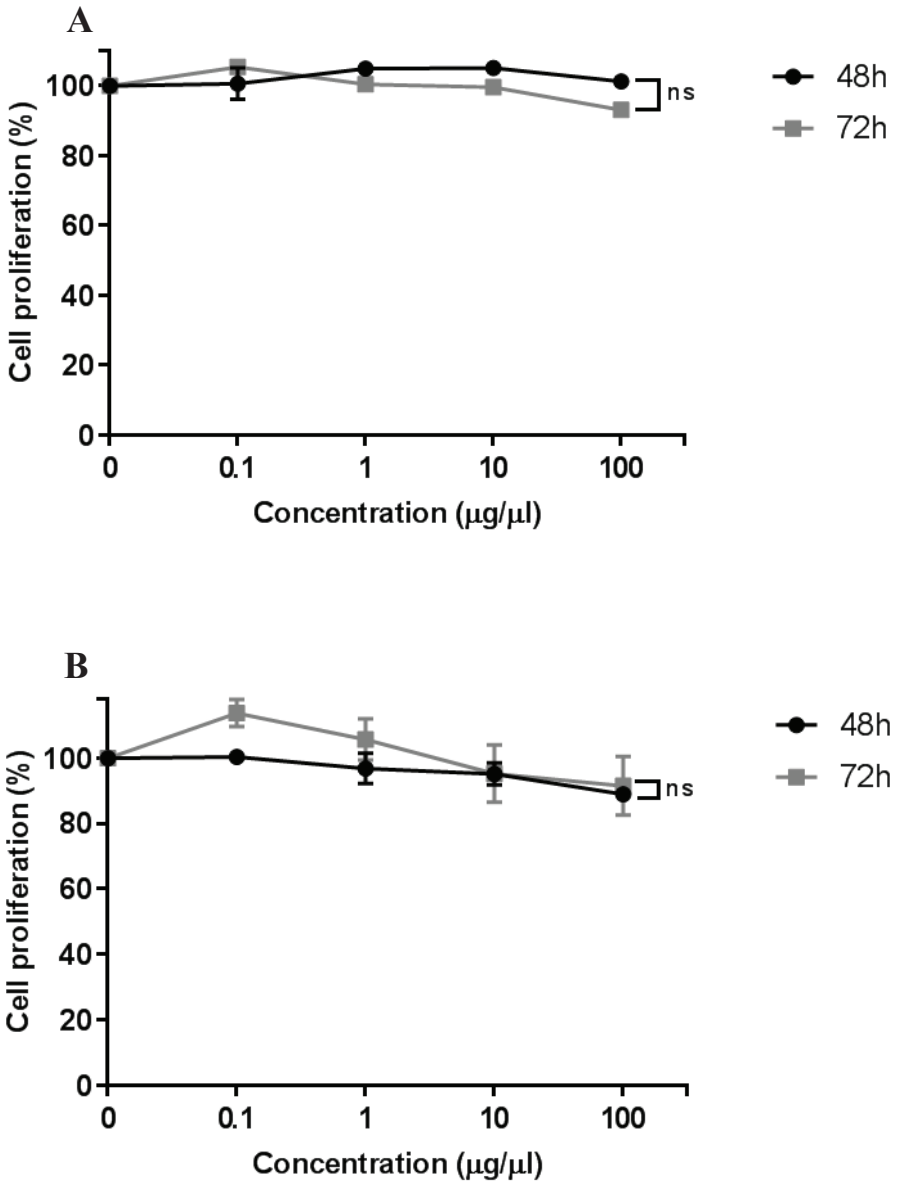

Figure 3.3. Cytotoxic effects of free NCs-2 on cell proliferation of SKBR-3 (A) and MCF-10A (B) cells at 48- and 72h.

Cytotoxic effects of second free NCs-2 were determined by XTT cell proliferation assay for SKBR-3 and MCF-10A cells. Experiments were done in triplicate in at least three independent experiments, and statistical analysis was done using paired t-test, $p<0.05$:*; $p<0.01$:**; $p<0.001$:*** were considered significant. The error bars represent the standard deviations. The error bars are not seen when they are smaller than the thickness of the lines on the graphs (Figure 3.3).

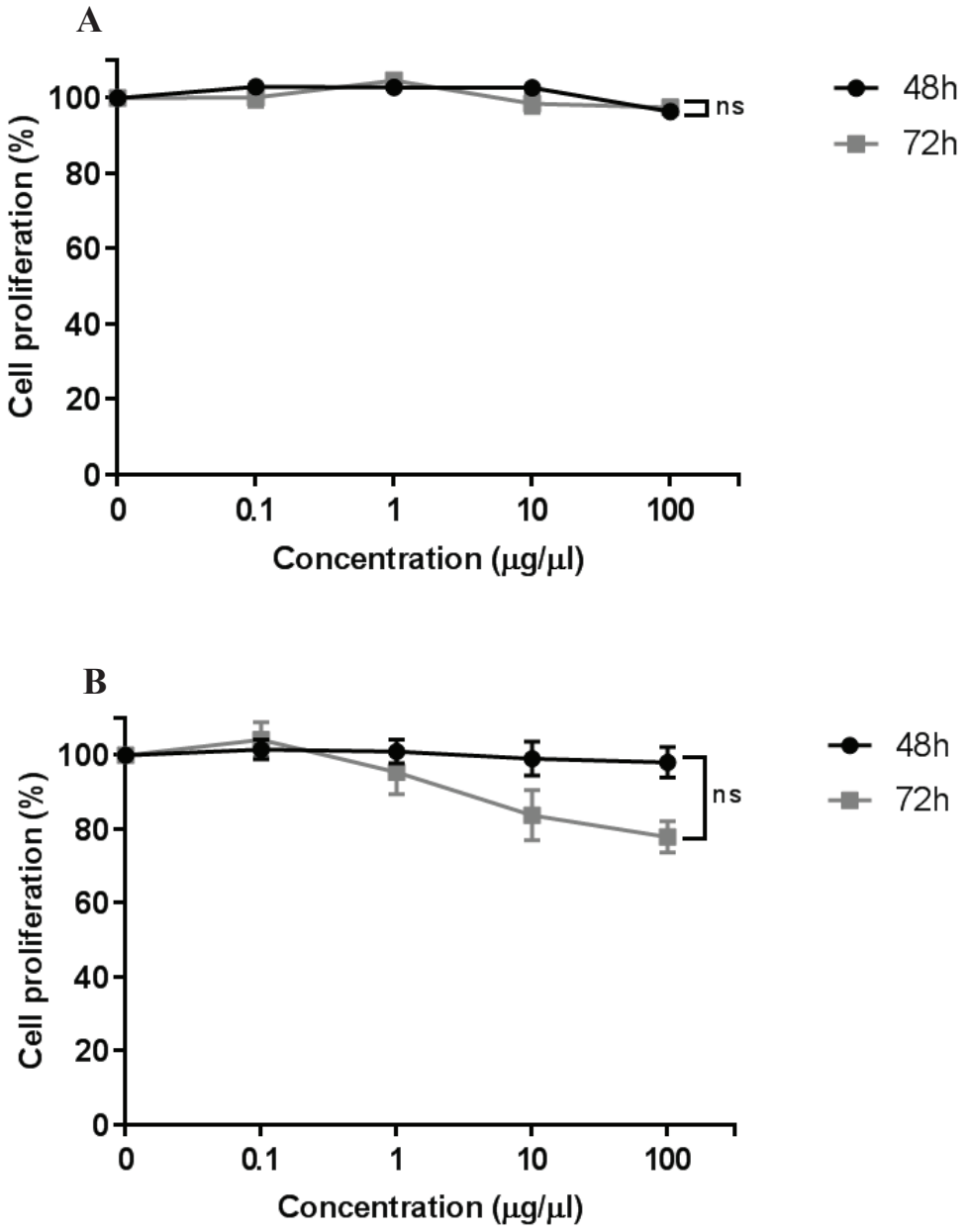

Figure 3.4. Cytotoxic effects of free HER-2-NCs-2 on cell proliferation of SKBR-3 (A) and MCF-10A (B) cells at 48- and 72h.

Cytotoxic effects of second free NCs-2 were determined by XTT cell proliferation assay for SKBR-3. Experiments were done in triplicate in at least three independent experiments, and statistical analysis was done using paired t-test, $p<0.05$:*; $p<0.01$:**; $p<0.001$:*** were considered significant. The error bars represent the standard deviations. The error bars are not seen when they are smaller than the thickness of the lines on the graphs (Figure 3.4).

Furthermore, the effects of NCs size on cell proliferation were determined by using the same method (XTT cell proliferation assay). The size of free NCs-2 is 115nm that is higher than 80nm of free NCs-1. Also, the results showed that increasing size of NCs did not cause any significant change on cell proliferation (Figure 3.3A-3.3B & Figure 3.4A-3.4B).

3.3 DOX-HER-2-NCs is more effective on cell proliferation of SKBR-3 cells compared to DOX-NCs

For this part, the cytotoxic effect of DOX was examined to determine the optimal concentration of DOX-NCs and DOX-HER-2-NCs. Step-wise increasing concentrations of DOX (0,1- to 5 μM) for SKBR-3 cells and DOX (0,05- to 1 μM) for MCF-10A cells were used to determine inhibitory concentration (IC50) value at 48- and 72h.

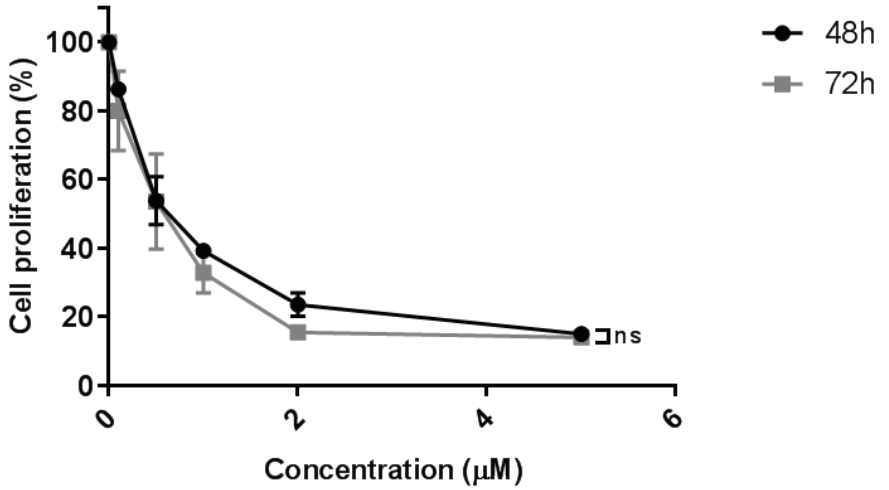

Figure 3.5. Cytotoxic effect of DOX on cell proliferation of SKBR-3 cells at 48- and 72h.

Cytotoxic effects of DOX were determined by XTT cell proliferation assay for SKBR-3. Experiments were done in triplicate in at least three independent experiments, and statistical analysis was done using paired t-test, $p<0.05$:*; $p<0.01$:**; $p<0.001$:*** were considered significant. The error bars represent the standard deviations. The error bars are not seen when they are smaller than the thickness of the lines on the graphs (Figure 3.5).

The IC50 values of DOX was calculated and found as 0.65- and 0.61 μM for SKBR-3 cells at 48- and 72h, respectively (Figure 3.5).

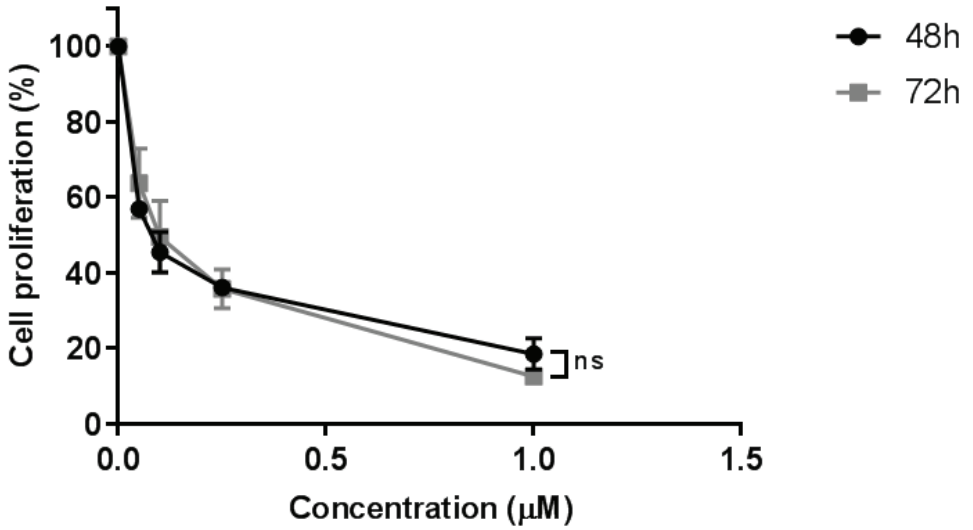

Figure 3.6. Cytotoxic effect of DOX on cell proliferation of MCF-10A cells at 48- and 72h.

Cytotoxic effects of DOX were determined by XTT cell proliferation assay for MCF-10A. Experiments were done in triplicate in at least three independent experiments, and statistical analysis was done using paired t-test, $p<0.05$:*; $p<0.01$:**; $p<0.001$:*** were considered significant. The error bars represent the standard deviations. The error bars are not seen when they are smaller than the thickness of the lines on the graphs (Figure 3.6).

Besides, The IC50 values of DOX were 0.08- and 0.1μM for MCF-10A cells at 48- and 72h, respectively (Figure 3.6). These results helped us to determine DOX effects

on cells for the continuation of the next processes which are decision of doses of DOX-NCs and DOX-HER-2-NCs.

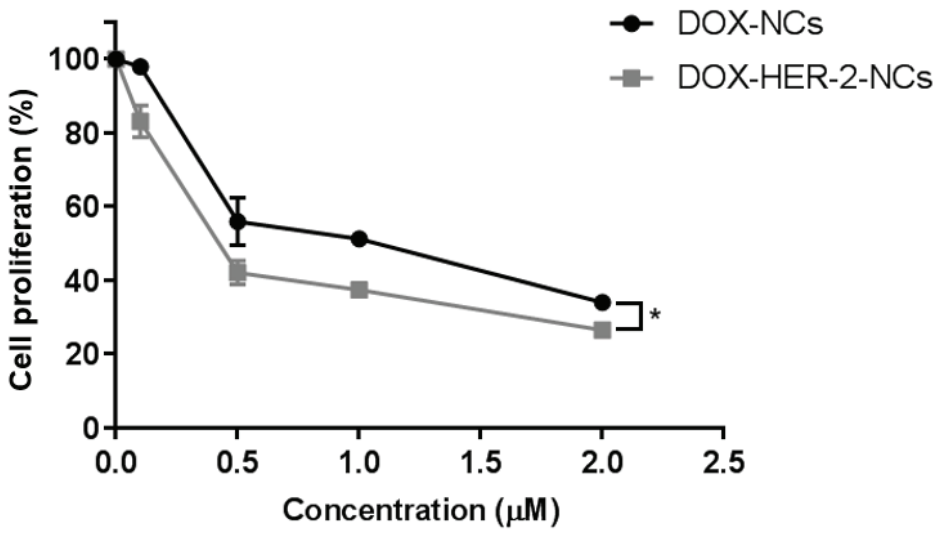

Figure 3.7. Cytotoxic effect of DOX-NCs and DOX-HER-2-NCs on cell proliferation of SKBR-3 cells at 48h.

Cytotoxic effects of DOX-NCs and DOX-HER-2-NCs were determined by XTT cell proliferation assay for SKBR-3. Experiments were done in triplicate in at least three independent experiments, and statistical analysis was done using paired t-test, $p<0.05$:*; $p<0.01$:**; $p<0.001$:*** were considered significant. The error bars represent the standard deviations. The error bars are not seen when they are smaller than the thickness of the lines on the graphs (Figure 3.7).

The results shown that IC50 values of DOX-NCs and DOX-HER-2-NCs were 0.45- and 1.07 μM for SKBR-3 cells at 48h, respectively (Figure 3.7). The significant change was on both DOX-NCs and DOX-HER-2-NCs. According to IC50 values, DOX-HER-2-NCs was 2-fold more effective on SKBR-3 cells as compared to DOX-NCs (Figure 3.7).

Additionally, the results showed that IC50 values of DOX-NCs and DOX-HER-2-NCs were 0.15- and 0.18 μM for MCF-10A cells at 48h, respectively (Figure 3.8). DOX-NCs and DOX-HER-2-NCs exhibited almost similar cytotoxic effect on MCF-10A. Also, there was no significant change. The effects of DOX-HER-2-NCs were higher

on HER-2 overexpressed SKBR-3 cells. However, HER-2 conjugated NCs does not have significant effects on proliferation of MCF-10A cells.

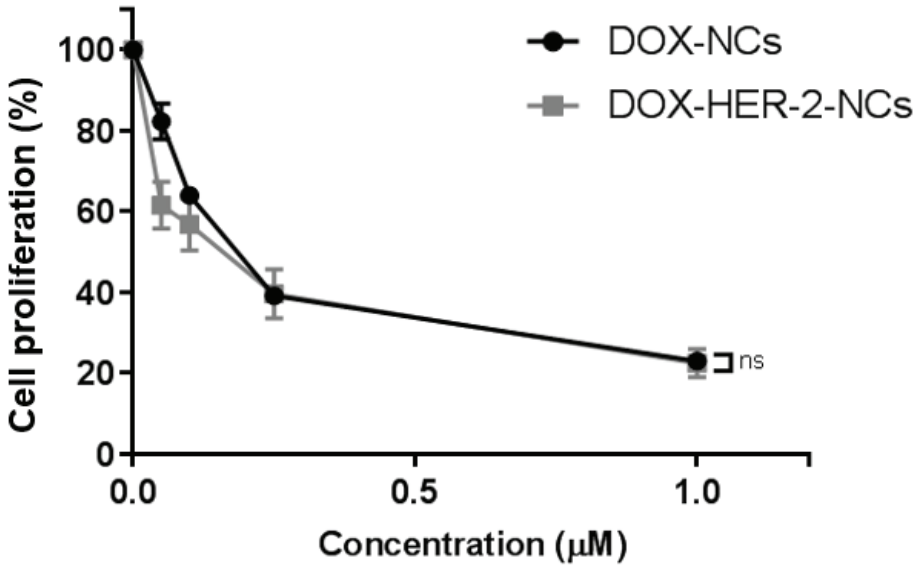

Figure 3.8. Cytotoxic effect of DOX-NCs and DOX- HER-2-NCs on cell proliferation of MCF-10A cells at 48h.

Cytotoxic effects of DOX-NCs and DOX- HER-2-NCs were determined by XTT cell proliferation assay for MCF-10A. Experiments were done in triplicate in at least three independent experiments, and statistical analysis was done using paired t-test, $p< 0.05$:*; $p<0.01$:**; $p<0.001$:*** were considered significant. The error bars represent the standard deviations. The error bars are not seen when they are smaller than the thickness of the lines on the graphs (Figure 3.8).

According to XTT cell proliferation assay, comparison of DOX-HER-2-NCs and DOX-NCs was determined at 48h application because the DOX molecule is more affective on SKBR-3 and MCF-10A cells at 48h. The IC50 value of DOX was 0.65 μM at 48h while IC50 value of DOX-NCs was 1.07 μM. The DOX conjugated micelles application decreased effects of DOX on SKBR-3 cells. However, IC50 values of DOX-HER-2-NCs was 0.45μM. DOX conjugated HER-2 micelles increased effects of DOX as compared to both only DOX molecules application and DOX-NCs at 48h application.

These results were analyzed by using t-test. According to that, when all doses of DOX-NCs and DOX-HER-2-NCs were compared, DOX-NCs and DOX-HER-2-NCs have significant difference on SKBR-3 cells at 48h application.

3.4 Increasing concentration of DOX-HER-2-NCs reduced cell viability on SKBR-3 cells significantly, rather than DOX-NCs

The cytotoxic effects of NCs on SKBR-3 and MCF-10A cells was explored by step-wise increasing concentrations of both DOX-NCs and DOX-HER-2-NCs at 48 and 72h.

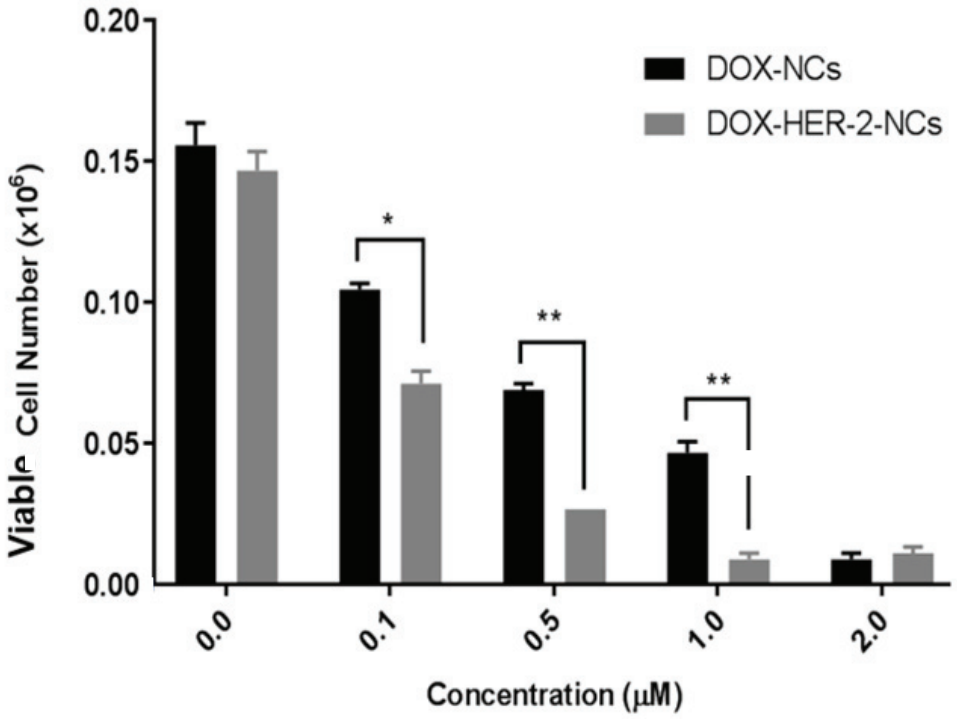

Figure 3.9. Cytotoxic effect of DOX-NCs and DOX-HER-2-NCs on cell number of SKBR-3 cells at 48h.

Cells, grown in 24-well plates ($3x10^4$ cells/well), were treated in increasing doses of DOX-NCs and DOX-HER-2-NCs at 48h. Cell viability was determined using trypan blue dye exclusion assay. Experiments were done in triplicate in at least three independent experiments, and statistical analysis was done using paired t-test, $p<0.05$:*; $p<0.01$:**;

p<0.001:*** were considered significant. The error bars represent the standard deviations. The error bars are not seen when they are smaller than the thickness of the lines on the graphs (Figure 3.9).

Treatments with 0.1- to 2 μM of DOX-NCs and DOX-HER-2-NCs on SKBR-3 cells at 48h were determined by counting live cells under the microscope. The cell viability decreased as the concentration of NCs increased. For 0.1 μM of DOX-NCs and DOX-HER-2-NCs have significantly decreased. In addition, increased concentrations (at 0.5- and 1 μM) caused more significant change as compared to 0.1 μM dose of NCs. However, 2 μM for both DOX-NCs and DOX-HER-2-NCs had significant cytotoxic effects on cells (Figure 3.9).

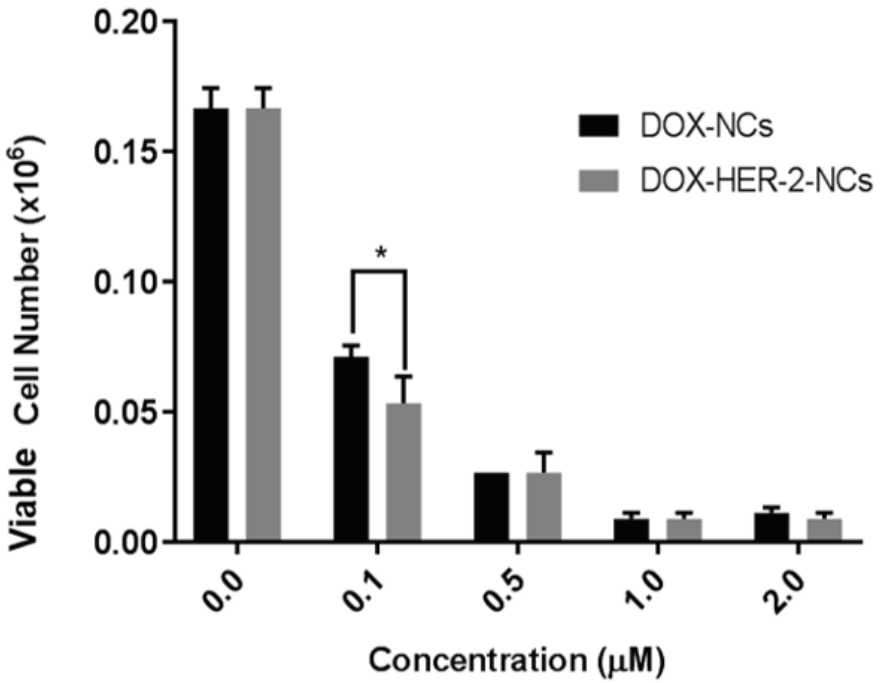

Figure 3.10. Cytotoxic effect of DOX-NCs and DOX-HER-2-NCs on cell number of SKBR-3 cells at 72h.

Cells grown in 24-well plates ($3x10^4$ cells/well), were treated in increased doses of DOX-NCs and DOX-HER-2-NCs at 72h. Cell viability was determined using trypan blue dye exclusion assay. Experiments were done in triplicate in at least three independent experiments, and statistical analysis was done using paired t-test, p<0.05:*; p<0.01:**;

p<0.001:*** were considered significant. The error bars represent the standard deviations. The error bars are not seen when they are smaller than the thickness of the lines on the graphs (Figure 3.10).

On the other hand, time points also affected significant change at different concentration. Only at 0.1 μM, that is low dose of both DOX-NCs and DOX-HER-2-NCs, caused significant change (Figure 3.10). These result showed that, NCs have significant effects on cell viability of SKBR-3 cells in a dose- and time dependent manner.

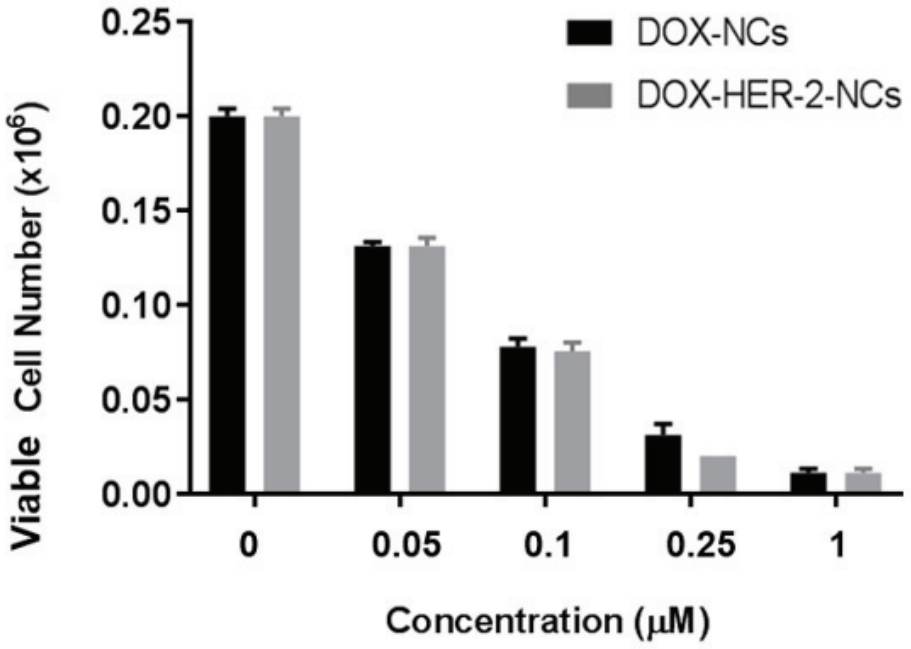

Figure 3.11. Cytotoxic effect of DOX-NCs and DOX-HER-2-NCs on cell number of MCF-10A cells at 48h.

Cells grown in 24-well plates ($1x10^4$ cells/well), were treated in increasing doses of DOX-NCs and DOX-HER-2-NCs at 48h. Cell viability was determined using trypan blue dye exclusion assay. Experiments were done in triplicate in at least three independent experiments, and statistical analysis was done using paired t-test, p<0.05:*; p<0.01:**; p<0.001:*** were considered significant. The error bars represent the standard deviations. The error bars are not seen when they are smaller than the thickness of the lines on the graphs (Figure 3.11).

Treatment with increasing concentration of DOX-NCs and DOX-HER-2-NCs between 0.05- and 1μM at 48h and 72h decrease viability of MCF-10A cells, whereas there was no change in cell number of MCF-10A cells as compared to each dose. The decreased viable cell number was analyzed by t-test. According to t-test analysis, there were not significant changes in all of doses compare to DOX-NCs and DOX-HER-2-NCs (Figure 3.11 and Figure 3.12). So, these results demonstrated that DOX-NCs and DOX-HER-2-NCs have similar effects on cell viability of MCF-10A cells at both 48h and 72h.

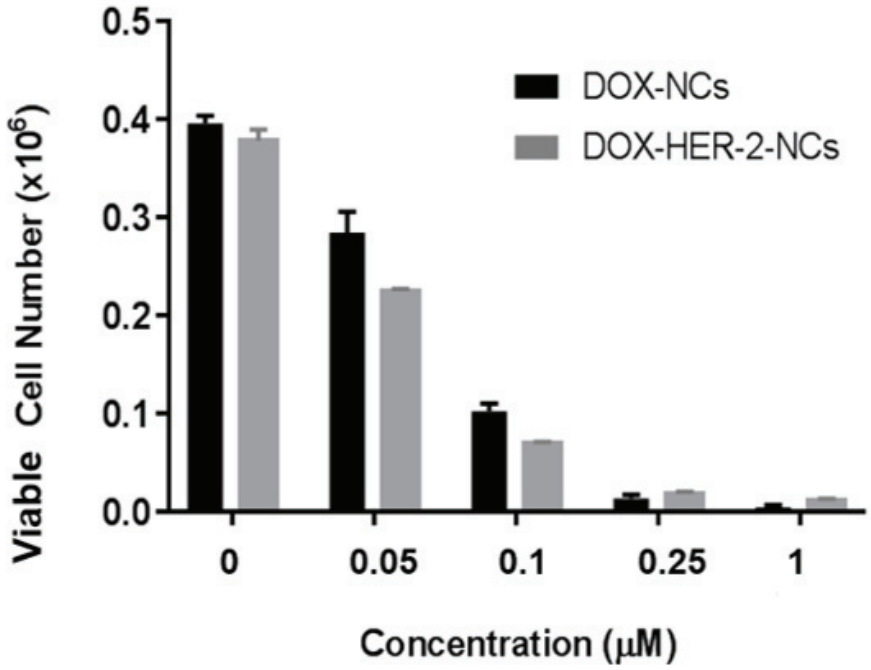

Figure 3.12. Cytotoxic effect of DOX-NCs and DOX- HER-2-NCs on MCF-10A cells at 72h.

Cells grown in 24-well plates ($1x10^4$ cells/well), were treated in increasing doses of DOX-NCs and DOX- HER-2-NCs at 48h. Cell viability was determined using trypan blue dye exclusion assay. Experiments were done in triplicate in at least three independent experiments, and statistical analysis was done using paired t-test, $p<0.05$:*; $p<0.01$:**; $p<0.001$:*** were considered significant. The error bars represent the standard deviations. The error bars are not seen when they are smaller than the thickness of the lines on the graphs (Figure 3.12).

3.5 Treatment of DOX-NCs-HER-2 on co-cultured SKBR-3 and K562 cells decreased cell viability of SKBR-3 significantly

The role of DOX-NCs and DOX-HER-2-NCs on co-culture of SKBR-3 and K562 cells was explored by applying increasing concentrations of both NCs (0.1- to 2 μM) at 48h. This method aids to determine the selectivity and specificity of DOX-NCs and DOX-HER-2-NCs on cell viability of SKBR-3 and K562 at the same condition.

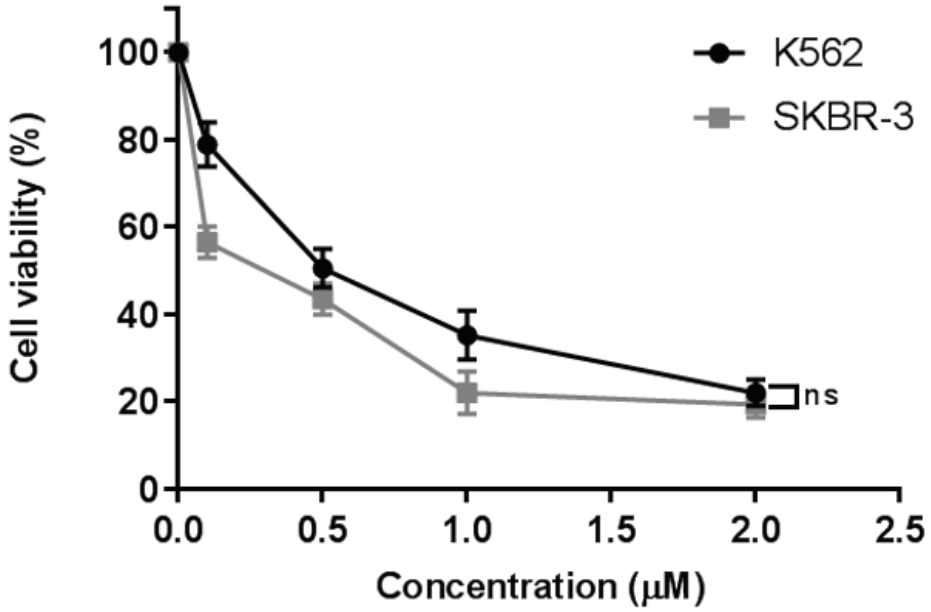

Figure 3.13. Cytotoxic effect of DOX-NCs on co-culture SKBR-3 and K562 cells at 48h.

Cells grown in 24-well plates ($3x10^4$ cells/well for both SKBR-3 and K562), were treated in increasing doses of DOX-NCs at 48h. Cell viability was determined using trypan blue dye exclusion assay. Experiments were done in triplicate in at least three independent experiments, and statistical analysis was done using paired t-test, $p<0.05$:*; $p<0.01$:**; $p<0.001$:*** were considered significant. The error bars represent the standard deviations. The error bars are not seen when they are smaller than the thickness of the lines on the graphs (Figure 3.13).

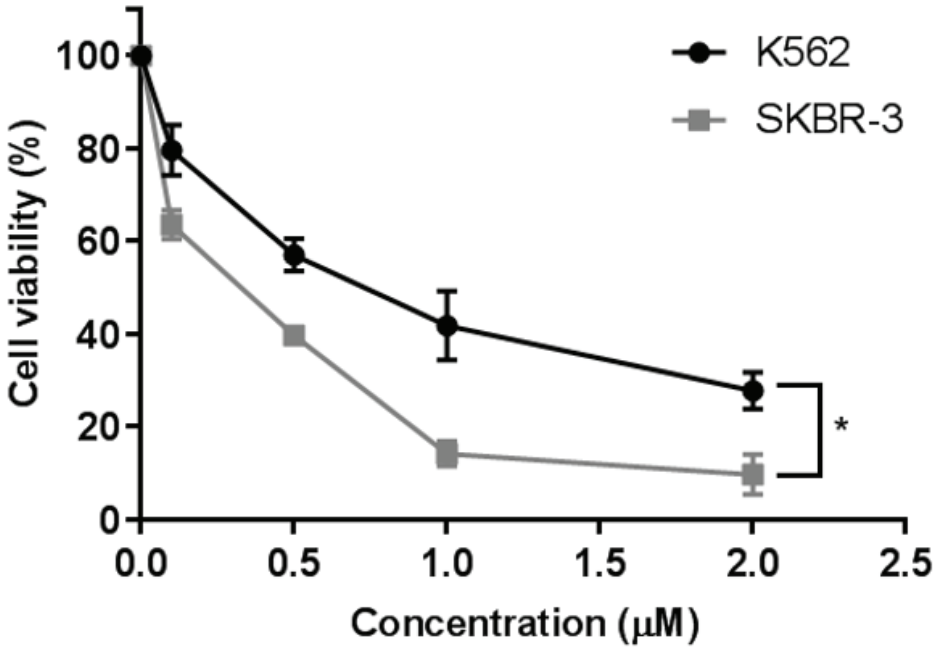

Figure 3.14. Cytotoxic effect of DOX-NCs-HER-2 on co-culture SKBR-3 and K562 cells at 48h.

Cells grown in 24-well plates ($3x10^4$ cells/well for both SKBR-3 and K562), were treated in increasing doses of DOX-HER-2-NCs at 48h. Cell viability was determined using trypan blue dye exclusion assay. Experiments were done in triplicate in at least three independent experiments, and statistical analysis was done using paired t-test, $p<0.05$:*; $p<0.01$:**; $p<0.001$:*** were considered significant. The error bars represent the standard deviations. The error bars are not seen when they are smaller than the thickness of the lines on the graphs (Figure 3.14).

K562 cells are HER-2 negative, similar to MCF-10A cells and the doubling time of K562 and SKBR-3 cells is similar. In addition, the IC50 value of DOX on SKBR-3 and K562 cells is similar. So, the comparison of DOX-NCs and DOX-HER-2-NCs on both cell lines is more reliable since the co-culture studies are important in determining the efficiency of NCs and DOX. The NCs application were occurred same condition and same wells. So, the effectivity of DOX-NCs and DOX-HER-2-NCs on HER-2 positive SKBR-3 and HER-2 negative MCF-10A cells were determined more significantly.

The treatment of DOX-NCs reduced cell viability of both SKBR-3 and K562 cells at 48h but there was not significant change (Figure 3.13). Additionally, treatments of

DOX-NCs-HER-2 decreased cell viability of both SKBR-3 and K562 cells. DOX-HER-2-NCs were significantly more effective on SKBR-3 cells (Figure 3.14).

Co-culture treatment studies revealed that DOX-HER-2-NCs causes significant decreases in cell viability as compared to DOX-NCs on SKBR-3 cells. These results also were compared by using t-test statistical analysis. The comparison of all doses of DOX-HER-2-NCs is more effective on SKBR-3 cells at 48h. This experimental result also showed drug selectivity on HER-2 positive and negative cells. The drug selectivity on SKBR-3 cells were more than on K562 cells as it was confirmed that viable cell number of SKBR-3 cells was less than K562 cells.

3.6 DOX-HER-2-NCs uptake was higher than DOX-NCs in SKBR-3 cells at 48h.

The uptake of 1.07 μM DOX-NCs (IC50 concentration) and 0.45 μM DOX-HER-2-NCs (IC50 concentration) by SKBR-3 cells at 48h were defined by fluorescence imaging. For this purpose, 10 different images were processed by using ImageJ.

The concentration of IC50 values of NCs for SKBR-3 cells was applied and it was swhoen that the fluorescence intensity density value of DOX-NCs-HER-2 is higher as compared to DOX-NCs despite a low concentration application of DOX-NCs-HER-2. The conjugated HER-2 peptide on NCs provided a high uptake rate by SKBR-3 cells (Figure 3.15).

After unpaired statistical analysis, the fluorescence intensity density value of DOX-NCs-HER-2 is fourfold more than DOX-NCs on SKBR-3 cells. This difference was also significant. This result revealed that the DOX-NCs-HER-2 was more effective than DOX-NCs on SKBR-3 HER-2 positive cells. High cytotoxic effects of DOX-HER-2-NCs on SKBR-2 cells can be explained by more uptake of DOX molecules.

Besides the determination of fluorescence intensity density on SKBR-3 cells for DOX-NCs and DOX-HER-2-NCs, the localization of DOX molecules was different. The localization of DOX molecules was determined by using FIJI imaging processes program. For this purpose, the co-localization analysis was used with localization of DAPI and DOX. The images of DAPI and DOX at different wavelength were merged and R-total

value was calculated by 3 images. The R-total value represents co-localization value. If it is closed to “1”, two different images from different fluorescence wavelengths are co-localized and determined by Pearson's correlation coefficient.

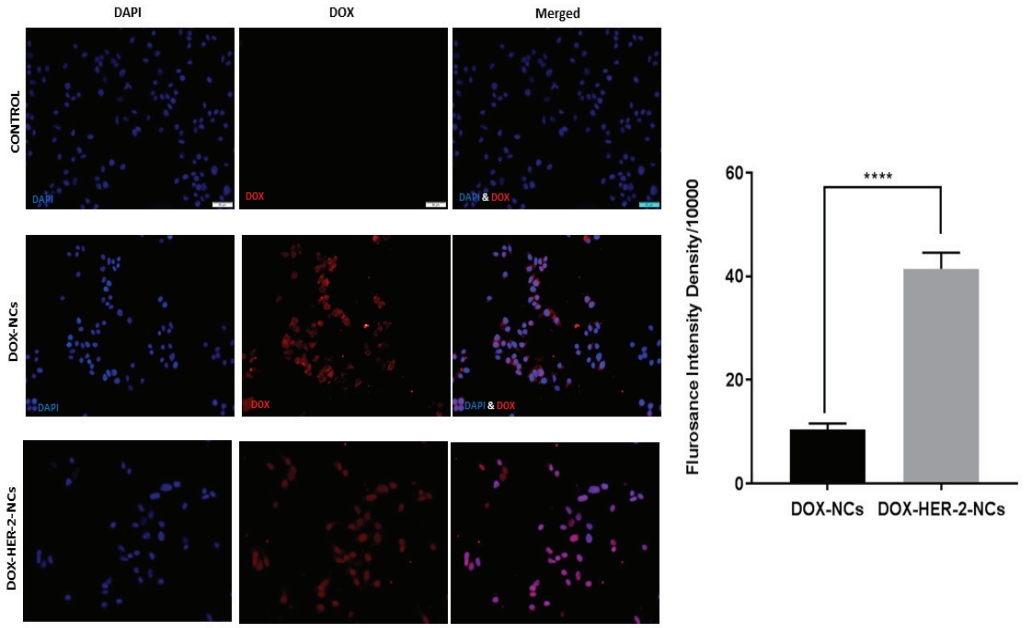

Figure 3.15. Fluorescence images and fluorescence intensity density of DOX-NCs and DOX-HER-2-NCs for SKBR-3 cells at 48h, Magnification: 20X, Blue: DAPI; Red: DOX

SKBR-3 cells grown in 6-well plates ($5x10^5$ cells/well) were treated with 1.07 µM DOX-NCs and 0.45 µM DOX-HER-2-NCs at 48h. Experiments were done in triplicate in at least three independent experiments, and statistical analysis was done using unpaired t-test, $p<0.05$:*; $p<0.01$:**; $p<0.001$:*** were considered significant for 10 different images sections. The error bars represent the standard deviations (Figure 3.15).

Drug release rate and efficiency of DOX-HER-2-NCs was higher than DOX-NCs. Besides, the distribution of DOX is different for DOX-HER-2-NCs and DOX-NCs that was identified by the co-localization analysis of DOX (red) and DAPI (nuclei dye-blue).

These results showed that targeted DOX-HER-2-NCs increased uptaken DOX by HER-2 enriched SKBR-3 cells. The co-localization value of DOX-HER-2-NCs was higher than DOX-NCs on SKBR-3 cells. This difference was determined by using unpaired t-test statistical analysis. So, the significant change was found between the application of DOX-NCs and DOX-HER-2-NCs on SKBR-3 cells (Figure 3.16).

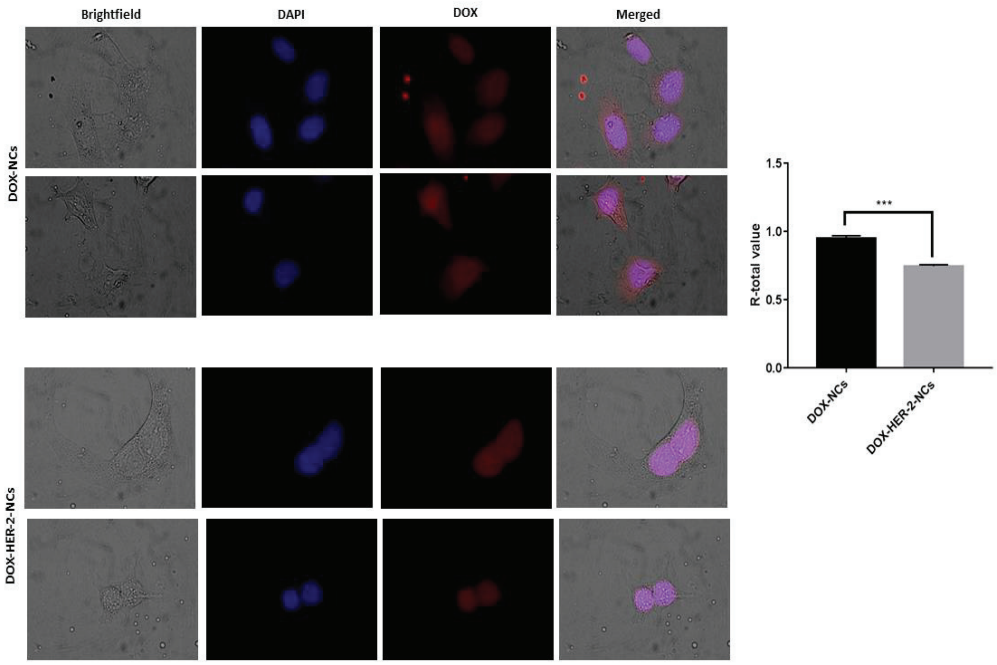

Figure 3.16. R-total value (co-localization) of DOX-NCs and DOX-HER-2-NCs for SKBR-3 cells at 48h, Magnification: 100X, Blue: DAPI; Red: DOX

SKBR-3 cells grown in 6-well plates ($5x10^5$ cells/well) were treated with IC50 of DOX-NCs and DOX-HER-2-NCs at 48h. The statistical analysis was done using unpaired t-test, $p<0.05$:*; $p<0.01$:**; $p<0.001$:*** were considered significant for three different images sections. The error bars represent the standard deviations. The error bars are not seen when they are smaller than the thickness of the lines on the graphs (Figure 3.16).

The localization of drug in cells is important to understand targeting mechanism of drug. This diffence can be occurred because of application dose of NCs and drug release mechanism. According to this images, effective mechanism of NCs was different on SKBR-3 cells.

The localization of DOX-NCs and DOX-HER-2-NCs were different. This event can be occured two possibilities. One is the drug concantration. The application doses of DOX-NCs and DOX-HER-2-NCs were different because their IC50 values were different. Other possibilitiy was effects of drug mechanism on SKBR-3 cells. The targeted property of DOX-HER-2-NCs induce tracking of nucleus in SKBR-3 cells. However, it

was not occured after application of DOX-NCs. So, DOX-NCs were localized in cytoplasm.

3.7 DOX-NCs-HER-2 uptake was similar to DOX-NC uptake in MCF-10A cells at 48h

The uptake of 0.15 μM DOX-NCs (IC50 value) and 0.18 μM DOX-HER-2-NCs (IC50 value) by SKBR-3 and MCF-10A cells at 48h were defined by fluorescence imaging.

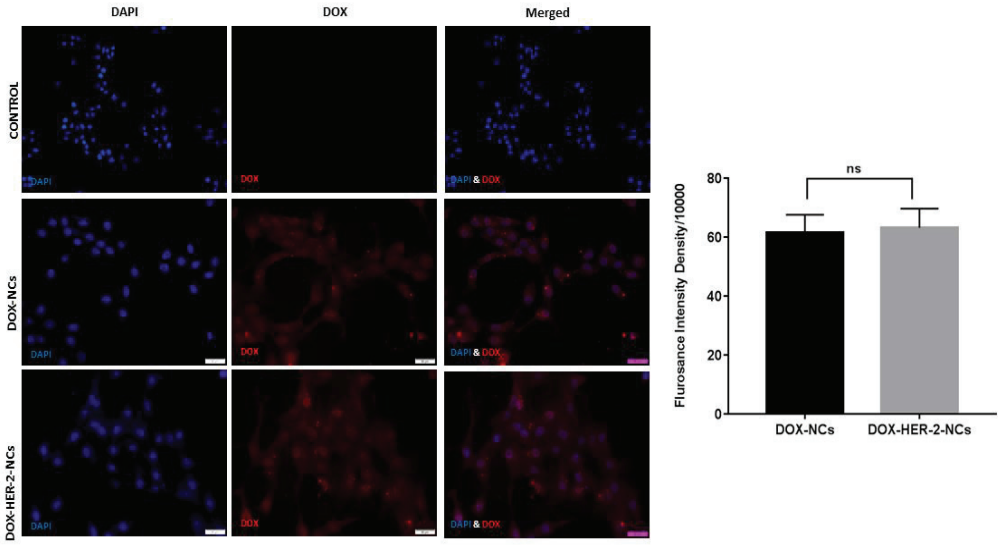

Figure 3.17. Flurosance images and fluorescence intensity density of DOX-NCs and DOX-NCs-HER-2 for MCF-10A cells at 48h, Magnification: 10X-20X, Scale bars= 50 μm, Blue: DAPI; Red: DOX.

MCF-10 cells grown in 6-well plates ($3x10^5$ cells/well), were treated with IC50 doses of DOX-NCs-HER-2 and DOX-NCs at 48h. Experiments were done in triplicate in at least three independent experiments, and statistical analysis was done using unpaired t-test, $p<0.05$:*; $p<0.01$:**; $p<0.001$:*** were considered significant for 10 different images sections. The error bars represent the standard deviations (Figure 3.17).

The IC50 value of NCs was applied to MCF-10A cells and the results showed that the fluorescence intensity density value of DOX-NCs-HER-2 and DOX-NCs was similar (Figure 3.17). Besides, there was not significant change because MCF-10A cells do not carry HER-2 receptor.

3.8 Increasing concentrations of DOX-NCs and DOX-HER-2-NCs induces apoptosis and necrosis in SKBR-3 cells.

IC50 and IC70 values of DOX-NCs and DOX-NCs-HER-2 were applied on SKBR-3 cells at 48h and apoptosis and necrosis percentage were defined by Annexin V/PI double staining assay.

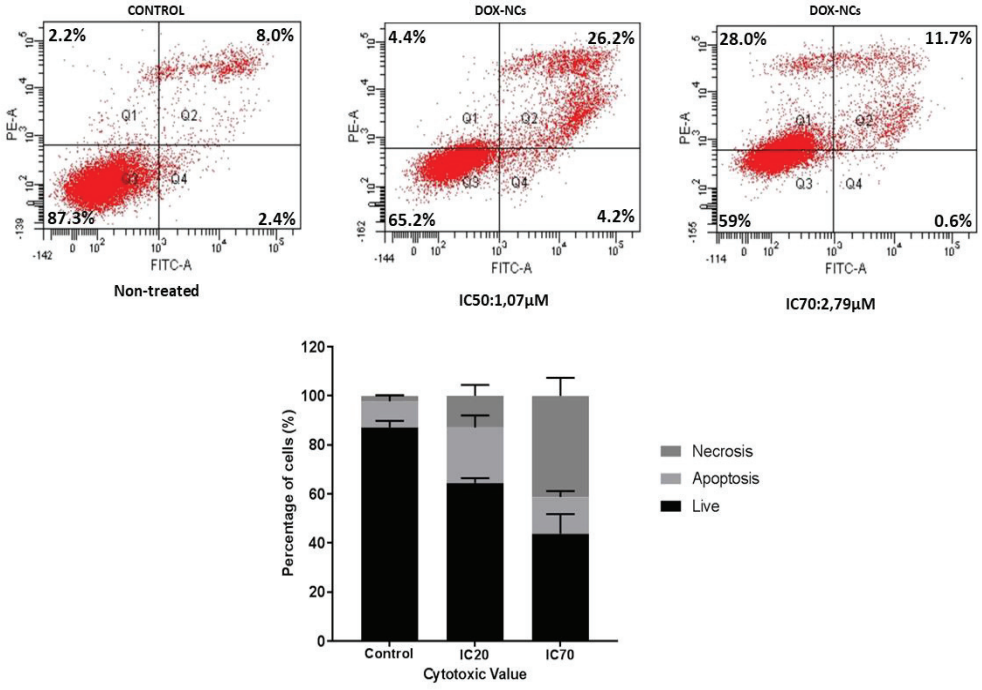

Figure 3.18. The percentage of DOX-NCs for SKBR-3 cells at 48h.

SKBR-3 cells grown in 6-well plates ($5x10^5$ cells/well) were treated with IC20 and IC70 doses of DOX-NCs at 48h. Experiments were done in triplicate in at least three independent experiments. The error bars represent the standard deviations (Figure 3.18).

The Annexin V-PI double staining was used to determine four different quadrants showing that Q1: necrosis; Q2: Late apoptosis; Q3: Live and Q4: Early apoptosis.

During Annexin V/PI double staining, all compensation adjustment was set up to for fluorescence crosstalk the following control by using unstained cells, Annexin V single labeling, PI single labeling, and Annexin V/PI double labeling. This step is very important to obtain singly stained cells.

The results revealed thattreatment of SKBR-3 with DOX-NCs induced apoptosis until 1.07 μM. Increasing dose of DOX-NCs increased percent of apoptotic cell population. However, increasing concentration of DOX-NCs induced necrosis to 28%. Moreover, the three independent experiments showed similar outcomes as shown in Figure 3.18.

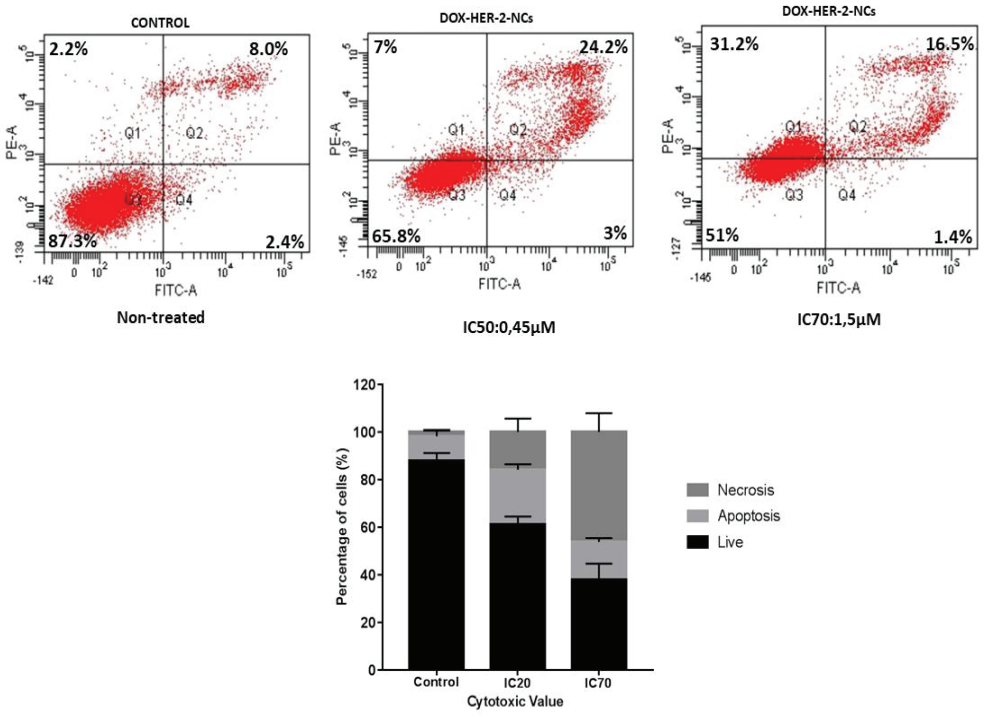

Figure 3.19. The percentage of DOX-HER-2-NCs for SKBR-3 cells at 48h.

SKBR-3 cells grown in 6-well plates ($5x10^5$ cells/well) were treated with IC20 and IC70 doses of DOX-HER-2-NCs at 48h. Experiments were done in triplicate in at least three independent experiments. The error bars represent the standard deviations (Figure 3.19).

The results showed that treatment of SKBR-3 cells with DOX-HER-2-NCs triggered apoptosis. Increasing doses of DOX-HER-2-NCs increased percent of apoptotic cell population. However, increasing concentration of DOX-HER-2-NCs induced necrosis. Moreover, similar results were observed from three independent experiments as shown in Figure 3.19.

3.9 Mitochondrial membrane potential did not change in SKBR-3 cells treated with DOX-NCs and DOX-HER-2-NCs at 48h.

The effects of DOX-NCs and DOX-NCs-HER-2 (0.5-5μM) on mitochondrial membrane potential (MMP) of SKBR-3 cells at 48h were determined by JC-1 MMP assay.

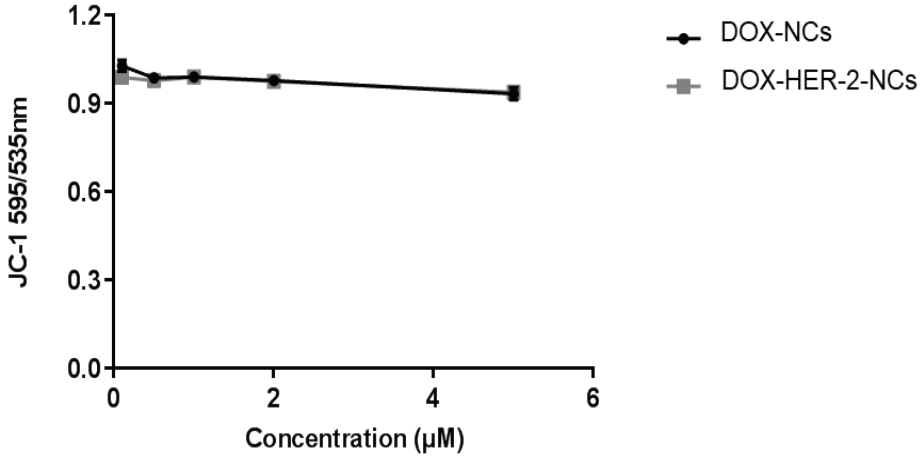

Figure 3.20. Effects of DOX-NCs and DOX-HER-2-NCs on mitochondrial membrane potential for SKBR-3 at 48h.

SKBR-3 cells grown in 96-well plates ($5x10^3$ cells/well) were treated with 0.5-5μM doses of DOX-NCs and DOX-HER-2-NCs for 48h. Experiments were done in triplicate in at least three independent experiments. The error bars represent the standard deviations (Figure 3.20).

SKBR-3 cells were treated with increasing concentrations of DOX-NCs and DOX-HER-2-NCs and changes in mitochondrial membrane potential was determined. The results showed that increasing doses of both DOX-NCs and DOX-HER-2-NCs did not effects MMP of SKBR-3 cells (Figure 3.20). This result also showed that DOX-NCs and DOX-HER-2-NCs induced necrosis instead of apoptosis confirming our Annexin V/PI double staining results (Figure 3.18 and Figure 3.19).

3.10 Bcl-2 protein levels was not changed in SKBR-3 cells treated with DOX-NCs and DOX-HER-2-NCs at 48h.

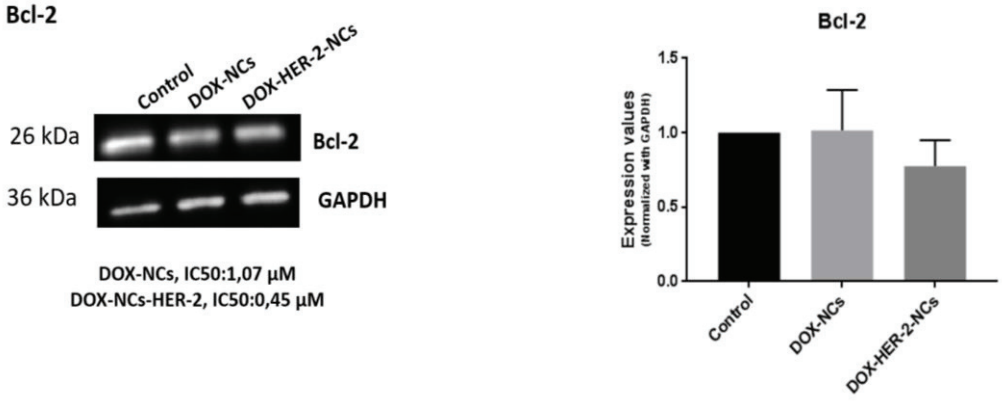

Figure 3.21. Effects of DOX-NCs and DOX-HER-2-NCs on Bcl-2 protein level for SKBR-3 cells at 48h.

SKBR-3 cells grown in 6-well plates ($5x10^5$ cells/well) were treated with IC50 doses of DOX-NCs and DOX-HER-2-NCs at 48h. Experiments were done in triplicate in at least three independent experiments. The error bars represent the standard deviations (Figure 3.21).

Bcl-2 protein is involved in the regulation of apoptotic cell death. In this experiment, GAPDH was used as internal positive control to understand the changes in protein levels of Bcl-2. The results showed that there was a small decreased in protein levels of Bcl-2 was in response to DOX-HER-2-NCs application (Figure 3.21). During this experiment, 1.07µM of DOX-NCs and 0.45µM of DOX-HER-2-NCs were used to determined Bcl-2 protein level. In this step, IC50 value was trailed because the apoptosis was observed in Annexin V/PI double staining while increaseing doses of DOX-NCs and DOX-HER-2-NCs induced necrosis.

Bcl-2 protein has roles in a critical life-death decision point in the common pathway. Application of DOX-NCs and DOX-HER-2-NCs decreased protein levels of Bcl-2. However, the protein levels of Bcl-2 decreased in response to DOX-HER-2-NCs application as compared to DOX-NCs and control.

3.11 Bax protein level was increased and Caspase-3 protein was cleavage for SKBR-3 cells after treated with DOX-NCs and DOX-HER-2-NCs at 48h.

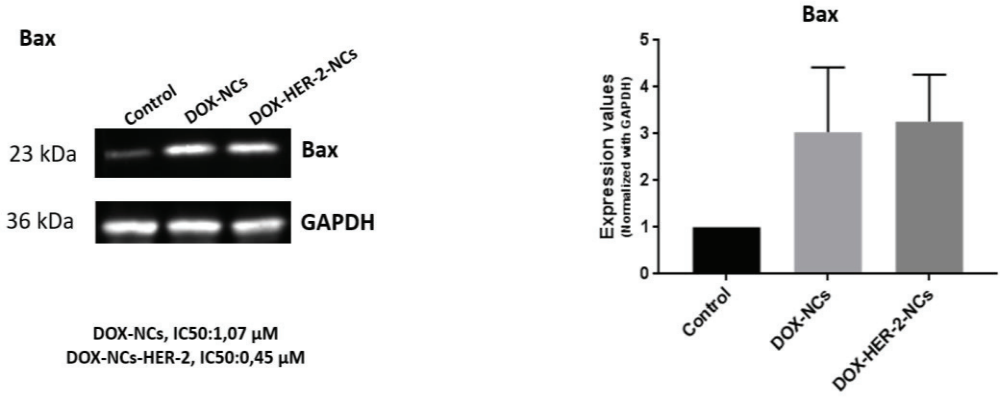

Figure 3.22. Effects of DOX-NCs and DOX-HER-2-NCs on Bax protein level for SKBR-3 cells at 48h.

SKBR-3 cells grown in 6-well plates ($5x10^5$ cells/well) were treated with IC50 doses of DOX-NCs and DOX-HER-2-NCs at 48h. Experiments were done in triplicate in at least two independent experiments. The error bars represent the standard deviations (Figure 3.22).

In parallel with determining the protein levels of pro-apoptotic Bax protein,we analysed protein levels of GAPDH which is used as internal positive control. The results showed that the protein levels of Bax was increased in response to DOX-NCs and DOX-HER-2-NCs as compared to control (Figure 3.21). During this experiment, 1.07µM of DOX-NCs and 0.45µM of DOX-HER-2-NCs were used to determine protein levels of Bax.

Application of DOX-NCs and DOX-HER-2-NCs increased protein levels of pro-apoptotic Bax. Besides, low dose of DOX-HER-2-NCs and high dose of DOX-NCs had a similar effect. So, low dose of DOX-HER-2-NCs was more effective than high dose of DOX-NCs. The effective mechanism of DOX-HER-2-NCs was related to Bax protein. Low dose of DOX-HER-2-NCs induce Bax protein without Bcl-2 protein.

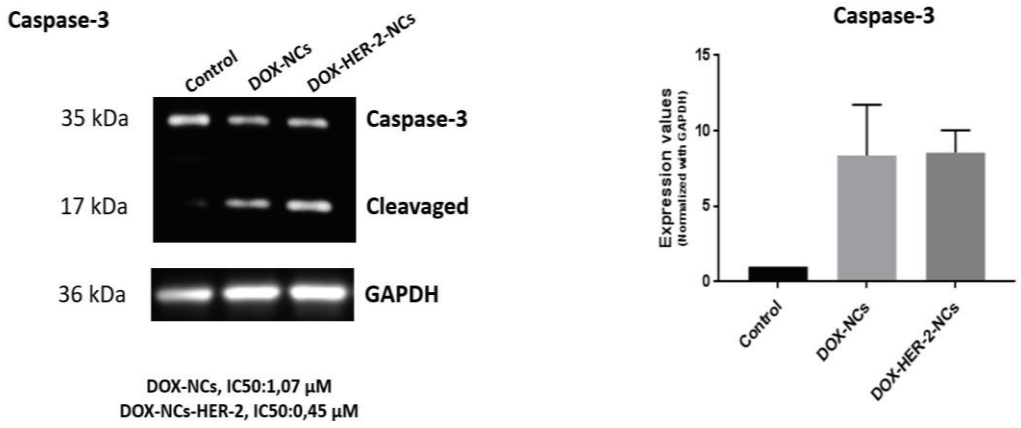

Figure 3.23. Effects of DOX-NCs and DOX-HER-2-NCs on Caspase-3 protein level for SKBR-3 cells at 48h.

SKBR-3 cells grown in 6-well plates ($5x10^5$ cells/well for) were treated with IC50 doses of DOX-NCs and DOX-HER-2-NCs at 48h. Experiments were done in triplicate in at least three independent experiments. The error bars represent the standard deviations (Figure 3.23).

Apoptotic pathways are orchestrated by caspases, a family of cysteine proteases and cleavage on the carboxy-terminal side of specific aspartic acid residues. Caspase-3 protein is member of Caspase family. The cleavage of Caspase-3 provide fragment formation that is detected with substrate-specific antibodies. These fragments are determined by western blotting.

The results revealed that, Caspase-3 was cleavage and observed as 17kDa and 35kDa in response to IC50 doses of DOX-NCs and DOX-HER-2-NCs at 48h. The rate of cleavage of Caspase-3 was increased as compared to control. However, the Caspase-3 cleavage were not observed. Besides, this result showed that treatment of DOX-NCs and DOX-HER-2-NCs at 48h induce apoptosis. In addition, the DOX-HER-2-NCs is more effective than DOX-NCs on SKBR-3 cells since low dose of DOX-HER-2-NCs and high dose of DOX-NCs had similar effects. The IC50 dose of DOX-NCs is 1.07µM and IC50 dose of DOX-HER-2-NCs was 0.45µM (Figure 3.23).

3.12 Increasing doses of DOX-NCs and DOX-HER-2-NCs change the cell cycle profile of SKBR-3 cells.

In addition to determining cytotoxic and apoptotic effects of the agents on the cells, we determined the cell cycle profiles of SKBR-3 cells exposed to IC20, IC50, and IC80 doses of DOX-NCs and DOX-HER-2-NCs by flow cytometry (Figure 3.24 & Figure 3.25).

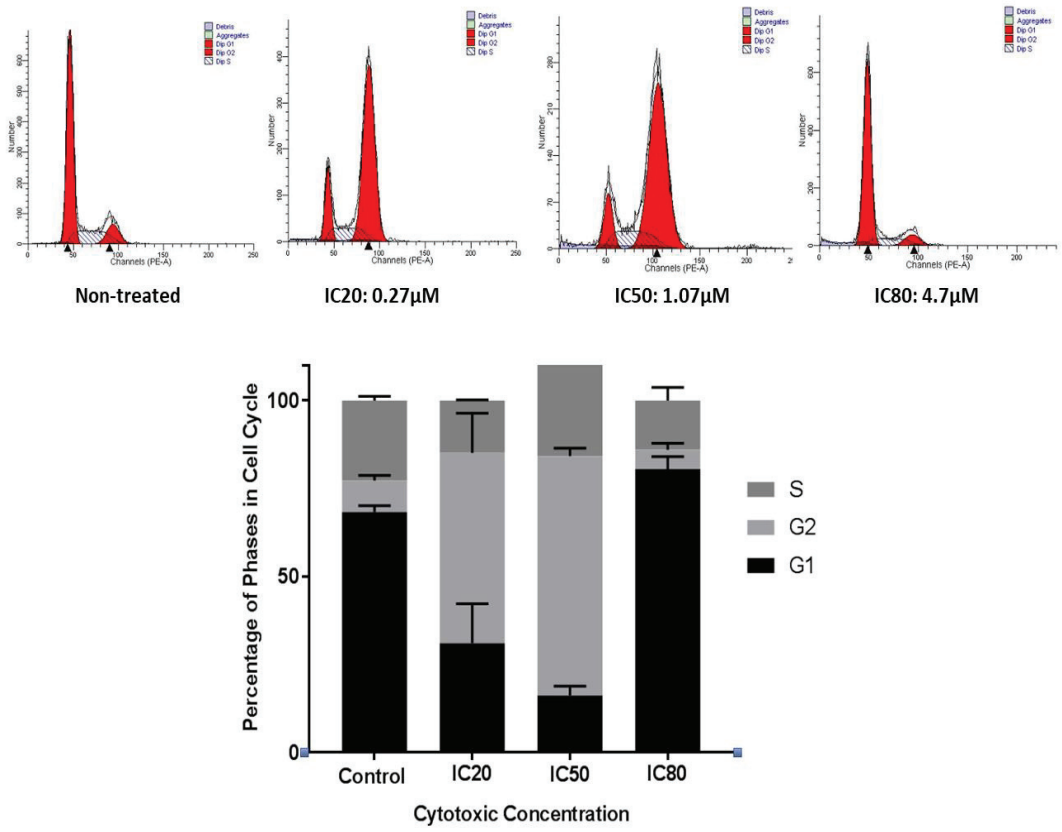

Figure 3.24. Effects of DOX-NCs on cell cycle phases of SKBR-3 at 48h.

SKBR-3 cells grown in 6-well plates ($5x10^5$ cells/well) were treated with IC20, IC50, and IC80 doses of DOX-NCs at 48h. Experiments were done in triplicate in at least three independent experiments. The error bars represent the standard deviations.

SKBR-3 cells treated with 0.27µM- and 1.07µM of DOX-NCs increased G2 phase and decreased G1 phase of the cell cycle. However, applications of 4.7µM of DOX-NCs on SKBR-3 cells increased G1 phases of cell cycle (Figure 3.24).

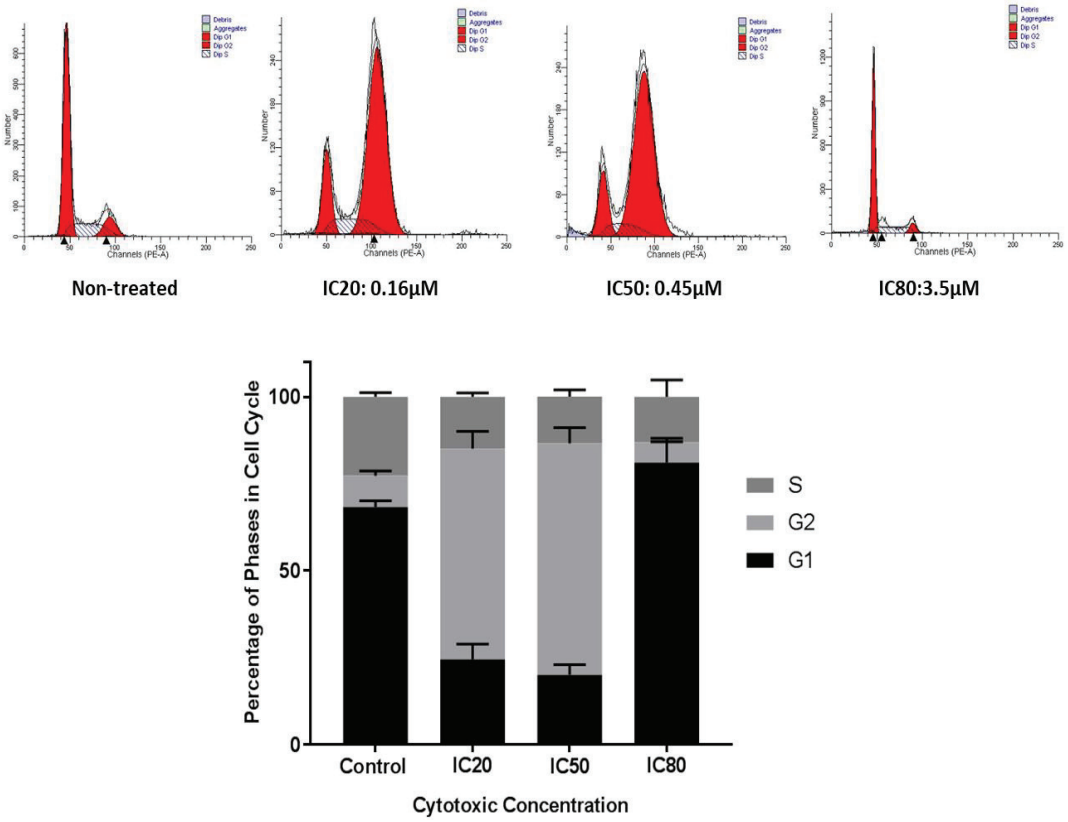

Figure 3.25. Effects of DOX-HER-2-NCs on cell cycle phases for SKBR-3 at 48h.

SKBR-3 cells grown in 6-well plates ($5x10^5$ cells/well) were treated with IC20, IC50, and IC80 doses of DOX-HER-2-NCs at 48h. Experiments were done in triplicate in at least three independent experiments. The error bars represent the standard deviations (Figure 3.25).

SKBR-3 cells treated with 0.16µM and 0.45µM of DOX-HER-2-NCs increased G2 phase and decreased G1 phase in cell cycle. However, there were no significant differences between 0.16µM and 0.45µM. The applications of 3.5µM of DOX-HER-2-NCs on SKBR-3 cells increased G1 phase of cell cycle (Figure 3.25).

The effects of DOX-NCs and DOX-HER-2-NCs on cell cycle progression of SKBR-3 were similar. Although, lower doses of DOX-HER-2-NCs were applied as compare to DOX-NCs, the results showed that DOX-HER-2-NCs were more specific and selective for SKBR-3 cells than DOX-NCs.

CHAPTER 4

CONCLUSION

Breast cancer is a common type of cancer. According to statistical analysis, this type of cancer is the second leading cause of cancer mortality for women in worldwide. Additionally, breast cancer is seen frequently in 154 countries of 185 countries according to statixtical analysis. Besides, leading cause of cancer death is breast cancer in more than 100 countries. 1 of every 4 women is diagnosed with breast cancer in worldwide (1). 1.7 million new cases of breast cancer were diagnosed according to 2012 data (5). Approximately, 2.1 million new diagnosed female breast cancer cases were estimated with respect to 2018 data (1). It is clear from these articles that the rate of a breast cancer diagnosis is increasing day by day.

There are different therapeutic options for breast cancer, such as surgery, chemotherapy, radiotherapy, hormone therapy, and novel targeted therapy that is based on pathological and clinical outcomes (166). The traditional treatment of breast cancer including surgery, radiotherapy, and chemotherapy contain many side effects such as anxiety, depression, decreasing life quality, vomiting, pain, and disruption of sleep disturbance (167). So, new treatment strategies are developing to overcome cancer. At this point, targeted therapy is important to manage the treatment of cancer, reduce treatment-related side effects, and to improve more specific and efficient treatment methods.

For the effective treatment of cancer, different nanoparticle or nanocarriers such as quantum dots, nanotubes, lipids, polymers, porous silica, and micelles can be used. All of them have different properties in terms of physicochemical characterization such as size, charge, shape, surface, drug loading and releasing capacity. These features can be modified with targeting molecules such as peptide and antibody. On the other hand, anti-cancer agents such as DOX, cisplatin, and 5-fluorouracil can be loaded to these carriers.

HER-2 is called as human epidermal growth factor receptor that has a role in cell proliferation and growth. The receptor directed nanoparticles or nanocarriers provide

stabilization of drug delivery capacity and pharmacokinetic regulation to manage synergy of drugs that have a role in targeted therapy of cancer (168).

In this study, we highlighted the critical role of targeting nanocarriers by using HER-2 peptide on breast cancer as well as HER-2 enriched breast cancer cell types. HER-2 enriched breast cancer SKBR-3 and HER-2 negative normal breast cells MCF-10-A cells were used to determine specificity and effectivity of DOX-HER-2-NCs. For this purpose, the cytotoxic, apoptotic and cytostatic effects of the agents on these cells were determined by cell proliferation, apoptosis, and cell cycle assays.

Firstly, the cytotoxic role of two different free NCs (80nm and 115nm) and free HER-2-NCs (160nm and 200nm) at 48h and 72h were determined in terms of size. They did show cytotoxic effects on SKBR-3 and MCF-10A cells. These NCs have biocompatible properties because of their low toxic effects. In addition, micelles have a dynamic structure that is also called as problem for cancer treatment since dynamic structure cause leak out of drug and minimal circulation time. These problems were solved by using cross-linking of core moiety that provides stability. The acid-sensitive crosslinking also provided cleavage by two sites of pH-effect and drug release. Next, the effect of DOX was identified to define applied doses of DOX-NCs and DOX-HER-2-NCs.

In this study, unused VSSTQDFP peptide sequences were conjugated with NCs. These peptide sequences have never been used with nanocarriers according to literature. Only Abbineni *et. al.* demonstrate the role of VSSTQDFP peptide with using filamentous phage on SKBR-3 cells. Their results showed that VSSTQDFP peptide has a role in cell internalization by the reorganization of actin filament in SKBR-3 cells that was critical for cellular cytoskeleton (169). At this point, using VSSTQDFP peptide sequence has a critical role in targeted HER-2 overexpressed SKBR-3 cells and cellular internalization.

Our results showed that DOX-HER-2-NCs reduced cell proliferation significantly as compared to DOX-NCs as determined by XTT cell proliferation assay and trypan-blue staining for cell viability assay. Firstly, we examined a range of DOX doses that were also supported by literature information to determine doses of DOX-NCs and DOX-HER-2-NCs. The IC50 doses of DOX-NCs and DOX-HER-2-NCs were 1.07 μM and 0.45μM for SKBR-3 respectively. However, DOX-NCs and DOX-HER-2-NCs had similar effects on MCF-10A cells since their IC50 values were determined as 0.15 μM and 0.18 μM, respectively. These results revealed that DOX-HER-2-NCs is more effective on SKBR-3

cells at 48h because of HER-2 receptor on these cells. In addition, the unpaired t-test also showed significant differences between DOX-NCs and DOX-HER-2-NCs.

The important part of our study was the co-culture experiments that was established with SKBR-3 (HER-2 enriched) and K562 (HER-2 negative). The results of this part is critical for *ex-vivo* studies. We analyzed the selectivity of DOX-HER-2-NCs at the same condition for two different cells. The effects of 0.5-, 1-, and 2 μM of DOX-NCs and DOX-HER-2-NCs was determined by trypan blue staining. The DOX-HER-2-NCs was more effective than DOX-NCs on SKBR-3 cells. In addition, the selectivity of DOX-HER-2-NCs was more on SKBR-3 cells as compared to K562 cells and these results were supported by unpaired t-test statistical analysis. However, DOX-NCs had similar effects on SKBR-3 and MCF-10A cells.

One of the main problems in chemotherapy is drug distribution in the body. So, this problem can be solved by nanocarriers that penetrate specific cancer cells with enhanced permeability and retention. Thise effects also provide increased drug efficiency and decreased drug resistance. We demonstrated increased uptake of DOX by SKBR-3 and MCF-10A cells after treatment with DOX-NCs and DOX-HER-2-NCs as determined by fluorescence intensity density analyses using fluoresce microscopy. The fluorescence intensity density in SKBR-3 cells was higher when these cells were treated with DOX-HER-2-NCs as compared to DOX-NCs. DOX-HER-2-NCs and DOX-NCs had the same effects on MCF-10A cells in terms of fluorescence intensity density. In addition to that, we also observed different localization of DOX in SKBR-3 cells treated with DOX-HER-2-NCs and DOX-NCs. The DOX-HER-2-NCs was localized in the nucleus of SKBR-3 cells but DOX-NCs was scattered in the cytoplasm. Next, we focus on the co-localization of DOX and DAPI that is also known nuclei dye for comparison of DOX-HER-2-NCs and DOX-NCs permeability effects.

Annexin-V/PI double staining ecperiments demonstrated that low dose of DOX-HER-2-NCs and DOX-NCs triggered apoptosis. However, increasing doses of DOX-HER-2-NCs and DOX-NCs induced necrosis. These results show that two different possibilities could occur like Figure 31 (170). In addition to that, there was no loss of mitochondrial membrane potential in SKBR-3 cells. Apoptosis analysis demonstrated that the rate of apoptosis increased until doses at IC50 of DOX-HER-2-NCs and DOX-NCs but increasing doses induced necrosis. So, the mitochondrial change at increasing doses was not observed by both Annexin V/PI double staining and JC-1 mitochondrial

membrane potential assay. After this application, two different possibilities were concluded in terms of cell death pathways (Figure 4.1).

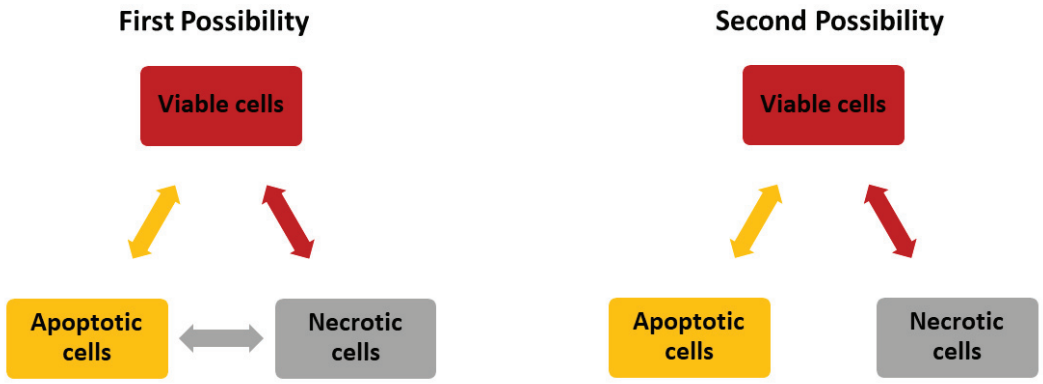

Figure 4.1 The possibility of drug effect on apoptosis and necrosis of SKBR-3 cells.

Bcl-2, Bax, and Caspase-3 protein was determined by using western blotting. Each protein was used to determine its role in the apoptosis signaling pathway. Our result shown that there was no decrease in protein levels of Bcl-2 but the protein levels of Bax increased in experimental group as compared to control group and normalized to internal positive gene, GAPDH. After this experiment, we have two main question marks; I. "Application of DOX conjugated NCs induce necrosis or apoptosis" and, II. "Application of DOX conjugated NCs induce apoptosis without Bcl-2 protein". After this application, the changes in protein level of Caspase-3 in response to DOX-NCs and DOX-HER-2-NCs were determined. Our results showed that Caspase-3 was cleavaged after NCs application. Whelan R.S. et al. explained that Bax protein regulates primary necrosis through mitochondrial dynamics (171). So, the apoptosis can be regulated through Bax protein. Next, the apoptosis can be regulated without mitochondrial membrane dynamics because Bcl-2 protein expression did not chande as compared to control. Bcl-2 protein was known as the main regulator of the apoptotic pathway by activation-deactivation of this protein. However, Bax protein regulates primary necrosis. In addition, Rogers C. *et. al.* showed that cleavage of Caspase-3 during apoptosis regulate the secondary necrotic/pyroptotic cell death (172). Our results also showed that the Caspase-3 cleavage occurred after NCs application. In agreement with the literature, our studies demonstrated that application of DOX-NCs and DOX-HER-2-NCs induced apoptosis and primary

necrosis. It is also known that apoptosis induces secondary necrosis. So, the increasing doses of DOX-NCs and DOX-HER-2-NCs induced necrosis.

On the other hand, G1, S, and G2 cell cycle phases were identified by the cytostatic analysis. DOX is known as topoisomerase inhibitor blocking topoisomerase-II-DNA complexes in G2 and S phases (173). In this section, IC20, IC50, and IC80 doses were used to determine the dose-dependent effects of the agents on the cell cycle progression. The application of 0.27- and 1.07µM DOX-NCs increased percent of cells in G2 phase. This event represents that SKBR-3 cells were more susceptible to increasing dose of DOX-NCs. However, a high dose of DOX-NCs (4.7µM) induced DNA damage was more in G1 phases than either in S or G2 phases. The application of 0.16- and 0.45 µM DOX-HER-2-NCs increased cell population in G2 phase. The lower dose of DOX-HER-2-NCs had the same effects with DOX-NCs. As a result, these experiments confirmed that DOX-HER-2-NCs is more selective and effective in SKBR-3 cells.

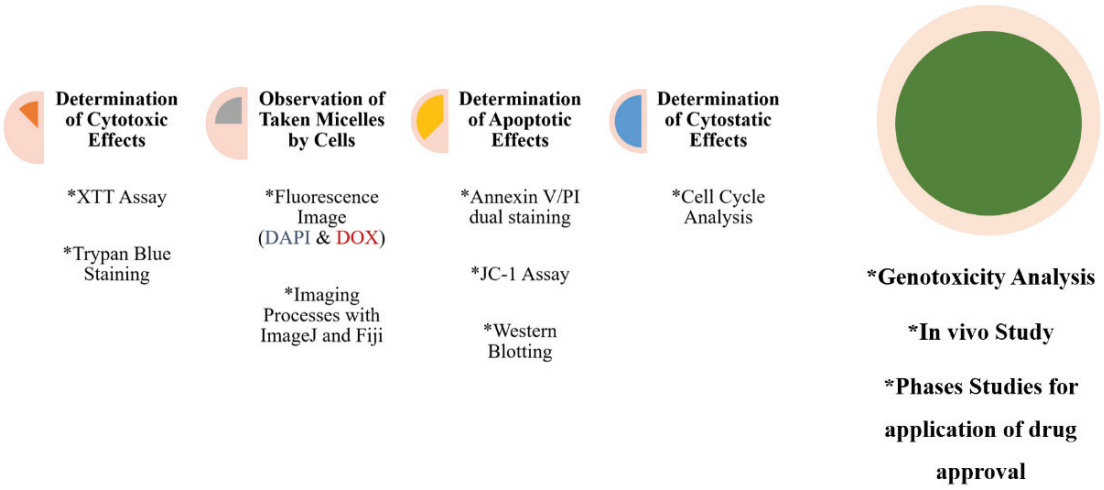

Figure 4.2. Past and future plan in this project.

Taken together all these results showed that the novel synthesized NCs can be used for effective treatment of HER-2 positive breast cancer patients. However, the genotoxicity analysis is necessary to continue *in vivo* and phase studies for the application of drug approval (Figure 4.2). In addition, the physicochemical characteristic of NCs also will be developed to increase drug efficiency by modification of acid-sensitive drug linking.

In different studies, nanoparticle or nanocarriers are referred to as “Trojan horses” (174). From this perspective, the micelles used in our study are the “Trojan horses” and DOX is the soldiers placed in the “Trojan horse” to fight with breast cancer cells. Using specific HER-2 peptide could be referred to as the blanket over “Trojan horses” that provides protection from outside of cells until full delivery inside the cells.

REFERENCES

1. Bray F, Ferlay J, Soerjomataram I, Siegel RL, Torre LA, Jemal A. Global cancer statistics 2018: GLOBOCAN estimates of incidence and mortality worldwide for 36 cancers in 185 countries. CA: A Cancer Journal for Clinicians. 2018;68(6):394-424.

2. Harrington KJ. The biology of cancer. Medicine. 2016;44(1):1-5.

3. Deborde S, Omelchenko T, Lyubchik A, Zhou Y, He S, McNamara WF, et al. Schwann cells induce cancer cell dispersion and invasion. The Journal of Clinical Investigation. 2016;126(4):1538-54.

4. Rahman MS, Suresh S, Waly MI. Risk Factors for Cancer: Genetic and Environment. In: Waly MI, Rahman MS, editors. Bioactive Components, Diet and Medical Treatment in Cancer Prevention. Cham: Springer International Publishing; 2018. p. 1-23.

5. Torre LA, Siegel RL, Ward EM, Jemal A. Global Cancer Incidence and Mortality Rates and Trends—An Update. Cancer Epidemiology Biomarkers & Prevention. 2016;25(1):16-27.

6. Miller KD, Siegel RL, Lin CC, Mariotto AB, Kramer JL, Rowland JH, et al. Cancer treatment and survivorship statistics, 2016. CA: A Cancer Journal for Clinicians. 2016;66(4):271-89.

7. Basch E, Deal AM, Kris MG, Scher HI, Hudis CA, Sabbatini P, et al. Symptom Monitoring With Patient-Reported Outcomes During Routine Cancer Treatment: A Randomized Controlled Trial. J Clin Oncol. 2016;34(6):557-65.

8. Lin JJ. Cancer Treatment. In: Nekhlyudov L, Goel MS, Lin JJ, Overholser L, Peairs KS, editors. Caring for Patients Across the Cancer Care Continuum: Essentials for Primary Care. Cham: Springer International Publishing; 2019. p. 93-123.

9. Zhang C-L, Huang T, Wu B-L, He W-X, Liu D. Stem cells in cancer therapy: opportunities and challenges. Oncotarget. 2017;8(43):75756-66.

10. Chan KS, Koh CG, Li HY. Mitosis-targeted anti-cancer therapies: where they stand. Cell Death Dis. 2012;3(10):e411-e.

11. Postow MA, Sidlow R, Hellmann MD. Immune-Related Adverse Events Associated with Immune Checkpoint Blockade. New England Journal of Medicine. 2018;378(2):158-68.

12. O'Donnell JS, Hoefsmit EP, Smyth MJ, Blank CU, Teng MWL. The promise of neoadjuvant immunotherapy and surgery for cancer treatment. Clinical Cancer Research. 2019:clincanres.2641.019.

13. Baskar R, Dai J, Wenlong N, Yeo R, Yeoh K-W. Biological response of cancer cells to radiation treatment. Front Mol Biosci. 2014;1:24-.

14. Sagar J, Chaib B, Sales K, Winslet M, Seifalian A. Role of stem cells in cancer therapy and cancer stem cells: a review. Cancer Cell Int. 2007;7:9-.

15. Cristofanilli M, Turner NC, Bondarenko I, Ro J, Im S-A, Masuda N, et al. Fulvestrant plus palbociclib versus fulvestrant plus placebo for treatment of hormone-receptor-positive, HER2-negative metastatic breast cancer that progressed on previous endocrine therapy (PALOMA-3): final analysis of the multicentre, double-blind, phase 3 randomised controlled trial. The Lancet Oncology. 2016;17(4):425-39.

16. James ND, Sydes MR, Clarke NW, Mason MD, Dearnaley DP, Spears MR, et al. Addition of docetaxel, zoledronic acid, or both to first-line long-term hormone therapy in prostate cancer (STAMPEDE): survival results from an adaptive, multiarm, multistage, platform randomised controlled trial. The Lancet. 2016;387(10024):1163-77.

17. Mayer IA, Arteaga CL. The PI3K/AKT Pathway as a Target for Cancer Treatment. Annual Review of Medicine. 2016;67(1):11-28.

18. Zou W, Wolchok JD, Chen L. PD-L1 (B7-H1) and PD-1 pathway blockade for cancer therapy: Mechanisms, response biomarkers, and combinations. Science Translational Medicine. 2016;8(328):328rv4-rv4.

19. Takebe N, Miele L, Harris PJ, Jeong W, Bando H, Kahn M, et al. Targeting Notch, Hedgehog, and Wnt pathways in cancer stem cells: clinical update. Nature Reviews Clinical Oncology. 2015;12:445.

20. Aronson SJ, Rehm HL. Building the foundation for genomics in precision medicine. Nature. 2015;526:336.

21. Khoury MJ, Bowen MS, Clyne M, Dotson WD, Gwinn ML, Green RF, et al. From public health genomics to precision public health: a 20-year journey. Genetics In Medicine. 2017;20:574.

22. Lacal PM, Graziani G. Therapeutic implication of vascular endothelial growth factor receptor-1 (VEGFR-1) targeting in cancer cells and tumor microenvironment by competitive and non-competitive inhibitors. Pharmacological Research. 2018;136:97-107.

23. Bisht S, Nolting J, Schütte U, Haarmann J, Jain P, Shah D, et al. Cyclin-Dependent Kinase 5 (CDK5) Controls Melanoma Cell Motility, Invasiveness, and Metastatic Spread—Identification of a Promising Novel therapeutic target. Translational Oncology. 2015;8(4):295-307.

24. Appert-Collin A, Hubert P, Crémel G, Bennasroune A. Role of ErbB Receptors in Cancer Cell Migration and Invasion. Frontiers in Pharmacology. 2015;6(283).

25. Arruebo M, Vilaboa N, Sáez-Gutierrez B, Lambea J, Tres A, Valladares M, et al. Assessment of the evolution of cancer treatment therapies. Cancers (Basel). 2011;3(3):3279-330.

26. Widakowich C, de Castro G, de Azambuja E, Dinh P, Awada A. Review: Side Effects of Approved Molecular Targeted Therapies in Solid Cancers. The Oncologist. 2007;12(12):1443-55.

27. Banerjee A, Pathak S, Subramanium VD, G D, Murugesan R, Verma RS. Strategies for targeted drug delivery in treatment of colon cancer: current trends and future perspectives. Drug Discovery Today. 2017;22(8):1224-32.

28. Kumar A, Lale SV, Aji Alex MR, Choudhary V, Koul V. Folic acid and trastuzumab conjugated redox responsive random multiblock copolymeric nanocarriers for breast cancer therapy: In-vitro and in-vivo studies. Colloids and Surfaces B: Biointerfaces. 2017;149:369-78.

29. Shi J, Votruba AR, Farokhzad OC, Langer R. Nanotechnology in drug delivery and tissue engineering: from discovery to applications. Nano letters. 2010;10(9):3223-30.

30. Hu Q, Sun W, Wang C, Gu Z. Recent advances of cocktail chemotherapy by combination drug delivery systems. Advanced drug delivery reviews. 2016;98:19-34.

31. Buduru S, Zimta AA, Ciocan C, Braicu C, Dudea D, Irimie AI, et al. RNA interference: new mechanistic and biochemical insights with application in oral cancer therapy. International journal of nanomedicine. 2018;13:3397-409.

32. Denic S, Agarwal MM. Breast cancer protection by genomic imprinting in close kin families. BMC Med Genet. 2017;18(1):136-.

33. Apostolou P, Fostira F. Hereditary breast cancer: the era of new susceptibility genes. Biomed Res Int. 2013;2013:747318-.

34. Bray F, McCarron P, Parkin DM. The changing global patterns of female breast cancer incidence and mortality. Breast Cancer Res. 2004;6(6):229-39.

35. van de Vijver MJ, He YD, van 't Veer LJ, Dai H, Hart AAM, Voskuil DW, et al. A Gene-Expression Signature as a Predictor of Survival in Breast Cancer. New England Journal of Medicine. 2002;347(25):1999-2009.

36. Makki J. Diversity of Breast Carcinoma: Histological Subtypes and Clinical Relevance. Clin Med Insights Pathol. 2015;8:23-31.

37. Lynch JA, Venne V, Berse B. Genetic tests to identify risk for breast cancer. Semin Oncol Nurs. 2015;31(2):100-7.

38. Sun Y-S, Zhao Z, Yang Z-N, Xu F, Lu H-J, Zhu Z-Y, et al. Risk Factors and Preventions of Breast Cancer. Int J Biol Sci. 2017;13(11):1387-97.

39. Llombart-Cussac A, Cortés J, Paré L, Galván P, Bermejo B, Martínez N, et al. HER2-enriched subtype as a predictor of pathological complete response following trastuzumab and lapatinib without chemotherapy in early-stage HER2-positive breast cancer (PAMELA): an open-label, single-group, multicentre, phase 2 trial. The Lancet Oncology. 2017;18(4):545-54.

40. Gianni L, Pienkowski T, Im Y-H, Tseng L-M, Liu M-C, Lluch A, et al. 5-year analysis of neoadjuvant pertuzumab and trastuzumab in patients with locally advanced, inflammatory, or early-stage HER2-positive breast cancer

(NeoSphere): a multicentre, open-label, phase 2 randomised trial. The Lancet Oncology. 2016;17(6):791-800.

41. Kawaguchi H, Yamashita T, Masuda N, Kitada M, Narui K, Hattori M, et al. Abstract P5-21-07: Phase II study of eribulin in combination with pertuzumab plus trastuzumab for human epidermal growth factor receptor 2 (HER2)-positive advanced or metastatic breast cancer. Cancer Research. 2018;78(4 Supplement):P5-21-07-P5-21-07.

42. Widatalla SE, Korolkova OY, Whalen DS, Goodwin JS, Williams KP, Ochieng J, et al. Lapatinib-induced annexin A6 upregulation as an adaptive response of triple negative breast cancer cells to EGFR tyrosine kinase inhibitors. Carcinogenesis. 2018.

43. Lee JH, Nan A. Combination drug delivery approaches in metastatic breast cancer. J Drug Deliv. 2012;2012:915375-.

44. Botrel TEA, Paladini L, Clark OAC. Lapatinib plus chemotherapy or endocrine therapy (CET) versus CET alone in the treatment of HER-2-overexpressing locally advanced or metastatic breast cancer: systematic review and meta-analysis. Core Evid. 2013;8:69-78.

45. Mohan N, Jiang J, Dokmanovic M, Wu WJ. Trastuzumab-mediated cardiotoxicity: current understanding, challenges, and frontiers. Antib Ther. 2018;1(1):13-7.

46. Inokuchi M, Ishikawa S, Furukawa H, Takamura H, Ninomiya I, Kitagawa H, et al. Treatment of capecitabine-induced hand-foot syndrome using a topical retinoid: A case report. Oncol Lett. 2014;7(2):444-8.

47. Prat A, Pineda E, Adamo B, Galván P, Fernández A, Gaba L, et al. Clinical implications of the intrinsic molecular subtypes of breast cancer. The Breast. 2015;24:S26-S35.

48. Netanely D, Avraham A, Ben-Baruch A, Evron E, Shamir R. Expression and methylation patterns partition luminal-A breast tumors into distinct prognostic subgroups. Breast Cancer Research. 2016;18(1):74.

49. Widodo I, Dwianingsih EK, Anwar SL, Fx Ediati T, Utoro T, Aryandono T, et al. Prognostic Value of Clinicopathological Factors for Indonesian Breast

Carcinomas of Different Molecular Subtypes. Asian Pac J Cancer Prev.18(5):1251-6.

50. Alluri P, Newman LA. Basal-like and triple-negative breast cancers: searching for positives among many negatives. Surg Oncol Clin N Am. 2014;23(3):567-77.

51. Gonçalves H, Jr., Guerra MR, Duarte Cintra JR, Fayer VA, Brum IV, Bustamante Teixeira MT. Survival Study of Triple-Negative and Non-Triple-Negative Breast Cancer in a Brazilian Cohort. Clin Med Insights Oncol. 2018;12:1179554918790563-.

52. Zuo T, Zeng H, Li H, Liu S, Yang L, Xia C, et al. The influence of stage at diagnosis and molecular subtype on breast cancer patient survival: a hospital-based multi-center study. Chinese journal of cancer. 2017;36(1):84-.

53. Joensuu K, Leidenius M, Kero M, Andersson LC, Horwitz KB, Heikkilä P. ER, PR, HER2, Ki-67 and CK5 in Early and Late Relapsing Breast Cancer-Reduced CK5 Expression in Metastases. Breast Cancer (Auckl). 2013;7:23-34.

54. Yersal O, Barutca S. Biological subtypes of breast cancer: Prognostic and therapeutic implications. World J Clin Oncol. 2014;5(3):412-24.

55. Tessier-Cloutier B, Asleh-Aburaya K, Shah V, McCluggage WG, Tinker A, Gilks CB. Molecular subtyping of mammary-like adenocarcinoma of the vulva shows molecular similarity to breast carcinomas. Histopathology. 2017;71(3):446-52.

56. Cava C, Colaprico A, Bertoli G, Bontempi G, Mauri G, Castiglioni I. How interacting pathways are regulated by miRNAs in breast cancer subtypes. BMC Bioinformatics. 2016;17(12):348.

57. Wang J, Sang D, Xu B, Yuan P, Ma F, Luo Y, et al. Value of Breast Cancer Molecular Subtypes and Ki67 Expression for the Prediction of Efficacy and Prognosis of Neoadjuvant Chemotherapy in a Chinese Population. Medicine. 2016;95(18):e3518-e.

58. Hu Z, Fan C, Oh DS, Marron JS, He X, Qaqish BF, et al. The molecular portraits of breast tumors are conserved across microarray platforms. BMC genomics. 2006;7:96.

59. Esserman LJ, Perou C, Cheang M, DeMichele A, Carey L, Veer LJvt, et al. Breast cancer molecular profiles and tumor response of neoadjuvant doxorubicin and paclitaxel: The I-SPY TRIAL (CALGB 150007/150012, ACRIN 6657). Journal of Clinical Oncology. 2009;27(18_suppl):LBA515-LBA.

60. Tran B, Bedard PL. Luminal-B breast cancer and novel therapeutic targets. Breast Cancer Res. 2011;13(6):221-.

61. Turner N, Grose R. Fibroblast growth factor signalling: from development to cancer. Nature Reviews Cancer. 2010;10:116.

62. Iqbal N, Iqbal N. Human Epidermal Growth Factor Receptor 2 (HER2) in Cancers: Overexpression and Therapeutic Implications. Molecular biology international. 2014;2014:852748.

63. Wee P, Wang Z. Epidermal Growth Factor Receptor Cell Proliferation Signaling Pathways. Cancers (Basel). 2017;9(5):52.

64. Jarvinen TA, Tanner M, Rantanen V, Barlund M, Borg A, Grenman S, et al. Amplification and deletion of topoisomerase IIalpha associate with ErbB-2 amplification and affect sensitivity to topoisomerase II inhibitor doxorubicin in breast cancer. The American journal of pathology. 2000;156(3):839-47.

65. Yao H, He G, Yan S, Chen C, Song L, Rosol TJ, et al. Triple-negative breast cancer: is there a treatment on the horizon? Oncotarget. 2016;8(1):1913-24.

66. Badowska-Kozakiewicz AM, Budzik MP. Immunohistochemical characteristics of basal-like breast cancer. Contemp Oncol (Pozn). 2016;20(6):436-43.

67. Toft DJ, Cryns VL. Minireview: Basal-like breast cancer: from molecular profiles to targeted therapies. Mol Endocrinol. 2011;25(2):199-211.

68. El Hachem G, Gombos A, Awada A. Recent advances in understanding breast cancer and emerging therapies with a focus on luminal and triple-negative breast cancer [version 1; peer review: 2 approved]. F1000Research. 2019;8(591).

69. Milioli HH, Tishchenko I, Riveros C, Berretta R, Moscato P. Basal-like breast cancer: molecular profiles, clinical features and survival outcomes. BMC Med Genomics. 2017;10(1):19-.

70. Choo JR, Nielsen TO. Biomarkers for Basal-like Breast Cancer. Cancers (Basel). 2010;2(2):1040-65.

71. González-González A, Muñoz-Muela E, Marchal JA, Cara FE, Molina MP, Cruz-Lozano M, et al. Activating Transcription Factor 4 Modulates TGFβ-Induced Aggressiveness in Triple-Negative Breast Cancer via SMAD2/3/4 and mTORC2 Signaling. Clinical Cancer Research. 2018;24(22):5697-709.

72. Helleday T. The underlying mechanism for the PARP and BRCA synthetic lethality: clearing up the misunderstandings. Mol Oncol. 2011;5(4):387-93.

73. Anders CK, Winer EP, Ford JM, Dent R, Silver DP, Sledge GW, et al. Poly(ADP-Ribose) polymerase inhibition: "targeted" therapy for triple-negative breast cancer. Clin Cancer Res. 2010;16(19):4702-10.

74. Dias K, Dvorkin-Gheva A, Hallett RM, Wu Y, Hassell J, Pond GR, et al. Claudin-Low Breast Cancer; Clinical & Pathological Characteristics. PLoS One. 2017;12(1):e0168669-e.

75. Vidal M, Peg V, Galván P, Tres A, Cortés J, Ramón y Cajal S, et al. Gene expression-based classifications of fibroadenomas and phyllodes tumours of the breast. Mol Oncol. 2015;9(6):1081-90.

76. Ping Tang, Gary M. Tse. Immunohistochemical Surrogates for Molecular Classification of Breast Carcinoma: A 2015 Update. Archives of Pathology & Laboratory Medicine. 2016;140(8):806-14.

77. Goldhirsch A, Wood WC, Coates AS, Gelber RD, Thurlimann B, Senn HJ. Strategies for subtypes--dealing with the diversity of breast cancer: highlights of the St. Gallen International Expert Consensus on the Primary Therapy of Early Breast Cancer 2011. Annals of oncology : official journal of the European Society for Medical Oncology. 2011;22(8):1736-47.

78. Goldhirsch A, Winer EP, Coates AS, Gelber RD, Piccart-Gebhart M, Thürlimann B, et al. Personalizing the treatment of women with early breast cancer: highlights of the St Gallen International Expert Consensus on the Primary Therapy of Early Breast Cancer 2013. Annals of oncology : official journal of the European Society for Medical Oncology. 2013;24(9):2206-23.

79. Tong CWS, Wu M, Cho WCS, To KKW. Recent Advances in the Treatment of Breast Cancer. Front Oncol. 2018;8:227-.

80. Sanchez-Vega F, Mina M, Armenia J, Chatila WK, Luna A, La KC, et al. Oncogenic Signaling Pathways in The Cancer Genome Atlas. Cell. 2018;173(2):321-37.e10.

81. Wang D-Y, Gendoo DMA, Ben-David Y, Woodgett JR, Zacksenhaus E. A subgroup of microRNAs defines PTEN-deficient, triple-negative breast cancer patients with poorest prognosis and alterations in RB1, MYC, and Wnt signaling. Breast Cancer Research. 2019;21(1):18.

82. Knudsen ES, Zacksenhaus E. The vulnerability of RB loss in breast cancer: Targeting a void in cell cycle control. Oncotarget. 2018;9(57):30940-1.

83. Witkiewicz AK, Chung S, Brough R, Vail P, Franco J, Lord CJ, et al. Targeting the Vulnerability of RB Tumor Suppressor Loss in Triple-Negative Breast Cancer. Cell reports. 2018;22(5):1185-99.

84. Liu JC, Granieri L, Shrestha M, Wang D-Y, Vorobieva I, Rubie EA, et al. Identification of CDC25 as a Common Therapeutic Target for Triple-Negative Breast Cancer. Cell Reports. 2018;23(1):112-26.

85. Fedele M, Cerchia L, Chiappetta G. The Epithelial-to-Mesenchymal Transition in Breast Cancer: Focus on Basal-Like Carcinomas. Cancers. 2017;9(10):134.

86. Li X, Zheng L, Zhang F, Hu J, Chou J, Liu Y. STARD13-correlated ceRNA network inhibits EMT and metastasis of breast cancer. Oncotarget. 2016;7.

87. van Nimwegen MJ, Verkoeijen S, van Buren L, Burg D, van de Water B. Requirement for Focal Adhesion Kinase in the Early Phase of Mammary Adenocarcinoma Lung Metastasis Formation. Cancer Research. 2005;65(11):4698-706.

88. Provenzano PP, Inman DR, Eliceiri KW, Beggs HE, Keely PJ. Mammary Epithelial-Specific Disruption of Focal Adhesion Kinase Retards Tumor Formation and Metastasis in a Transgenic Mouse Model of Human Breast Cancer. The American Journal of Pathology. 2008;173(5):1551-65.

89. Hu Y, Yu K, Wang G, Zhang D, Shi C, Ding Y, et al. Lanatoside C inhibits cell proliferation and induces apoptosis through attenuating Wnt/β-catenin/c-Myc

signaling pathway in human gastric cancer cell. Biochemical Pharmacology. 2018;150:280-92.

90. Wang E, Sorolla A, Cunningham PT, Bogdawa HM, Beck S, Golden E, et al. Tumor penetrating peptides inhibiting MYC as a potent targeted therapeutic strategy for triple-negative breast cancers. Oncogene. 2019;38(1):140-50.

91. Baker A, Wyatt D, Bocchetta M, Li J, Filipovic A, Green A, et al. Notch-1-PTEN-ERK1/2 signaling axis promotes HER2+ breast cancer cell proliferation and stem cell survival. Oncogene. 2018;37(33):4489-504.

92. Cabrera RM, Mao SPH, Surve CR, Condeelis JS, Segall JE. A novel neuregulin - jagged1 paracrine loop in breast cancer transendothelial migration. Breast cancer research : BCR. 2018;20(1):24.

93. Shah D, Wyatt D, Baker AT, Simms P, Peiffer DS, Fernandez M, et al. Inhibition of HER2 Increases JAGGED1-dependent Breast Cancer Stem Cells: Role for Membrane JAGGED1. Clinical Cancer Research. 2018;24(18):4566-78.

94. Hossain F, Sorrentino C, Ucar DA, Peng Y, Matossian M, Wyczechowska D, et al. Notch Signaling Regulates Mitochondrial Metabolism and NF-κB Activity in Triple-Negative Breast Cancer Cells via IKKα-Dependent Non-canonical Pathways. Frontiers in oncology. 2018;8:575-.

95. Walker A, Singh A, Tully E, Woo J, Le A, Nguyen T, et al. Nrf2 signaling and autophagy are complementary in protecting breast cancer cells during glucose deprivation. Free Radical Biology and Medicine. 2018;120:407-13.

96. He J-L, Zhou Z-W, Yin J-J, He C-Q, Zhou S-F, Yu Y. Schisandra chinensis regulates drug metabolizing enzymes and drug transporters via activation of Nrf2-mediated signaling pathway. Drug design, development and therapy. 2014;9:127-46.

97. Nakanishi T, Ross DD. Breast cancer resistance protein (BCRP/ABCG2): its role in multidrug resistance and regulation of its gene expression. Chin J Cancer. 2012;31(2):73-99.

98. Lou Y, Guo Z, Zhu Y, Zhang G, Wang Y, Qi X, et al. Astragali radix and its main bioactive compounds activate the Nrf2-mediated signaling pathway to

induce P-glycoprotein and breast cancer resistance protein. Journal of ethnopharmacology. 2019;228:82-91.

99. Mundi PS, Sachdev J, McCourt C, Kalinsky K. AKT in cancer: new molecular insights and advances in drug development. Br J Clin Pharmacol. 2016;82(4):943-56.

100. Valkov A, Kilvaer TK, Sorbye SW, Donnem T, Smeland E, Bremnes RM, et al. The prognostic impact of Akt isoforms, PI3K and PTEN related to female steroid hormone receptors in soft tissue sarcomas. J Transl Med. 2011;9:200-.

101. McClurg UL, Robson CN. Deubiquitinating enzymes as oncotargets. Oncotarget. 2015;6(12):9657-68.

102. Yang W-L, Wu C-Y, Wu J, Lin H-K. Regulation of Akt signaling activation by ubiquitination. Cell Cycle. 2010;9(3):487-97.

103. Wang G, Gao Y, Li L, Jin G, Cai Z, Chao J-I, et al. K63-linked ubiquitination in kinase activation and cancer. Front Oncol. 2012;2:5-.

104. Szymonowicz K, Oeck S, Malewicz NM, Jendrossek V. New Insights into Protein Kinase B/Akt Signaling: Role of Localized Akt Activation and Compartment-Specific Target Proteins for the Cellular Radiation Response. Cancers (Basel). 2018;10(3):78.

105. Huang F, Shi Q, Li Y, Xu L, Xu C, Chen F, et al. HER2/EGFR–AKT Signaling Switches TGFβ from Inhibiting Cell Proliferation to Promoting Cell Migration in Breast Cancer. Cancer Research. 2018;78(21):6073-85.

106. Kunihiro AG, Brickey JA, Frye JB, Luis PB, Schneider C, Funk JL. Curcumin, but not curcumin-glucuronide, inhibits Smad signaling in TGFβ-dependent bone metastatic breast cancer cells and is enriched in bone compared to other tissues. The Journal of Nutritional Biochemistry. 2019;63:150-6.

107. Veenstra C, Karlsson E, Mirwani SM, Nordenskjöld B, Fornander T, Pérez-Tenorio G, et al. The effects of PTPN2 loss on cell signalling and clinical outcome in relation to breast cancer subtype. Journal of Cancer Research and Clinical Oncology. 2019.

108. Tiganis T. The Role of TCPTP in Cancer. In: Neel BG, Tonks NK, editors. Protein Tyrosine Phosphatases in Cancer. New York, NY: Springer New York; 2016. p. 145-68.

109. Bence KK. Protein-Tyrosine Phosphatases: Linking Metabolism and Cancer. In: Neel BG, Tonks NK, editors. Protein Tyrosine Phosphatases in Cancer. New York, NY: Springer New York; 2016. p. 307-33.

110. Kim M, Morales LD, Baek M, Slaga TJ, DiGiovanni J, Kim DJ. UVB-induced nuclear translocation of TC-PTP by AKT/14-3-3σ axis inhibits keratinocyte survival and proliferation. Oncotarget. 2017;8(53):90674-92.

111. Buszard BJ, Johnson TK, Meng T-C, Burke R, Warr CG, Tiganis T. The nucleus- and endoplasmic reticulum-targeted forms of protein tyrosine phosphatase 61F regulate Drosophila growth, life span, and fecundity. Mol Cell Biol. 2013;33(7):1345-56.

112. Hsu JL, Hung M-C. The role of HER2, EGFR, and other receptor tyrosine kinases in breast cancer. Cancer Metastasis Rev. 2016;35(4):575-88.

113. Wieduwilt MJ, Moasser MM. The epidermal growth factor receptor family: biology driving targeted therapeutics. Cell Mol Life Sci. 2008;65(10):1566-84.

114. Carpenter G, King L, Jr., Cohen S. Epidermal growth factor stimulates phosphorylation in membrane preparations *in vitro*. Nature. 1978;276(5686):409-10.

115. Schulz R, Streller F, Scheel AH, Rüschoff J, Reinert MC, Dobbelstein M, et al. HER2/ErbB2 activates HSF1 and thereby controls HSP90 clients including MIF in HER2-overexpressing breast cancer. Cell Death &Amp; Disease. 2014;5:e980.

116. de Melo Gagliato D, Jardim DLF, Marchesi MSP, Hortobagyi GN. Mechanisms of resistance and sensitivity to anti-HER2 therapies in HER2+ breast cancer. Oncotarget. 2016;7(39):64431-46.

117. Luque-Cabal M, García-Teijido P, Fernández-Pérez Y, Sánchez-Lorenzo L, Palacio-Vázquez I. Mechanisms behind the Resistance to Trastuzumab in HER2-Amplified Breast Cancer and Strategies to Overcome It. Clinical Medicine Insights: Oncology. 2016;10s1:CMO.S34537.

118. Peddi PF, Hurvitz SA. Trastuzumab emtansine: the first targeted chemotherapy for treatment of breast cancer. Future Oncol. 2013;9(3):319-26.

119. Goel S, Wang Q, Watt AC, Tolaney SM, Dillon DA, Li W, et al. Overcoming Therapeutic Resistance in HER2-Positive Breast Cancers with CDK4/6 Inhibitors. Cancer Cell. 2016;29(3):255-69.

120. Jordan NV, Bardia A, Wittner BS, Benes C, Ligorio M, Zheng Y, et al. HER2 expression identifies dynamic functional states within circulating breast cancer cells. Nature. 2016;537:102.

121. Ebbesen SH, Scaltriti M, Bialucha CU, Morse N, Kastenhuber ER, Wen HY, et al. Pten loss promotes MAPK pathway dependency in HER2/neu breast carcinomas. Proceedings of the National Academy of Sciences. 2016;113(11):3030-5.

122. Tripathy J, Tripathy A, Thangaraju M, Suar M, Elangovan S. α-Lipoic acid inhibits the migration and invasion of breast cancer cells through inhibition of TGFβ signaling. Life Sciences. 2018;207:15-22.

123. Tanioka MFC, Parker JS, Hoadley KA, Hu Z, Li Y, Hyslop T, Pitcher BN, Soloway M, Spears PA, et al. Integrated analysis of RNA and DNA from the phase III trial CALGB 40601 identifies predictors of response to trastuzumab-based neoadjuvant chemotherapy in HER2-positive breast cancer. Clinical Cancer Research. 2018; in press.

124. Tanioka M, Mott KR, Hollern DP, Fan C, Darr DB, Perou CM. Identification of Jun loss promotes resistance to histone deacetylase inhibitor entinostat through Myc signaling in luminal breast cancer. Genome Med. 2018;10(1):86.

125. Li J, Liu Y, Jiang Y, Shao Z. Breast Cancer-Specific Mortality Pattern and Its Changing Feature According to Estrogen Receptor Status in Two Time Periods. PLoS One. 2016;11(6):e0157322-e.

126. Desai NV, Torous V, Parker J, Auman JT, Rosson GB, Cruz C, et al. Intrinsic molecular subtypes of breast cancers categorized as HER2-positive using an alternative chromosome 17 probe assay. Breast Cancer Research. 2018;20(1):75.

127. Xue L, Maihle NJ, Yu X, Tang S-C, Liu HY. Synergistic Targeting HER2 and EGFR with Bivalent Aptamer-siRNA Chimera Efficiently Inhibits HER2-Positive Tumor Growth. Molecular Pharmaceutics. 2018;15(11):4801-13.

128. Arpino G, Milano M, De Placido S. Features of aggressive breast cancer. The Breast. 2015;24(5):594-600.

129. Romond EH, Perez EA, Bryant J, Suman VJ, Geyer CE, Davidson NE, et al. Trastuzumab plus Adjuvant Chemotherapy for Operable HER2-Positive Breast Cancer. New England Journal of Medicine. 2005;353(16):1673-84.

130. Perez EA, Romond EH, Suman VJ, Jeong J-H, Sledge G, Jr CEG, et al. Trastuzumab Plus Adjuvant Chemotherapy for Human Epidermal Growth Factor Receptor 2–Positive Breast Cancer: Planned Joint Analysis of Overall Survival From NSABP B-31 and NCCTG N9831. Journal of Clinical Oncology. 2014;32(33):3744-52.

131. Meric-Bernstam F, Johnson AM, Dumbrava EEI, Raghav K, Balaji K, Bhatt M, et al. Advances in HER2-Targeted Therapy: Novel Agents and Opportunities Beyond Breast and Gastric Cancer. Clinical Cancer Research. 2019;25(7):2033-41.

132. Di Modica M, Tagliabue E, Triulzi T. Predicting the Efficacy of HER2-Targeted Therapies: A Look at the Host. Dis Markers. 2017;2017:7849108-.

133. von Minckwitz G, Procter M, de Azambuja E, Zardavas D, Benyunes M, Viale G, et al. Adjuvant Pertuzumab and Trastuzumab in Early HER2-Positive Breast Cancer. New England Journal of Medicine. 2017;377(2):122-31.

134. Nami B, Maadi H, Wang Z. Mechanisms Underlying the Action and Synergism of Trastuzumab and Pertuzumab in Targeting HER2-Positive Breast Cancer. Cancers (Basel). 2018;10(10):342.

135. Xu Z-q, Zhang Y, Li N, Liu P-j, Gao L, Gao X, et al. Efficacy and safety of lapatinib and trastuzumab for HER2-positive breast cancer: a systematic review and meta-analysis of randomised controlled trials. BMJ Open. 2017;7(3):e013053.

136. Lambert JM, Chari RVJ. Ado-trastuzumab Emtansine (T-DM1): An Antibody–Drug Conjugate (ADC) for HER2-Positive Breast Cancer. Journal of Medicinal Chemistry. 2014;57(16):6949-64.

137. Amiri-Kordestani L, Blumenthal GM, Xu QC, Zhang L, Tang SW, Ha L, et al. FDA Approval: Ado-Trastuzumab Emtansine for the Treatment of Patients with HER2-Positive Metastatic Breast Cancer. Clinical Cancer Research. 2014;20(17):4436-41.

138. Canonici A, Gijsen M, Mullooly M, Bennett R, Bouguern N, Pedersen K, et al. Neratinib overcomes trastuzumab resistance in HER2 amplified breast cancer. Oncotarget. 2013;4(10):1592-605.

139. Blackwell KL, Zaman K, Qin S, Tkaczuk KHR, Campone M, Hunt D, et al. Neratinib in Combination With Trastuzumab for the Treatment of Patients With Advanced HER2-positive Breast Cancer: A Phase I/II Study. Clinical Breast Cancer. 2019;19(2):97-104.e4.

140. Beeram M, Krop I, Modi S, Tolcher A, Rabbee N, Girish S, et al. A phase I study of trastuzumab-MCC-DM1 (T-DM1), a first-in-class HER2 antibody-drug conjugate (ADC), in patients (pts) with HER2+ metastatic breast cancer (BC). Journal of Clinical Oncology. 2007;25(18_suppl):1042-.

141. Vogel CL, Burris HA, Limentani S, Borson R, O'Shaughnessy J, Vukelja S, et al. A phase II study of trastuzumab-DM1 (T-DM1), a HER2 antibody-drug conjugate (ADC), in patients (pts) with HER2+ metastatic breast cancer (MBC): Final results. Journal of Clinical Oncology. 2009;27(15_suppl):1017-.

142. Papachristos A, Pippa N, Demetzos C, Sivolapenko G. Antibody-drug conjugates: a mini-review. The synopsis of two approved medicines. Drug delivery. 2016;23(5):1662-6.

143. Finn RS, Crown JP, Lang I, Boer K, Bondarenko IM, Kulyk SO, et al. The cyclin-dependent kinase 4/6 inhibitor palbociclib in combination with letrozole versus letrozole alone as first-line treatment of oestrogen receptor-positive, HER2-negative, advanced breast cancer (PALOMA-1/TRIO-18): a randomised phase 2 study. The Lancet Oncology. 2015;16(1):25-35.

144. Patnaik A, Rosen LS, Tolaney SM, Tolcher AW, Goldman JW, Gandhi L, et al. Efficacy and Safety of Abemaciclib, an Inhibitor of CDK4 and CDK6, for Patients with Breast Cancer, Non–Small Cell Lung Cancer, and Other Solid Tumors. Cancer Discovery. 2016;6(7):740-53.

145. Diamantis N, Banerji U. Antibody-drug conjugates—an emerging class of cancer treatment. British Journal Of Cancer. 2016;114:362.

146. Martínez-Jothar L, Beztsinna N, van Nostrum CF, Hennink WE, Oliveira S. Selective Cytotoxicity to HER2 Positive Breast Cancer Cells by Saporin-Loaded Nanobody-Targeted Polymeric Nanoparticles in Combination with Photochemical Internalization. Molecular Pharmaceutics. 2019;16(4):1633-47.

147. Cai Z, Chattopadhyay N, Yang K, Kwon YL, Yook S, Pignol J-P, et al. 111In-labeled trastuzumab-modified gold nanoparticles are cytotoxic *in vitro* to HER2-positive breast cancer cells and arrest tumor growth in vivo in athymic mice after intratumoral injection. Nuclear Medicine and Biology. 2016;43(12):818-26.

148. Hayward SL, Francis DM, Kholmatov P, Kidambi S. Targeted Delivery of MicroRNA125a-5p by Engineered Lipid Nanoparticles for the Treatment of HER2 Positive Metastatic Breast Cancer. Journal of Biomedical Nanotechnology. 2016;12(3):554-68.

149. Su C-Y, Chen M, Chen L-C, Ho Y-S, Ho H-O, Lin S-Y, et al. Bispecific antibodies (anti-mPEG/anti-HER2) for active tumor targeting of docetaxel (DTX)-loaded mPEGylated nanocarriers to enhance the chemotherapeutic efficacy of HER2-overexpressing tumors. Drug Delivery. 2018;25(1):1066-79.

150. Kulhari H, Pooja D, Kota R, Reddy TS, Tabor RF, Shukla R, et al. Cyclic RGDfK Peptide Functionalized Polymeric Nanocarriers for Targeting Gemcitabine to Ovarian Cancer Cells. Molecular Pharmaceutics. 2016;13(5):1491-500.

151. Choi YH, Yu AM. ABC transporters in multidrug resistance and pharmacokinetics, and strategies for drug development. Current pharmaceutical design. 2014;20(5):793-807.

152. Ozcelikkale A, Moon H-R, Linnes M, Han B. *In vitro* microfluidic models of tumor microenvironment to screen transport of drugs and nanoparticles. Wiley Interdiscip Rev Nanomed Nanobiotechnol. 2017;9(5):10.1002/wnan.460.

153. Qi SS, Sun JH, Yu HH, Yu SQ. Co-delivery nanoparticles of anti-cancer drugs for improving chemotherapy efficacy. Drug delivery. 2017;24(1):1909-26.

154. Singh R, Lillard JW, Jr. Nanoparticle-based targeted drug delivery. Exp Mol Pathol. 2009;86(3):215-23.

155. Kumari A, Singla R, Guliani A, Yadav SK. Nanoencapsulation for drug delivery. EXCLI J. 2014;13:265-86.

156. Wang F, Li C, Cheng J, Yuan Z. Recent Advances on Inorganic Nanoparticle-Based Cancer Therapeutic Agents. Int J Environ Res Public Health. 2016;13(12):1182.

157. Deshpande PP, Biswas S, Torchilin VP. Current trends in the use of liposomes for tumor targeting. Nanomedicine (Lond). 2013;8(9):1509-28.

158. Matea CT, Mocan T, Tabaran F, Pop T, Mosteanu O, Puia C, et al. Quantum dots in imaging, drug delivery and sensor applications. Int J Nanomedicine. 2017;12:5421-31.

159. Soga O, van Nostrum CF, Fens M, Rijcken CJ, Schiffelers RM, Storm G, et al. Thermosensitive and biodegradable polymeric micelles for paclitaxel delivery. Journal of controlled release : official journal of the Controlled Release Society. 2005;103(2):341-53.

160. Singh SK, Singh S, Lillard JW, Jr., Singh R. Drug delivery approaches for breast cancer. Int J Nanomedicine. 2017;12:6205-18.

161. Yamaguchi H, Hayama K, Sasagawa I, Okada Y, Kawase T, Tsubokawa N, et al. HER2-Targeted Multifunctional Silica Nanoparticles Specifically Enhance the Radiosensitivity of HER2-Overexpressing Breast Cancer Cells. Int J Mol Sci. 2018;19(3):908.

162. Li J, Xu W, Yuan X, Chen H, Song H, Wang B, et al. Polymer-lipid hybrid anti-HER2 nanoparticles for targeted salinomycin delivery to HER2-positive breast cancer stem cells and cancer cells. Int J Nanomedicine. 2017;12:6909-21.

163. Jin H, Pi J, Zhao Y, Jiang J, Li T, Zeng X, et al. EGFR-targeting PLGA-PEG nanoparticles as a curcumin delivery system for breast cancer therapy. Nanoscale. 2017;9(42):16365-74.

164. Nakanishi T, Fukushima S, Okamoto K, Suzuki M, Matsumura Y, Yokoyama M, et al. Development of the polymer micelle carrier system for doxorubicin. Journal of controlled release : official journal of the Controlled Release Society. 2001;74(1-3):295-302.

165. Matsumura Y, Hamaguchi T, Ura T, Muro K, Yamada Y, Shimada Y, et al. Phase I clinical trial and pharmacokinetic evaluation of NK911, a micelle-encapsulated doxorubicin. Br J Cancer. 2004;91(10):1775-81.

166. Nounou MI, ElAmrawy F, Ahmed N, Abdelraouf K, Goda S, Syed-Sha-Qhattal H. Breast Cancer: Conventional Diagnosis and Treatment Modalities and Recent Patents and Technologies. Breast Cancer (Auckl). 2015;9(Suppl 2):17-34.

167. Satija A, Bhatnagar S. Complementary Therapies for Symptom Management in Cancer Patients. Indian J Palliat Care. 2017;23(4):468-79.

168. Park JW, Hong K, Kirpotin DB, Colbern G, Shalaby R, Baselga J, et al. Anti-HER2 Immunoliposomes. Enhanced Efficacy Attributable to Targeted Delivery. 2002;8(4):1172-81.

169. Abbineni G, Modali S, Safiejko-Mroczka B, Petrenko VA, Mao C. Evolutionary selection of new breast cancer cell-targeting peptides and phages with the cell-targeting peptides fully displayed on the major coat and their effects on actin dynamics during cell internalization. Molecular pharmaceutics. 2010;7(5):1629-42.

170. D'Suze G, Rosales A, Salazar V, Sevcik C. Apoptogenic peptides from Tityus discrepans scorpion venom acting against the SKBR3 breast cancer cell line. Toxicon. 2010;56(8):1497-505.

171. Whelan RS, Konstantinidis K, Wei AC, Chen Y, Reyna DE, Jha S, et al. Bax regulates primary necrosis through mitochondrial dynamics. Proceedings of the National Academy of Sciences of the United States of America. 2012;109(17):6566-71.

172. Rogers C, Fernandes-Alnemri T, Mayes L, Alnemri D, Cingolani G, Alnemri ES. Cleavage of DFNA5 by caspase-3 during apoptosis mediates progression to secondary necrotic/pyroptotic cell death. Nature communications. 2017;8:14128.

173. Potter AJ, Gollahon KA, Palanca BJA, Harbert MJ, Choi YM, Moskovitz AH, et al. Flow cytometric analysis of the cell cycle phase specificity of DNA damage induced by radiation, hydrogen peroxide and doxorubicin. Carcinogenesis. 2002;23(3):389-401.

174. Liu D, Auguste DT. Cancer targeted therapeutics: From molecules to drug delivery vehicles. J Control Release. 2015;219:632-43.